VOLUME 32 | SUPPLEMENT 2 | MARCH 2019

MODERN PATHOLOGY

USCAP 2019

ABSTRACTS

PANCREAS, GALLBLADDER, AMPULLA, AND EXTRA-HEPATIC BILIARY TREE (1667-1734)

USCAP 108TH ANNUAL MEETING

UNLOCKING YOUR INGENUITY

MARCH 16-21, 2019

National Harbor, Maryland
Gaylord National Resort & Convention Center

Published by
SPRINGER NATURE
www.ModernPathology.org

USCAP Creating a Better Pathologist
AN OFFICIAL JOURNAL OF THE UNITED STATES AND CANADIAN ACADEMY OF PATHOLOGY

EDUCATION COMMITTEE

Jason L. Hornick, Chair
Rhonda K. Yantiss, Chair, Abstract Review Board and Assignment Committee
Laura W. Lamps, Chair, CME Subcommittee
Steven D. Billings, Interactive Microscopy Subcommittee
Shree G. Sharma, Informatics Subcommittee
Raja R. Seethala, Short Course Coordinator
Ilan Weinreb, Subcommittee for Unique Live Course Offerings
David B. Kaminsky (Ex-Officio)
Aleodor (Doru) Andea
Zubair Baloch
Olca Basturk
Gregory R. Bean, Pathologist-in-Training
Daniel J. Brat
Ashley M. Cimino-Mathews
James R. Cook
Sarah M. Dry
William C. Faquin
Carol F. Farver
Yuri Fedoriw
Meera R. Hameed
Michelle S. Hirsch
Lakshmi Priya Kunju
Anna Marie Mulligan
Rish Pai
Vinita Parkash
Anil Parwani
Deepa Patil
Kwun Wah Wen, Pathologist-in-Training

ABSTRACT REVIEW BOARD

Benjamin Adam
Michelle Afkhami
Narasimhan (Narsi) Agaram
Rouba Ali-Fehmi
Ghassan Allo
Isabel Alvarado-Cabrero
Christina Arnold
Rohit Bhargava
Justin Bishop
Jennifer Boland
Elena Brachtel
Marilyn Bui
Shelley Caltharp
Joanna Chan
Jennifer Chapman
Hui Chen
Yingbei Chen
Benjamin Chen
Rebecca Chernock
Beth Clark
James Conner
Alejandro Contreras
Claudiu Cotta
Timothy D'Alfonso
Farbod Darvishian
Jessica Davis
Heather Dawson
Elizabeth Demicco
Suzanne Dintzis
Michelle Downes
Daniel Dye
Andrew Evans
Michael Feely
Dennis Firchau
Larissa Furtado
Anthony Gill
Ryan Gill
Paula Ginter
Tamara Giorgadze
Raul Gonzalez
Purva Gopal
Anuradha Gopalan
Jennifer Gordetsky
Rondell Graham
Alejandro Gru
Nilesh Gupta
Mamta Gupta
Krisztina Hanley
Douglas Hartman
Yael Heher
Walter Henricks
John Higgins
Mai Hoang
Mojgan Hosseini
Aaron Huber
Peter Illei
Doina Ivan
Wei Jiang
Vickie Jo
Kirk Jones
Neerja Kambham
Chiah Sui (Sunny) Kao
Dipti Karamchandani
Darcy Kerr
Ashraf Khan
Rebecca King
Michael Kluk
Kristine Konopka
Gregor Krings
Asangi Kumarapeli
Alvaro Laga
Cheng-Han Lee
Zaibo Li
Haiyan Liu
Xiuli Liu
Yan-Chun Liu
Tamara Lotan
Anthony Magliocco
Kruti Maniar
Jonathan Marotti
Emily Mason
Jerri McLemore
Bruce McManus
David Meredith
Anne Mills
Neda Moatamed
Sara Monaco
Atis Muehlenbachs
Bita Naini
Dianna Ng
Tony Ng
Ericka Olgaard
Jacqueline Parai
Yan Peng
David Pisapia
Alexandros Polydorides
Sonam Prakash
Manju Prasad
Peter Pytel
Joseph Rabban
Stanley Radio
Emad Rakha
Preetha Ramalingam
Priya Rao
Robyn Reed
Michelle Reid
Natasha Rekhtman
Michael Rivera
Michael Roh
Andres Roma
Avi Rosenberg
Esther (Diana) Rossi
Peter Sadow
Safia Salaria
Steven Salvatore
Souzan Sanati
Sandro Santagata
Anjali Saqi
Frank Schneider
Jeanne Shen
Jiaqi Shi
Wun-Ju Shieh
Gabriel Sica
Deepika Sirohi
Kalliopi Siziopikou
Lauren Smith
Sara Szabo
Julie Teruya-Feldstein
Gaetano Thiene
Khin Thway
Rashmi Tondon
Jose Torrealba
Evi Vakiani
Christopher VandenBussche
Sonal Varma
Endi Wang
Christopher Weber
Olga Weinberg
Sara Wobker
Mina Xu
Shaofeng Yan
Anjana Yeldandi
Akihiko Yoshida
Gloria Young
Minghao Zhong
Yaolin Zhou
Hongfa Zhu
Debra Zynger

1667 Intracholecystic Papillary-Tubular Neoplasms: Is a Size Cut-Off Justified?

Heba Abdelal[1], Deyali Chatterjee[2]
[1]Washington University School of Medicine, St. Louis, MO, [2]Washington University, St. Louis, MO

Disclosures: Heba Abdelal: None; Deyali Chatterjee: None

Background: In the current WHO classification of tumors of the gallbladder (2010), polypoid well-demarcated intra-cholecystic lesions are classified as adenomas or intracystic papillary neoplasms, without a clear demarcation between the two entities. The term intracholecystic papillary-tubular neoplasms (ICPN) has subsequently been suggested to encompass all discrete noninvasive epithelial neoplasms in gallbladder, including adenomas. There is also a general consensus to use a size cut-off of 1 cm for ICPN. In our study, we wanted to explore the prognostic significance of smaller discrete polypoid lesions < 1cm (PL) in gallbladder, and how they relate to conventional ICPN.

Design: We searched our pathology database for all retrospective cholecystectomies (1995-2017) which had a grossly identifiable discrete polypoid lesion, and slides available for review. Polypoid lesions microscopically showing a cellular proliferation of glandular elements, arranged in various combinations of tubular and/or papillary configuration, were selected. Focal mucosal papillary hyperplasia in relation to chronic cholecystitis or cholesterolosis, and polypoid adenomyoma were excluded. Cases were classified based on greatest gross dimension, into PL (< 1cm) and ICPN (>=1cm). The clinical and follow-up information were reviewed from the electronic medical records.

Results: In our cohort, there were 22 cholecystectomy specimens (from 8 males, 14 females; with mean age 61 years), all of which were received grossly intact. 6 among them were classified as PL, and 16 as ICPN. The clinicopathologic details for the two groups are outlined in Table 1. Both groups showed similar histologic features in terms of epithelial composition, dysplasia within lesion, background flat epithelial dysplasia, or associated invasive carcinoma. On follow-up, one patient each from non-invasive PL and ICPN cases, subsequently developed a biliary malignancy.

Clinicopathologic features	PL (< 1cm)	ICPN (>=1cm)
Average size	0.4 (0.2-0.7)	1.9 (1-4.3)
Total cases	6 (F=5, M=1)	16 (F=9, M=7)
mean age (years)	59.7	62.5
Multiplicity of lesions	2 (33.3%)	5 (31.3%)
Multiplicity of epithelial components	2 (33.3%)	9 (56.3%)
Epithelial types (in number of lesions)	Biliary (4), gastric (3), intestinal (1), clear cell change (1)	Biliary (14), gastric (5), intestinal (3), oncocytic (1)
Cytologic dysplasia	3 (50%) (low grade- 1, high grade- 2)	14 (87.5%) (low grade-2, high grade-12)
Associated invasive carcinoma	1 (16.7%)	6 (37.5%)
Background flat dysplasia	2 (33.3%); low grade	9 (56.3%); (low grade- 6, high grade-3)
Subsequent biliary malignancy for non-invasive lesions	1 of 5 (20%)	1 of 10 (10%)
Association with chronic cholecystitis	4 (66.7%)	8 (50%)
Association with cholelithiasis	3 (50%)	7 (43.8%)
Association with cholesterolosis	1 (16.7%)	5 (31.3%)
Association with primary sclerosing cholangitis	1 (16.7%)	2 (12.5%)

Conclusions: Our study shows that clinical and pathologic findings between the two groups (PL and ICPN) are similar. Although the risk of high-grade dysplasia and invasive adenocarcinoma increases with size of the non-invasive lesion, they can be present in lesions less than 1 cm as well. There is also a subsequent risk of developing biliary tract malignancy elsewhere even if the lesion in gallbladder is less than 1 cm. Therefore, we feel, all discrete polypoid lesions in gallbladder have similar neoplastic potential and can be considered as ICPN irrespective of their size.

1668 Intraoperative Electroporation: Initial Observations In Whipple Resection Specimens

Andrea Agualimpia Garcia[1], Sarah Hackman[1], Danielle Fritze[1], Daniel Mais[2]
[1]UT Health San Antonio, San Antonio, TX, [2]The University of Texas Health Science Center at San Antonio, San Antonio, TX

Disclosures: Andrea Agualimpia Garcia: None; Sarah Hackman: None; Danielle Fritze: None; Daniel Mais: None

Background: Irreversible electroporation (IRE) constitutes an emerging component of the surgical approach to pancreatic cancer, particularly those in which there is involvement of major blood vessels. IRE consists of a series of short electrical pulses administered through electrodes placed astride the area of concern, creating small pores in cell membranes. The resulting impaired homeostasis leads to initiation of programmed cell death or apoptosis. This technique has been studied in porcine and mouse models, in some cases demonstrating significant thermal ('cautery') artifact. Distinctive morphologic abnormalities were noted in tissue harvested one or more hours after treatment, but the effect upon more immediately resected tissue has not been studied. The aim of this study was to investigate the immediate histologic effects of IRE administered during Whipple resection for pancreatic adenocarcinoma in human subjects.

Design: We retrospectively identified patients in whom IRE was applied to the vascular groove during resection and an equal number of patients in whom it was not used. We conducted blinded review of selected histologic sections from each specimen, including sections of vascular groove, uncinate margin, and tumor and parenchyma remote from specimen edges. Specific features in both tumor cells and benign elements (endothelial cells, vascular smooth muscle, lymphoid tissue, acinar, ductal, and islet cells) were noted, including apoptosis, necrosis, mitosis, thrombosis, extravasation, inflammatory cell infiltration, protoplasmic vacuolization, and 'cautery artifact.' We then compared these findings to those in other same-specimen sections and to specimens not exposed to IRE.

Results: We identified 8 patients in whom IRE was utilized and 8 patients in whom it was not. Among treated patients, all vascular groove tissue was free of cautery artifact and inflammatory cell infiltration. Some vascular groove sections from treated patients demonstrated apoptosis, mitotic activity, necrosis, thrombosis, extravasation, and vacuolization, but there was no difference in the frequency of these findings as compared to controls.

Conclusions: Histologic findings in tissue treated with IRE did not differ from findings in untreated tissue, and there was no specific histologic hallmark of IRE treatment. Damage to parenchymal and stromal elements in tissue treated with IRE was negligible, thereby minimizing tissue morphologic distortion.

1669 Prognostic Assessment of Immunogenicity in Ampullary Carcinoma Points Towards an Immunomodulatory Therapeutic Option

John Aird[1], Steve Kalloger[2], Christine Chow[3], Daniel Renouf[4], David Schaeffer[1]
[1]Vancouver General Hospital, Vancouver, BC, [2]University of British Columbia, Vancouver, BC, [3]Genetic Pathology Evaluation Centre, Vancouver, BC, [4]British Columbia Cancer Agency, Vancouver, BC

Disclosures: John Aird: None; Steve Kalloger: None; Christine Chow: None; Daniel Renouf: None; David Schaeffer: None

Background: The prognostication of ampullary carcinoma (AC) has largely relied on differentiation of the two main subtypes: pancreatobiliary (PB-Type) and intestinal (I-Type). Previous studies have shown that PB-Type has an inferior prognosis relative to I-Type. While much of the recent literature has focused on how best to categorize AC, little attention has been given to intrinsic characteristics such as immunogenicity which may have prognostic effects that transcend subtypes.

Design: A fully clinically annotated duplicate 0.6mm core tissue microarray of the epithelial and stromal components of 98 pathologically confirmed AC was assessed for CD8 & CD3 T-cells. Absolute counts were conducted for each core and the maximum count between cores was taken as the score for the histological component. Absolute counts and localization of the respective T-cell phenotypes were compared across histological subtypes and subjected to univariable and multivariable prognostic assessments. Associations with mismatch repair (MMR) deficiency and PD-L1 staining of the epithelial component were also performed.

Results: The I-Type (N=47) and PB-Type (N=51) had median ages of 70 and 68 and equivalent sex distribution (57% male, 43% female). The count data for CD3 & CD8 T-Cells did not demonstrate any statistically significant differences between the subtypes (Table 1). Parametric survival analysis using count data for CD8 and CD3 T-cells in each component demonstrated a positive association with survival (p<=0.04) in both univariable and multivariable analysis with ampullary subtype as the covariate. Intra-epithelial localization of both CD3+ and CD8+ T-Cells was associated with improved prognosis by univariable assessment (p<=0.04). However, only CD8+ T-cells conferred an improved prognosis on multivariable analysis with a risk ratio = 0.33 and 95%CI of [0.13-0.84]. No association with MMR deficiency was found for any of the CD3/CD8 and histological component combinations. Using a 1% cut-off for PD-L1 positivity, a significantly higher number of CD3+ & CD8+ T-Cells were found in both the stromal and epithelial components (p<= 0.03). The rate of PD-L1 positivity ranged from 18% in the PB-Type to 4% in the I-Type (p=0.03).

Mean Counts	I-Type	PB-Type	P-Value (ANOVA)

CD3+ Stromal	52.6	60.3	0.47
CD3+ Epithelial	12.3	6.3	0.06
CD8+ Stromal	23.5	30.2	0.23
CD8+ Epithelial	6.0	4.0	0.55

Conclusions: This study illustrates that increasing numbers of CD3+ and CD8+ T-Cells in either the stromal or epithelial component are associated with improved prognosis in AC regardless of PB-Type or I-Type histology. The strongest prognostic associations were conferred by CD8+ intraepithelial T-Cells.

1670 Histopathologic changes of pancreatic cysts after endoscopic ultrasound-guided ethanol and/or paclitaxel ablation therapy mimic pseudocysts

Soyeon An[1], Sung Joo Kim[2], Song Cheol Kim[2], Dong-Wan Seo[2], Seung-Mo Hong[3]
[1]Incheon St. Mary's Hospital, The Catholic University of Korea, Incheon, Korea, Republic of South Korea, [2]Asan Medical Center, Seoul, Korea, Republic of South Korea, [3]Asan Medical Center, Songpa-gu, Korea, Republic of South Korea

Disclosures: Soyeon An: None; Seung-Mo Hong: None

Background: Endoscopic ultrasound (EUS)-guided ablation therapy is a minimally invasive procedure for patients with pancreatic cystic tumors when they had preoperative comorbidities or were not indicated for surgical resection. However, histopathologic characteristics of pancreatic cysts after ablation have not been well-elucidated.

Design: Twelve cases of surgically resected pancreatic cysts after EUS-guided ablation with ethanol and/or paclitaxel injection were selected. Histopathologic parameters, including residual lining epithelia, inflammatory cell infiltrations, hyalinization, calcification, hemorrhage, pigmentation, cholesterol cleft, and fat necrosis, were evaluated.

Results: Mean patient age was 49.8±13.6 years with male-to-female ratio was 0.33. Clinical impression before EUS-guided ablation was predominantly mucinous cystic neoplasms. Mean pancreatic cyst size before and after ablation therapy was 3.7±1.0cm and 3.4±1.6cm, respectively (p=0.44). Median time between ablation therapy and surgical resection of pancreatic cysts was 18 (range, 1-59) months. Mean percent of residual lining epithelial cells were 23.1±37.0%. Eight cases (67%) showed no or minimal residual lining epithelia (6 cases, no lining epithelia; 2, 4% lining epithelia; 67%), while 4 cases (33%) showed various degree of residual mucinous epithelium (20% to 90%). Ovarian-type stroma was noted in 4 cases (33%). Other frequently observed histologic features were moderate chronic active inflammation (8 cases, 67%), histiocytic aggregation (8, 67%), marked stromal hyalinization (8, 67%), diffuse calcification along the cystic wall (7, 58%), and fat necrosis (2, 17%).

Conclusions: Diffuse calcification along the pancreatic cystic walls with focal residual lining epithelia are characteristic features of pancreatic cysts after ablation therapies with ethanol and/or paclitaxel injection. In addition, chronic active inflammation, histiocytic aggregation, and marked stromal hyalinization are also observed. Understanding of these pathologic features will be helpful for precise pathologic diagnosis of pancreatic cystic tumor after ablation therapies, even without knowing patient history of cystic ablation therapies.

1671 Characterizing the Pancreatic Adenocarcinoma Stromal Immune Microenvironment: Assessment of Tumor Associated Macrophages and Lymphocyte Immune Checkpoint Molecules

Shi Bai[1], Yiqin Xiong[2], Karen Dresser[3], Xiaofei Wang[3], Michelle Yang[4], Benjamin Chen[5]
[1]UMass Memorial Medical Center, Northborough, MA, [2]University of Massachusetts, Worcester, MA, [3]UMass Memorial Health Care, Worcester, MA, [4]University of Massachusetts Medical School, Worcester, MA, [5]UMass Memorial Medical Center, Worcester, MA

Disclosures: Shi Bai: None; Yiqin Xiong: None; Karen Dresser: None; Xiaofei Wang: None; Michelle Yang: None; Benjamin Chen: *Grant or Research Support*, TESARO Inc.

Background: The immune microenvironment of pancreatic adenocarcinoma (PDAC) is incompletely understood, and patients frequently fail to respond to currently available targeted immunotherapies. Recent evidence suggests that tumor-associated macrophages (TAMs) are important for tumorigenesis, and play a significant immunosuppressive role in PDAC. In this study, we sought to characterize by immunohistochemistry the relationship between TAMs, tumor infiltrating lymphocytes (TILs), and expression of checkpoint molecules PD-L1, TIM3, and LAG3 in PDAC.

Design: PDAC resection cases were retrospectively selected, and serial sections were stained with antibodies against CD3, PD-L1, TIM3, LAG3, and CD68. The percentage of stroma occupied by CD3+ TILs and CD68+ TAMs was scored. TIM3 and LAG3 were enumerated per

HPF. PD-L1 was evaluated by CPS score. Staining within a 40x field of tumor cells was scored. Patient age, sex, disease progression, pathologic stage, and treatment response were also reviewed.

Results: Sixty-four cases were examined, including 3 well-differentiated, 26 moderately-differentiated, 21 poorly-differentiated PDACs, and 14 PDACs that were treated with neoadjuvant therapy prior to surgery. CD3+ TILs were found to be relatively sparse in each of these groups, ranging from <5% to 20% of the tumor stroma, and with a trend toward fewer TILs with increasing grade. TIM3 and LAG3 were consistently expressed in a subset of TILs. Nearly all cases were negative for PD-L1 (CPS <1). CD68+ TAMs were consistently found in the tumor stroma, ranging from 5-40%, and with a trend toward greater TAMs with increasing grade. Of note, a sarcomatoid PDAC had about 70% CD68+ TAMs within the stroma.

Conclusions: These observations support the concept of TAMs promoting a tumorigenic immune environment for PDACs. The relative lack of TILs in PDAC potentially explains the general failure of current immunotherapies, although the presence of TIM3 and LAG3 on TILs reveals additional potential targets for immunotherapy.

1672 Screening of NTRK fusions in pancreatic ductal adenocarcinomas by immunohistochemistry and comparison with NGS

Prashant Bavi[1], Amy Zhang[2], Gun-Ho Jang[2], Robert Denroche[2], Ilinca Lungu[2], John Bartlett[2], Julie Wilson[2], Stefano Serra[3], Sandra Fischer[4], Grainne O'Kane[3], Jennifer Knox[5], Steven Gallinger[6]
[1]University of Toronto, Toronto, ON, [2]Ontario Institute for Cancer Research, Toronto, ON, [3]University Health Network, University of Toronto, Toronto, ON, [4]University Health Network, Toronto, ON, [5]University Health Network Medical Oncology, Toronto, ON, [6]University Health Network and Mount Sinai Hospital University of Toronto, Toronto, ON

Disclosures: Prashant Bavi: None; Amy Zhang: None; Gun-Ho Jang: None; Robert Denroche: None; Ilinca Lungu: None; John Bartlett: None; Julie Wilson: None; Stefano Serra: None; Grainne O'Kane: None; Jennifer Knox: None; Steven Gallinger: None

Background: The neurotrophic receptor kinase (NTRK) family includes three oncogenes (NTRK 1-3) that code for the Trk-family proteins (TrkA/B and C), are implicated in neuronal homeostasis. Clinical trials with TRK inhibitors in patients whose tumors harbor NTRK gene fusions, independent of histology type, have shown good results. However, there is no comprehensive data on prevalence of NTRK fusions and its expression in pancreatic ductal adenocarcinomas (PDACs), a lethal malignancy that has a dismal 5-year overall survival outcome of ~ 6-8%.

Design: PDAC samples with available RNAseq and WGS data were screened for NTRK fusions (Figure1). Fusion predictions were performed separately using 2 RNA seq based callers and 2 DNA based callers. We filtered for fusions detected by at least one RNA based caller and one DNA or two RNA based caller, generating a final list of potential fusions for downstream analyses (Figure 2). Immunohistochemistry (IHC) was also performed on a well characterized TMA cohort of 167 PDACs using a pan-Trk monoclonal antibody (mAb)clone EPR17341 (Abcam, Cambridge, MA) to detect Trk A/B/C expression. Fetal brain and ganglion cells served as a positive external control.

Results: We found two predicted NTRK3 fusions and the fusion partners were EML4 and KANK1. No NTRK1 and NTRK2 fusion were detected. Interestingly, PDAC with EML4-NTRK3 fusion, a previously reported oncogenic driver fusion, had a KRAS wild type tumour. NTRK IHC expression was negative in 130 PDACs; 37 cases were noninformative (TMA). High Ntrk gene expression was seen in 18 cases but without corresponding IHC expression in the TMA cores and further validation is being done on big sections for these 18 cases. Unfortunately, for the 2 cases with identified NTRK gene fusions, we are trying to procure FFPE tissue from our collaborators. IHC analysis of negative Pan-Trk IHC was concordant with RNAseq testing.

Figure 1 - 1672

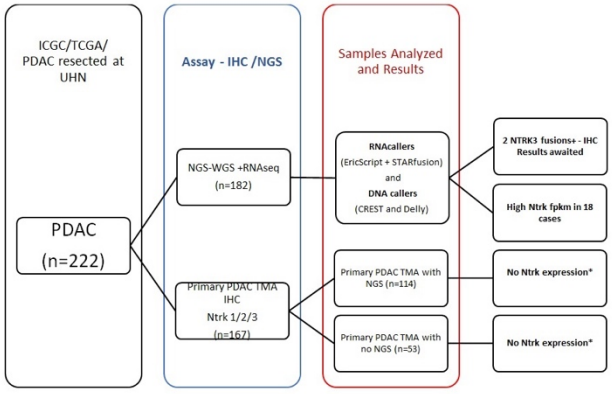

Figure 1. Study design of investigating NTRK fusion (NGS) and IHC expression in PDAC; PDAC: pancreatic ductal adenocarcinoma; Ntrk: neurotrophic receptor kinase; IHC: Immunohistochemistry; TMA: tissue microarrays; * 37 cases were non informative for IHC

Figure 2 - 1672

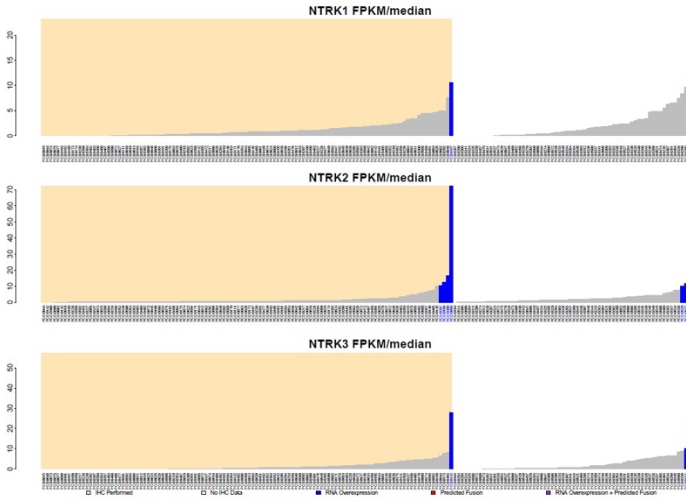

Figure 2. NTRK gene overexpression defined as 10x fold change over median fpkm, predicated fusions.

Conclusions: In this study we confirm the rarity of NTRK gene fusions and panTrk protein expression in both primary resected PDACs (< 1%), in concordance with earlier reports in GI tumors. IHC can be a reliable, quick, specific screening assay that can detect NTRK fusions. Therefore, detecting oncogenic fusions involving NTRK1-3 through a companion IHC diagnostic assay in conjunction with NGS is valuable to identify and elicit a potential therapeutic response in the rare PDAC harboring these alterations.

1673 Integrative Clinical Genomic Analysis of Advanced Pancreatic Adenocarcinoma: New Targets and Biomarkers

Shaham Beg[1], Kenneth Eng[2], Rohan Bareja[3], Ahmed Mohamed Kamal Ibrahim Halima[1], Evan Fernandez[1], Jose Jessurun[4], Rema Rao[5], David Wilkes[1], Sung-Suk Chae[1], John Stahl[6], Zenta Walther[6], Kimberly Johung[6], Terra McNary[1], Wei Song[7], Brian Robinson[1], Himisha Beltran[8], Allyson Ocean[1], Olivier Elemento[8], Andrea Sboner[1], Juan Miguel Mosquera[1]
[1]Weill Cornell Medicine, New York, NY, [2]Englander Institute for Precision Medicine, Brooklyn, NY, [3]Englander Institute for Precision Medicine, New York, NY, [4]New York Presbyterian Hospital, New York, NY, [5]New York-Presbyterian/Weill Cornell Medical Center, New York, NY, [6]Yale University School of Medicine, New Haven, CT, [7]Weill Cornell Medical College, Short Hills, NJ, [8]New York, NY

Disclosures: Shaham Beg: None; Kenneth Eng: None; Rohan Bareja: None; Ahmed Mohamed Kamal Ibrahim Halima: None; Evan Fernandez: None; Jose Jessurun: None; Rema Rao: None; Sung-Suk Chae: None; John Stahl: None; Zenta Walther: None; Kimberly Johung: None; Terra McNary: None; Wei Song: None; Brian Robinson: None; Olivier Elemento: None; Andrea Sboner: None; Juan Miguel Mosquera: None

Background: Despite surgery, chemotherapy and radiation therapy, pancreatic adenocarcinoma (PADC) has a dismal prognosis with ~1 year mean overall survival after diagnosis. Tumor mutational burden (TMB) and microsatellite instability (MSI) are biomarkers for immunotherapy and prognosis. Previously, recurrent *NRG1* Fusions in *KRAS* Wild-Type PADC have been described. Here we highlight findings of TMB and MSI status and transcriptome analysis of PADC with emphasis on patients with advanced disease.

Design: We studied 41 samples (31 metastatic and 10 primary) from 37 patients with advanced PADC. Whole-exome sequencing (WES) with algorithms to determine TMB and MSI status, and RNA-seq were performed as part of our NGS-based clinical trial. Tumor organoid development was attempted in 12 cases with available fresh tissue. Clinico-pathologic and molecular findings were correlated.

Results: All 31 metastatic and 10 primary tumors were microsatellite stable. MSIsensor score ranged from 0.00 to 0.93 (cut-off for MSI-H is ≥5). In a subset of patients, IHC was also performed and matched MSIsensor results. TMB ranged from 0.027 to 42.13 mutations/megabase (cut-off for high TMB ≥10). 4/41 (9.7%) samples from 2 patients showed high TMB, two metastases & 1 primary (one patient) and one primary (another patient). Both patients had long-term survival (12 years and 3 years, respectively). Total RNA-seq identified actionable genes with outlier expression levels in 14/25 (56%) interrogated patient samples. Common outliers included *CPS1, CDKN2A, ALDH2, ATIC, HDAC7, PDGFRB, PTPN6*. Further, 35 non-recurrent gene fusions were detected in 13/25 (52%) tumors including a potentially targetable *KDM4C-JAK2* fusion. We were able to successfully establish patient-derived tumor organoids in 3 patients and multi-drug sensitivity testing is in progress.

Conclusions: Although MSI-H has been reported in PADC (0-22% range), we did not find microsatellite instability in any of our primary or metastatic tumors. A high TMB was associated with significantly longer survival (up to 12 years in one case), consistent with the reported favorable prognosis for other solid tumors with this molecular feature. Transcriptome analysis of PADC revealed potential therapeutic targets, *i.e.* gene fusions and RNA-outliers. Ongoing functional validation and *ex vivo* testing of tumor organoids will determine if these findings could potentially be extrapolated to the clinical setting

1674 SATB2 Expression in Primary Pancreatobiliary and Gastrointestinal Neoplasms

Simona De Michele[1], Stephen Lagana[2], Susan Hsiao[3], Helen Remotti[4]
[1]New York-Presbyterian/Columbia University Medical Center, New York, NY, [2]New York, NY, [3]New York-Presbyterian/Columbia University Medical Center, Flushing, NY, [4]Columbia University Medical Center, Dobbs Ferry, NY

Disclosures: Simona De Michele: None; Stephen Lagana: None; Susan Hsiao: None; Helen Remotti: None

Background: SATB2 (special AT-rich binding protein 2) is involved in transcription regulation and chromatin remodeling. In the gastrointestinal tract, high levels of SATB2 are restricted to normal epithelial cells of the colon, rectum and appendix, and not seen in the small bowel (SB), stomach, or pancreatobiliary tract. SATB2 immunohistochemistry (IHC) has showed high sensitivity and specificity as a marker of primary and metastatic colorectal cancer (CRC). To date SATB2 expression has been noted in a small portion of gastric and SB adenocarcinomas (ADCA). The literature provides limited data on SATB2 expression in pancreatobiliary neoplasms (PBNs), particularly with respect to cholangiocarcinomas (CC), including intrahepatic (I-CC), hilar (H-CC) and distal (D-CC) sites. In this study we assessed SATB2 expression in a large cohort of PBNs in addition to gastric, SB and ampullary (AMP) ADCAs and compared the results to expression in colonic adenocarcinomas (CRC).

Design: Immunostaining for SATB2 (clone EP281) was performed in tissue microarrays (TMAs) of 166 cases of PBNs including 34 intraductal papillary mucinous neoplasms (IPMNs), 19 pancreatic ADCA, 113 CC (41 I-CC, 36 H-CC and 36 D-CC), in addition to 51 gastric, 17 SB, 43 AMP, and 46 CRC. SATB2 expression was evaluated in each case by two pathologists independently (100% concordance). A positive result was considered >5% nuclear staining. For positive cases, the percent of tumor staining varied from 5% to 70% in non-CRC cases and from 5% to >95% in CRC cases.

Results: Among all PBNs only 2 CC cases showed positivity for SATB2; 6/51 (12%) gastric ADCAs, 5/17 (29%) SB ADCAs, 2/43 (4%) of AMP ADCAs and 40/46 (87%) of CRCs were SATB2 positive. All pancreatic ADCA and IPMNs were negative for SATB2.

Tumor type	SATB2+	
IPMNs	0/34	(0%)
Pancreatic ADCA	0/19	(0%)
D-CC	1/36	(3%)
I-CC	0/41	(0%)
H-CC	1/36	(3%)
PBN (total)	2/166	(1%)
SB ADCA	5/17	(29%)
AMP ADCA	2/43	(4%)
Gastric ADCA	6/51	(12%)
CRC	40/46	(87%)

Conclusions: SATB2 expression by IHC may strongly favor CRC, in evaluating ADCAs of uncertain primary site. It is important to note that SATB2 may be expressed in other primary ADCAs (including 29% of SB, 12% of stomach, 4% of ampullary, 1.8% of CC) and these sites should also be considered in the differential diagnosis of SATB2 positive tumors.

1675 Rb-Inactivated Pancreatic Ductal Adenocarcinoma

Craig Dunseth[1], Rondell Graham[2], Andrew Bellizzi[3]
[1]Coralville, IA, [2]Mayo Clinic, Rochester, MN, [3]University of Iowa Hospitals and Clinics, Iowa City, IA

Disclosures: Craig Dunseth: None; Rondell Graham: None; Andrew Bellizzi: None

Background: A few years ago we encountered a woman with adenocarcinoma in the peritoneum with concurrent masses in the cervix and pancreas. p16 immunohistochemistry (IHC) was strongly positive. We could find no such report in pancreatic ductal adenocarcinoma (PDA), and, thus, favored tumor to be of cervical origin. This case spurred us to screen a large cohort of PDAs with p16 IHC. We found that 5% of 345 PDAs had p16 H-scores between 200-300, which we termed the "highly expressing pattern" (*Mod Pathol*. 2017;30(Suppl2):443A). We speculated this reflected Rb-inactivation due to a genetic (rather than viral oncogenic) mechanism but lacked the tools to further pursue this. We subsequently validated Rb IHC, which we now routinely use to distinguish spindle cell lipoma/genetically related tumors from histologic mimics and, more importantly, to distinguish poorly differentiated neuroendocrine carcinoma from non-neuroendocrine carcinoma and grade 3 well-differentiated neuroendocrine tumor.

Design: We performed total Rb protein (clone G3-245; 1:100) IHC on whole sections of 11 tumors from our previous series that demonstrated p16 H-scores >200, as well as 15 cases with H-scores <200. Rb IHC expression was assessed as intact (any tumor staining) or lost (complete absence of staining in the presence of internal control). We performed fluorescence in situ hybridization (FISH) for *RB1* and the enumeration probe *LAMP1* on 8 cases with lost and 5 cases with intact Rb IHC. Rb-inactivated tumors were assessed for any distinctive histologic features (e.g., grade, tumor type, prominent tumor-associated lymphoid stroma).

Results: Eight cases demonstrated Rb IHC loss (all with p16 H-scores >/=278); all other cases demonstrated intact Rb IHC. Rb IHC-deficient tumors showed relative or absolute loss of *RB1* in 4 cases; possible *RB1* amplification in 2; and normal FISH results in 1; 1 case failed to hybridize. Of the 5 Rb IHC-intact cases, 4 showed normal FISH and 1 trisomy/tetrasomy. Rb-inactivated cases showed no distinctive histologic features. Two cases with adjacent high-grade PanIN also showed Rb IHC loss in the PanIN (see Figure). Results of cases with concurrent FISH are summarized in the Table.

Case ID	p16 IHC H-score	Rb IHC Result	*RB1*/*LAMP1* FISH Result	*RB1* FISH Interpretation
A	300	Lost	1 *RB1* and 1 *LAMP1*signal	*RB1* LOH
B	300	Lost	1-4 *RB1* and 2-6 *LAMP1* signals	*RB1* relative loss
C	300	Lost	1-4 *RB1* and 3-6 *LAMP1* signals	*RB1* relative loss
D	300	Lost	1-3 *RB1* and 2-5 *LAMP1* signals	*RB1* relative loss
E	300	Lost	4-15 *RB1* and 1-6 *LAMP1* signals	Possible *RB1* amplification
F	300	Lost	4-15 *RB1* and 1-4 *LAMP1* signals	Possible *RB1* amplification
G	300	Lost	2 *RB1* and 2 *LAMP1* signals	Normal
H	278	Lost	Failed to hybridize	Failed to hybridize
I	175	Intact	2 *RB1* and 2 *LAMP1* signals	Normal
J	2	Intact	2 *RB1* and 2 *LAMP1* signals	Normal
K	0	Intact	2 *RB1* and 2 *LAMP1* signals	Normal
L	0	Intact	2 *RB1* and 2 *LAMP1* signals	Normal
M	10	Intact	3-4 *RB1* and 3-4 *LAMP1* signals	Trisomy/tetrasomy

Figure 1 - 1675

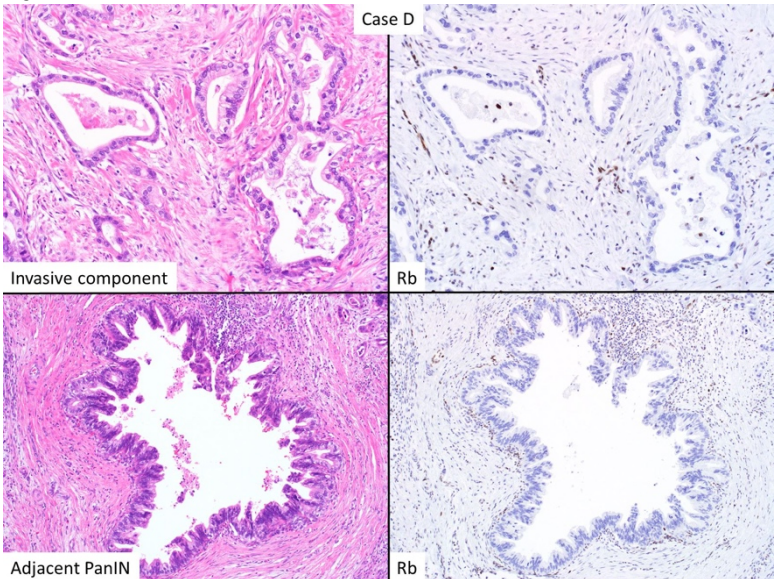

Conclusions: In rare PDAs, diffuse, strong p16 expression is attributable to Rb-inactivation, as demonstrated by IHC and FISH results. We are currently performing *RB1* sequencing. Biallelic *RB1* inactivation, though the genetic hallmark of small cell lung carcinoma, may rarely be seen in PDA.

1676 Characterizing the Cytotoxic Lymphocyte Antigen-4 (CTLA-4) or Programmed Cell Death Ligand 1 (PD-L1) Expression Landscape in Gallbladder Carcinoma: implications for treatment

David Escobar[1], Jessica Nguyen[2], Jennifer Pincus[3], Guang-Yu Yang[4], Maryam Pezhouh[2]
[1]McGaw Medical Center of Northwestern University, Chicago, IL, [2]Northwestern University Feinberg School of Medicine, Chicago, IL, [3]Northwestern Memorial Hospital, Chicago, IL, [4]Northwestern University, Chicago, IL

Disclosures: David Escobar: None; Jessica Nguyen: None; Jennifer Pincus: None; Guang-Yu Yang: None; Maryam Pezhouh: None

Background: Gallbladder carcinomas (GCs) are aggressive cancers of the biliary tree which usually present at advanced stage with limited therapeutic options. Current modalities include surgical resection followed by cytotoxic chemotherapy; however, metastatic rates and local recurrence rates are high, with poor overall survival. Immune checkpoint inhibitors, including anti-CTLA-4 and anti-PD-1 agents, have shown effectiveness against many high-grade malignancies, but the expression of CTLA-4 and PD-L1 in GC tumor cells (TCs) and associated tumor infiltrating lymphocytes (TILs) has not yet been fully explored

Design: We searched our pathology database and identified 22 cases of GCs. A group of chronic cholecystitis cases was included as a control group. PD-L1 and CTLA-4 expression were assessed in both TCs and TILs. CTLA-4 immunolabeling was quantified and scored by extent (1= >1%, 2= >25%, 3= >50% and 4= >75%) and intensity (0= none, 1= weak, 2= moderate, 3= strong). A composite score (CS) was computed by multiplying extent and intensity scores. PD-L1 expression was scored at the following cut-offs: 0= 0%, 1= >1%, 2= >10%, 3= >25%, and 4= >50%.

Results: Thirteen GCs (59%) expressed PD-L1 in TCs, of which five were score 2 or higher (5/22, 23%). One case, a poorly differentiated adenocarcinoma with signet ring features, showed score 4 PD-L1 expression (80% in TCs). Eighteen GCs (82%) showed PD-L1 expression in TILs, of which eleven were score 2 or higher (11/22, 50%). In comparison, only 40% of controls showed scattered PD-L1 expression in TILs, with none showing PD-L1 expression higher than 5% (score 1 or less) of TILs (p=0.0024). Five GCs (23%) expressed CTLA-4 in TCs, with an average composite score of 0.82. Nine GCs (41%) showed CTLA-4 expression in TILs, with an average composite score of 0.50. In comparison, CTLA-4 was not expressed in lymphocytes in controls (CS = 0) (p=0.043). Carcinoma subtype, histologic grade, necrosis, or presence of lymphovascular invasion were not significantly associated with PD-L1 and CTLA-4 expression.

Conclusions: Our results indicate that PD-L1 and CTLA-4 is expressed in GCs at an increased rate compared to controls. This suggests a potential target for immune-modulation therapy for patients with gallbladder carcinomas. Analysis of additional cases with long-term follow-ups is underway to further evaluate the role of PD-L1/CTLA-4 expression in GCs as a prognostic marker.

1677 Differences in histology, molecular features and cancer pathway between two types of intraductal papillary neoplasm of the bile duct

Yuki Fukumura[1], Reiko Doi[2], Hiroko Onagi[3], Momoko Tonosaki[2], Ayako Ura[2], Tsuyoshi Saito[4], Yuko Kinowaki[5], Masaru Takase[6], Takashi Yao[7]
[1]Juntendo University, Tokyo, Tokyo, Japan, [2]Juntendo University, Bunkyo-ku, Japan, [3]Juntendo University, Bunkyo-ku, Tokyo, Japan, [4]Juntendo University, School of Medicine, Tokyo, Japan, [5]Tokyo Medical and Dental University, Bunkyo-ku, Japan, [6]Koshigaya Municipal Hospital, Koshgaya, Japan, [7]Juntendo University, Tokyo, Japan

Disclosures: Yuki Fukumura: None; Reiko Doi: None; Hiroko Onagi: None; Momoko Tonosaki: None; Ayako Ura: None; Tsuyoshi Saito: None; Yuko Kinowaki: None; Masaru Takase: None; Takashi Yao: None

Background: Intraductal papillary neoplasms of the bile duct is one type of precursor/preinvasive neoplastic lesions of the biliary tract. In the Japan-Korea meetings held in 2017, a recommendation was proposed to classify IPNBs into two types; where type 1 IPNB is histologically similar to intraductal papillary mucinous neoplasms of the pancreas and typically develops in the intrahepatic bile ducts, and type 2 IPNB has more complex histological architecture with irregular papillary branching and typically involves the extrahepatic bile ducts. Herein, we compared histopathological and molecular differences as well as differences in genes of cancer pathway between two types of IPNBs.

Design: Surgically resected IPNB cases including 8 cases of type 1 and 9 cases of type 2 IPNBs were enrolled in this study. Tumor site was intrahepatic for 6 and perihilar for 2 cases of type 1, while all except one intrahepatic case were extrahepatic for type 2. Stromal invasion was seen in 2 cases of type 1 and 8 cases of type 2. As histological evaluation, stalk of the tumor papilla was investigated with CD34 and SMA stains. Loss of smad4 protein was investigated immunohistochemically. Mutational analyses were conducted with Sanger method for *GNAS*, *KRAS*, *RNF43*, and *PIK3CA*. mRNA of 770 cancer pathway genes were quantified with nanostring method.

Results: Different features of type 1 and type2 were (1) the distribution of CD34-positive vessels and the amount of SMA-positive myofibroblasts, (2) Somatic mutation for *KRAS*, *GNAS*, or *RNF43* was observed only in type 1, but not in type 2. (3) By cancer pathway analysis, the amount of mRNA of genes of cell cycle, chromatin remodeling, and DNA repair were different between the two types.

Figure 1 - 1677

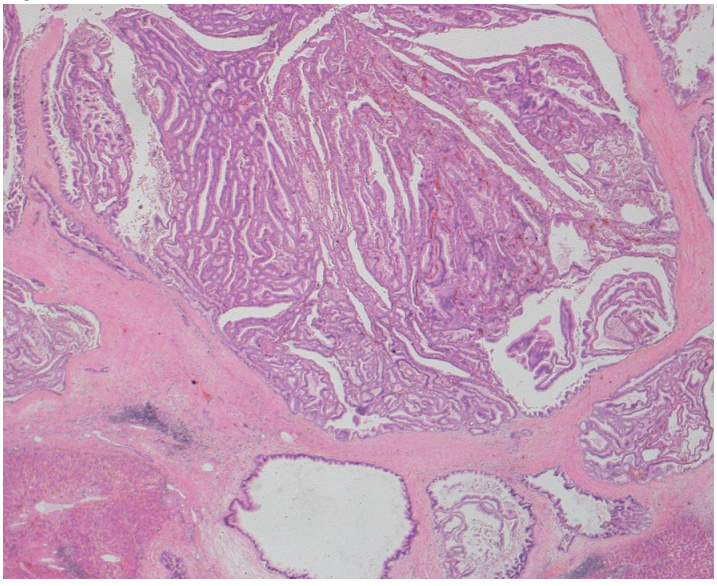

Figure 2 - 1677

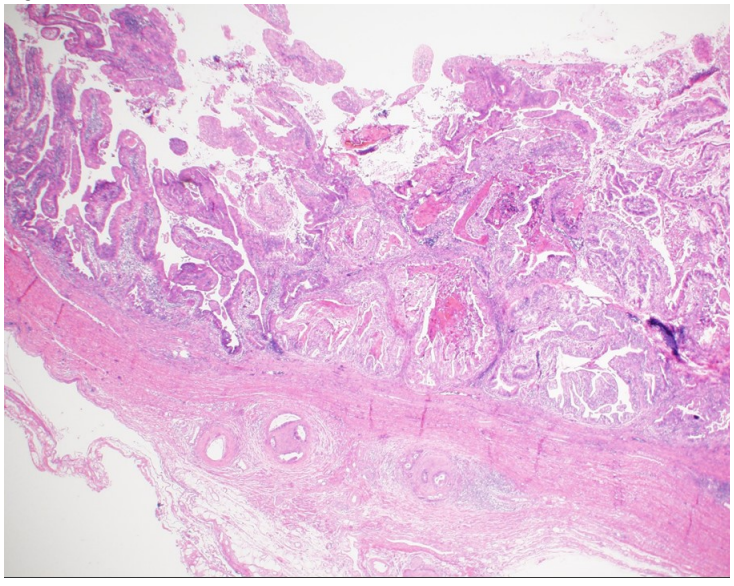

Conclusions: Type 1 and type 2 IPNBs were found to be very different, histologically and molecularly, hence it seems important to study IPNBs by dividing type 1 and type 2.

1678 EBV-Associated Biliary Tumors Frequently Show Typical Cholangiocarcinoma Morphology and Immunoreactivity for PD-L1

Clifton Fulmer[1], Lindsay Alpert[2], Erika Hissong[3], Meredith Pittman[3], John Hart[2], Rhonda Yantiss[4]
[1]Weill Cornell Medicine, New York, NY, [2]University of Chicago, Chicago, IL, [3]New York-Presbyterian/Weill Cornell Medical Center, New York, NY, [4]Weill Cornell Medical College, New York, NY

Disclosures: Clifton Fulmer: None; Lindsay Alpert: None; Erika Hissong: None; Meredith Pittman: None; John Hart: None; Rhonda Yantiss: None

Background: Cholangiocarcinomas account for 3% of all gastrointestinal malignancies and tend to have a poor prognosis. We have recently encountered a handful of EBV-positive tumors and found them to strongly express PD-L1, a marker used in other sites to evaluate patients for potential checkpoint inhibitor therapy. We performed this study to assess the prevalence of EBV-associated carcinomas among biliary tumors and evaluate them for PD-L1 staining compared with EBV-negative tumors.

Design: We identified 122 cholangiocarcinomas diagnosed during a 10-year period, including 61 biopsy and 61 resection specimens. All cases were subjected to *in situ* hybridization for EBV-encoded RNAs (EBER) and PD-L1 immunostains. EBV-negative tumors with a CPS>1 for PD-L1 were also stained with MLH1, PMS2, MSH2, and MSH6. Results of PD-L1 immunohistochemistry were assessed with respect to EBV and mismatch repair status.

Results: The clinical features are summarized in Table 1. Strong, diffuse EBER signal was detected in 7 (6%) tumors. Four (57%) showed solid growth or single infiltrating cells with a marked lymphoplasmacytic infiltrate (Figure 1), and 3 (43%) contained infiltrative glands, sclerotic stroma, and occasional peritumoral lymphoid aggregates (Figure 2). Ten (8%) equivocal cases showed weak to moderate signal in a minority of tumor cells; none of these displayed lymphoepitheliomatous histology, but 40% contained intratumoral lymphocytes and 60% featured peritumoral lymphoid aggregates. Overall, 46 (38%) cholangiocarcinomas were positive for PD-L1 (mean CPS: 25), including all EBV-positive tumors (mean CPS: 50), 80% of cases with equivocal EBER signal (mean CPS: 18), and both tumors with loss of MLH1/PMS2 staining (Mean CPS: 60). In contrast, 30% of EBV-negative tumors were positive for PD-L1 (mean CPS: 23). The differences between EBV-positive and EBV-/MMR-proficient tumors were statistically significant ($p<0.05$). Cases with equivocal EBER staining showed more frequent PD-L1 positivity than EBV-/MMR-proficient tumors ($p<0.05$).

Clinicopathologic Features of Cholangiocarcinoma					
		EBV-positive (n=7)	EBV-equivocal (n=10)	Mismatch Repair-Defificient (n=2)	Misatch Repair Proficient/EBV-negative (n=29)
	Sex Ratio (M:F)	2:5	5:5	0:2	20:9
	Age (Mean)	46	63	66	68
Location	Intrahepatic (n=60)	5	5	2	16
	Hilar/Perhilar (n=35)	2	4	0	3
	Distal (n=27)	0	1	0	10
Ethnicity	Asian (n=11)	2	4	1	4
	Non-Asian (n=37)	5	6	1	25

Figure 1 - 1678

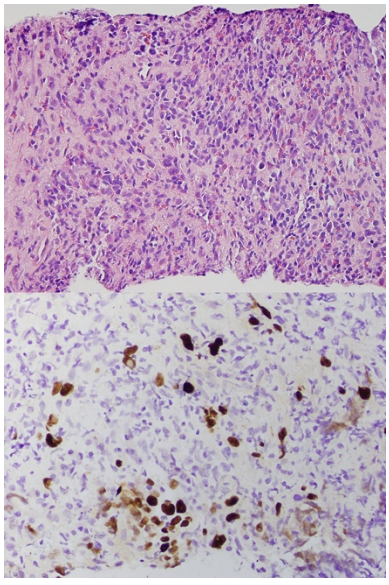

Figure 2 - 1678

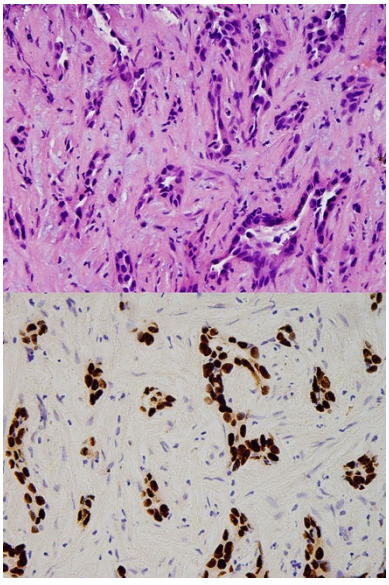

Conclusions: EBV-associated cholangiocarcinomas usually occur in the hilum or within the liver. They can exhibit lymphoepithelioma-like or ductular histology, often with intratumoral lymphocytes and peritumoral lymphoid aggregates. EBV-associated tumors show strong PD-L1 immunoreactivity comparable to that seen in MMR-deficient carcinomas. Even tumors with equivocal EBER ISH results show more frequent PD-L1 positivity than MMR-proficient, EBV-negative carcinomas ($p<0.05$).

1679 The Interleukin 21 (IL21) – receptor (IL21R) axis is associated with a poor survival of pancreatic cancer patients

Matthias Gaida[1], Peter Schirmacher[2], Alica Linnebacher[3], Philipp Mayer[4], Frank Bergmann[1], Thilo Hackert[1]
[1]University of Heidelberg, Heidelberg, Germany, [2]Institute of Pathology, Heidelberg University Hospital, Heidelberg, Germany, [3]Ruprecht-Karls-University Heidelberg, Heidelberg, Germany, [4]University Hospital Heidelberg, Heidelberg, Germany

Disclosures: Matthias Gaida: None; Peter Schirmacher: None; Philipp Mayer: None

Background: Pancreatic ductal adenocarcinoma (PDAC) displays a marked fibro-inflammatory microenvironment in which infiltrated immune cells often fail to eliminate the tumor cells but paradoxically can even promote tumor progression due their cytokines. The role of the T cell cytokine IL21 in PDAC is unknown.

Design: A PDAC tissue microarray (n=264 patients) was created and stained with antibodies for CD3, IL21, IL21R, and Blimp1 followed by multivariate analysis. Pancreatic cancer cell lines (AsPC1, BxPC3, Panc1) were stimulated with IL21, followed by Western blot analysis for downstream products pERK, pp38, pSTAT3, and Blimp1. IL21 stimulated cells were used for wound healing assays and invasion assays. Furthermore incubation of tumor cells with IL21 and clinically used chemotherapeutic agent Gemcitabine was performed, as were colony formation assays.

Results: All tested PDAC samples were infiltrated by CD3-IL21+ T cells. The tumor cells showed an expression of IL21R (221/264) and the downstream factor Blimp1 (199/264), expression of which was significantly associated with poor patient survival. In vitro, IL21 activated ERK- and STAT3 pathways and upregulated the transcription factor Blimp1, whereas the p38 MAPK pathway was not involved. Functionally, a significantly higher PDAC cell invasivity was seen, as was an increased tumor cell migration, colony formation, and resistance to the chemotherapeutic agent Gemcitabine.

Conclusions: The IL21-IL21R axis in PDAC is associated with poor patient survival and promotes invasivity and chemoresistance.

1680 The Spectrum of Ampulla of Vater Biopsy Findings and Discrepancies in Followup Specimens: 10 Year Review of 318 Cases

Denise Gamble[1], Wendy Frankel[2], Christina Arnold[2], Martha Yearsley[2], Wei Chen[2]
[1]The Ohio State University, Columbus, OH, [2]The Ohio State University Wexner Medical Center, Columbus, OH

Disclosures: Denise Gamble: None; Wendy Frankel: None; Christina Arnold: None; Martha Yearsley: None; Wei Chen: None

Background: Biopsies from the ampulla of Vater are challenging due to poor specimen sampling, small size, and interventional artifacts. We examined the initial and subsequent ampulla of Vater samples to determine the discrepancy rates.

Design: We retrospectively reviewed 318 ampulla of Vater biopsy specimens from 252 patients over a 10-year period. Clinical indications for endoscopy and pathologic diagnosis were noted. The biopsy findings were compared to those in subsequent resection specimens (pancreaticoduodenectomies and 1 ileal resection).

Results: Of the 318 biopsy cases, 96 were diagnosed as low-grade adenomas, 8 high-grade adenomas, 20 adenocarcinomas, and 5 other carcinomas/tumors, including well differentiated neuroendocrine tumors (2), high-grade neuroendocrine carcinomas (2), and metastatic squamous cell carcinoma of the cervix (1). Of the 90 cases with follow-up specimens, 55 cases (61%) had concordant results and 35 (39%) were discordant. 29% (10) of the discordant cases had major discrepancies (benign biopsy diagnosis with malignant resection diagnosis); all likely due to sampling issues. The benign diagnoses included ulcer and acute inflammation (4), reactive changes (6), rare atypical cells (1), and adenoma/low-grade dysplasia (1). The most common malignancy found on resection was adenocarcinoma (ampullary - 13, distal bile duct - 6, pancreatic - 1). 71% (25) of the discordant cases had minor discrepancies (normal, reactive, atypical, and dysplastic).

Conclusions: We found that 11% (10/90) of benign ampullary biopsies with followup resection contained malignancy, likely secondary to sampling issues. Careful correlation with endoscopic and imaging findings is necessary. When malignancy is suspected clinically, additional sampling may be helpful.

1681 Tumor-insular Complex in Neoadjuvant Treated Pancreatic Ductal Adenocarcinoma is Associated with Higher Residual Tumor

Iván González[1], Greg Williams[2], Esther Lu[3], William Hawkins[1], Deyali Chatterjee[2]
[1]Washington University School of Medicine, St. Louis, MO, [2]Washington University, St. Louis, MO, [3]St. Louis, MO

Disclosures: Iván González: None; Greg Williams: None; Esther Lu: None; William Hawkins: None; Deyali Chatterjee: None

Background: In recent years, the role of the tumor stroma in pancreatic ductal adenocarcinoma (PDAC) has gained recognition as playing a vital role in treatment resistance, tumor progression and clinical outcome. This is shedding new light on the intimate association of the tumor cells and supporting tissues. Here, we describe an unusual pathologic feature involving neoplastic and non-neoplastic cells that appears in a subset of PDAC tumors, particularly when patients have received neoadjuvant therapy (PDAC-NAT). The tumor cells show intimate association with non-neoplastic islet cells to form characteristic structures which appear to recapitulate ducto-insular complexes, therefore we have named this as tumor-insular complexes (TIC). We further investigate the clinical significance of the appearance of these TICs in PDAC-NAT, and discuss the implications on prognosis and survival.

Design: Archival slides of 84 resections of PDAC-NAT were retrospectively identified. Diagnostic features for identification of TIC (Fig-1) were established. Slides were reviewed independently by two pathologists to assess the percentage of residual tumor (%RT) and TIC. An arbitrary cut-off of >10% tumor cells involved in TICs was used for classifying the cases positive for this feature. TIC was compared to multiple clinicopathologic prognostic parameters, including two newly established parameters: treatment response groups (TRG) 0 and 1 (RT <5% and =>5% respectively), and residual tumor index (RTI).

Results: The mean age at presentation was 64 years (M:F=1:0.9). Perineural invasion (PNI) and lymphovascular invasion was noted in 76% and 46% of the cases respectively. The mean values of tumor bed size (TBS) was 2.6 cm, %RT = 38%, and RTI = 1.1. 15 and 69 cases belonged to TRG 0 and 1 respectively. TIC was significantly associated with PNI (p=0.002), TBS (p=0.04), %RT (p=0.011), RTI

(p=0.004), lymph node involvement (p=0.03), and TRG (p=0.016). The clinicopathologic characteristics and associations are summarized in Table-1.

Table-1. Patient and Tumor Characteristics		
	N = 84	
Gender		
Male	41, 48.8%	
Female	43, 51.2%	
Age at diagnosis (mean, SD)	64.03 years, 10.2	
Race		
Caucasian	76, 90.5%	
African American	8, 9.5%	
BMI (mean, SD)	26.9, 5.7	
Neoadjuvant radiation	84, 100%	
Neoadjuvant chemotherapy		
FOLFIRINOX	40, 47.6%	
Gemcitabine + Abraxane	17, 20.2%	
Gemcitabine	22, 26.2%	
FOLFOX	3, 3.6%	
Unknown	2, 2.4%	
Surgical procedure		
Standard	51, 60.7%	
Pylorus sparing	19, 22.6%	
WATSA	9, 10.7%	
Total pancreatectomy	5, 6.0%	
Tumor differentiation		
Well	3, 3.5%	
Moderate	45, 53.6%	
Poorly	36, 42.9%	
Tumor-insular Complex		
Present	28, 33.3%	
Absent	56, 66.7%	
Lymphovascular invasion	39, 46.4%	
Perineural invasion	64, 76.2%	
Resection margin status		
Negative	47, 56.0%	
Positive	37, 44.0%	
Positive margin location		
Uncinate	14, 28.0%	
Portal vein groove	23, 46.0%	
Neck	5, 10.0%	
Common bile duct	1, 2.0%	
Posterior	5,10.0%	
Other	2, 4.0%	
Tumor bed size (mean, SD)	2.6 cm, 0.91	
Percentage of residual tumor (mean, SD)	38%, 27	
RTI (mean, SD)	1.1, 0.91	
Pathologic T stage		
T1a	4, 4.8%	
T1c	23, 27.4%	
T2	51, 60.7%	
T3	5, 5.9%	
No define mass identified	1, 1.2%	
Pathologic N stage		
N0	41, 48.9%	
N1	26, 30.9%	
N2	17, 20.2%	
Number of lymph nodes involved (mean, SD)	2.02, 3.1	
Pathologic AJCC stage		
IA	6, 7.1%	
IB	5, 6.0%	
IIA	29, 34.5%	
IIB	43, 51.2%	
IV	1, 1.2%	
Treatment response group		
0	15, 17.9%	
1	69, 82.1%	
	Frequency TIC	*P*
Tumor differentiation		
Well	0/3	0.6011
Moderate	15/45	
Poorly	13/36	
Lymphovascular invasion	16/39	0.1744
Perineural invasion	27/28	**0.0021**
Tumor bed size (mean, SD)		
Present	2.88 cm, 0.86	**0.0435**
Absent	2.50 cm, 0.91	
Percentage of residual tumor (mean, SD)		
Present	49%, 25	**0.0119**
Absent	33%, 27	
RTI (mean, SD)		

Present	1.38, 0.86	**0.0040**
Absent	0.89, 0.90	
RTI		
? 0.35	3/25	**0.0103**
> 0.35	25/59	
Pathologic T stage		
T1a	0/4	0.1915
T1c	5/23	
T2	21/51	
T3	2/5	
Pathologic N stage		
N0	11/41	0.0542
N1	7/26	
N2	10/17	
Number of lymph nodes involved (mean, SD)		
Present	3.39, 4.13	**0.0332**
Absent	1.34, 2.16	
Treatment response group		
0	1/15	**0.0160**
1	27/69	
Abbreviations: SD - Standard Deviation; BMI - Body Mass Index; FOLFIRINOX - 5 Fluorouracil, Irinotecan, Oxaliplatin, Leucovorin; FOLFOX - 5 Fluorouracil, Oxaliplatin; WATSA - Whipple at Splenic Artery; RTI - Residual Tumor Index; TIC - Tumor-insular Complex.		

Figure 1 - 1681

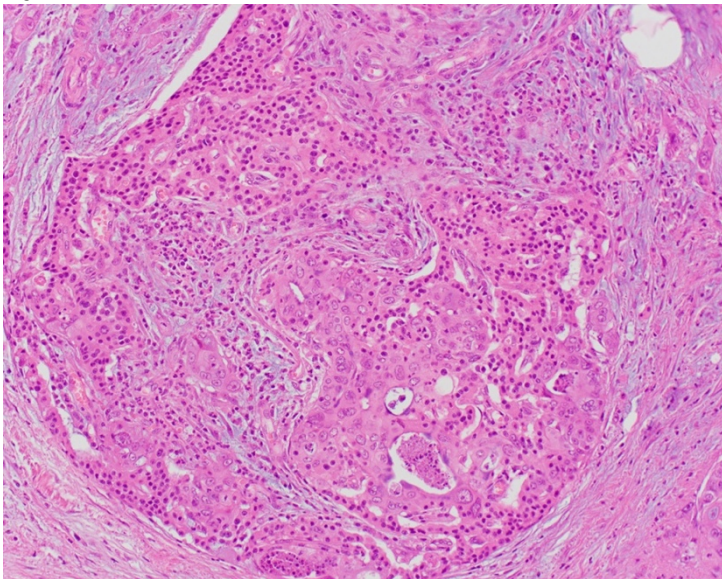

Figure 2 - 1681

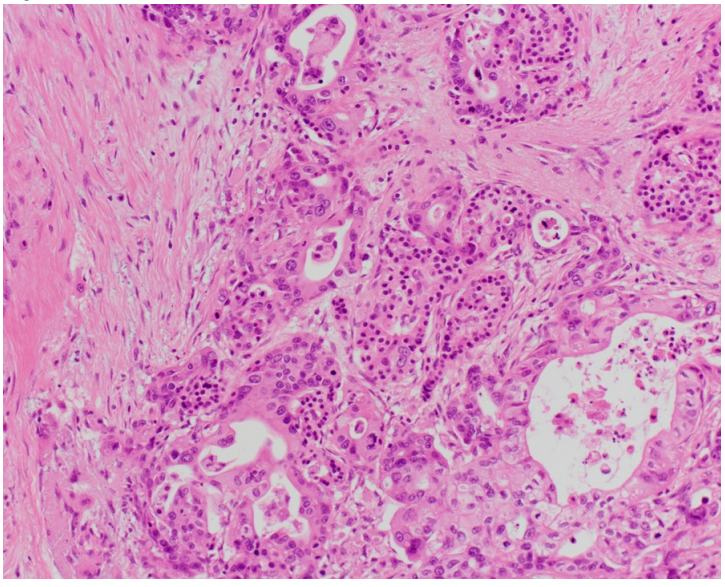

Conclusions: This is the first study describing the phenomenon of TIC, and although the pathogenesis is unknown, it is interesting to note that it is significantly associated with several prognostic pathologic parameters, including an inverse association to treatment response. This suggests that formation of TIC may act as a protective mechanism for tumor cells undergoing NAT. Further studies, especially insights into the molecular mechanisms, will be needed to better understand the biology of TICs.

1682 Performance of DAXX Immunohistochemistry as a Screen for DAXX Mutations in Pancreatic Neuroendocrine Tumors

Jaclyn Hechtman[1], David Klimstra[1], Gouri Nanjangud[1], Denise Frosina[1], Jinru Shia[1], Achim Jungbluth[1]
[1]Memorial Sloan Kettering Cancer Center, New York, NY

Disclosures: Jaclyn Hechtman: None; David Klimstra: *Consultant*, Paige.AI; *Consultant*, Merck; Gouri Nanjangud: None; Denise Frosina: None; Jinru Shia: None; Achim Jungbluth: None

Background: Inactivating *DAXX* mutations are frequent in pancreatic neuroendocrine tumors (PanNETs), are known to cause alternative lengthening of telomeres, and have significant clinical impact including poor prognosis. Many studies have adopted DAXX immunohistochemistry (IHC) as a surrogate for mutation testing, yet in depth studies of *DAXX* mutation-IHC correlation have not been performed.

Design: All PanNETs with MSK-IMPACT next generation sequencing data were interrogated for *DAXX* mutations. All PanNETs with *DAXX* mutations and available material were analyzed for DAXX expression by IHC using mAb clone E94. IHC for DAXX was also

performed on a subset of PanNETs with wild type *DAXX*. Telomere-specific fluorescence in situ hybridization (FISH) was performed in discordant cases to assess presence of alternative lengthening of telomeres (ALT).

Results: 46 of 154 (30%) of PanNETs harbored *DAXX* mutations. *DAXX* mutations were significantly associated with *TSC2* mutations (46% vs. 10%, p=0.0001), and trended with *MEN1* mutations (63% vs 49%, p=0.11), while they trended to be mutually exclusive with *ATRX* mutations (11% vs 25%, p=0.053). Of 27 *DAXX* mutant PanNETs with available material, 23 showed complete loss of DAXX expression on IHC (85.2%). All 4 *DAXX* mutants with retained protein expression harbored WT *ATRX* and had *DAXX* mutations in the last exon, within the SUMO-interacting motif. Telomere-specific FISH demonstrated ALT in all 4 cases. Of 20 PanNETs with wild type *DAXX*, protein expression was retained in 19 cases (95%).

Figure 1. Distibution of *DAXX* mutations across the gene. The first and last regions are SUMO-interaction motifs (SIMs). There are 2 helical segments including the DAXX helix bundle (DHB) domain. Towards the C terminal, the “acidic” region is present, followed by segments rich in Ser/Pro/Glu (SPE) and Ser/Pro/Thr (SPT) residues. Black dots: truncating mutations, green dots: missense mutations, brown dot: in frame indel.

Figure 2. Retained expression of DAXX in a distal *DAXX* mutant pancreatic neuroendocrine tumor with ALT. A) H&E; B) Nuclear retention of DAXX (IHC); C) A nonsense mutation with 72% VAF, signifying LOH; D) Large intranuclear FISH signals (Orange) indicative of ALT (arrows).

DAXX IHC results according to *DAXX* mutation.

DAXX IHC (mAb E94)	AA	NT	Exon	DOMAIN
negative/ lost	Y71*	213C>G	2	DHB
negative/ lost*	Q89*	265C>T	3	DHB
negative/ lost	E116*	346G>T	3	DHB
negative/ lost*	C118*	354C>A	3	DHB
negative/ lost	L146P	437T>C	3	DHB
negative/ lost	H175fs	524_527delACCT	3	
negative/ lost	Q205*	613C>T	3	Helical
negative/ lost	G262C; E466*	784G>T; 1396G>T	3, 5	Helical,
negative/ lost	N280S	839A>G	3	Helical
negative/ lost	N280K	840C>G	3	Helical
negative/ lost*	Q320*; G531R	958C>T; 1591G>A	3, 6	Helical, Helical
negative/ lost	R330*	988C>T	3	Helical
negative/ lost	C350R	1048T>C	3	Helical
negative/ lost*	Q395*	1183C>T	4	Helical
negative/ lost	D419fs	1255delG	4	
negative/ lost*	E466*	1396G>T	5	
negative/ lost	M482_Q483delinsI*	1446_1447delinsAT	5	SPE
negative/ lost	R602Gfs*12	1803delC	6	
negative/ lost	F625Lfs*31	1875_1878delCAAT	6	
negative/ lost	Q650*	1948C>T	6	
negative/ lost*	Y660*	1977-1_1979dupGCTA	6	
negative/ lost	H723Ifs*55	2156delC	7	SPT
medium / retained	E743*	2227G>T	8	SIM
medium/ retained	S749*	2246C>G	8	SIM
medium/ retained	D750fs	2247dupA	8	SIM
medium/ retained	D750V	2249A>T	8	SIM

DHB= DAXX helix bundle, SPE= domain rich in Ser/Pro/Glu residues, SPT= domain rich in Ser/Pro/Thr residues, SIM= sumo-interaction motif
*also tested with clone 25C12 with concordant results

Figure 1 - 1682

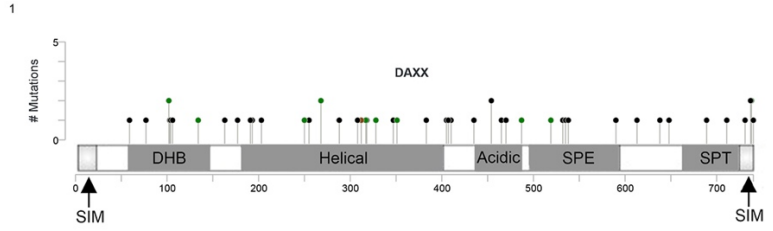

Figure 2 - 1682

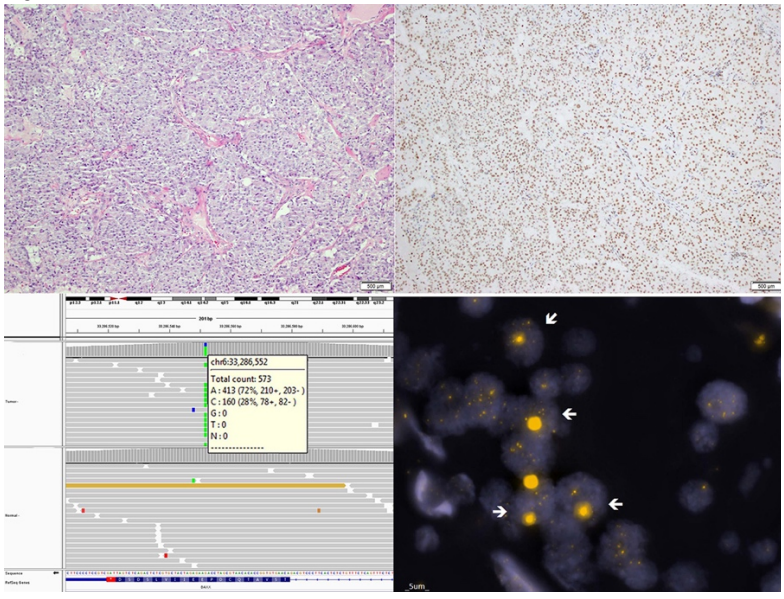

Conclusions: DAXX IHC has a sensitivity of approximately 85% for *DAXX* mutation, and a specificity of 95% in PanNETs. Mutations in the last exon disrupt important functional areas and are associated with ALT even though DAXX expression is retained, likely due to escape of non-mediated decay.

1683 Immunolabeling of Cleared Human Pancreata for Multiple Markers Provides Insights into Pancreatic Anatomy and Pathology

Seung-Mo Hong[1], Michael Noe[2], Tadashi Yoshizawa[3], Matthias Gaida[4], Elizabeth D Thompson[5], Christopher Wolfgang[6], Denis Wirtz[7], Pei-Hsun Wu[7], Braxton Alicia[8], Ashley Keimen[7], Ralph Hruban[3], Laura Wood[5]
[1]Asan Medical Center, Songpa-gu, Korea, Republic of South Korea, [2]Johns Hopkins School of Medicine, Baltimore, MD, [3]Johns Hopkins Medical Institutions, Baltimore, MD, [4]University of Heidelberg, Heidelberg, Germany, [5]Johns Hopkins Hospital, Baltimore, MD, [6]Johns Hopkins University School of Medicine, Baltimore, MD, [7]Johns Hopkins University, Baltimore, MD, [8]Johns Hopkins Medicine, Baltimore, MD

Disclosures: Seung-Mo Hong: None; Michael Noe: None; Tadashi Yoshizawa: None; Matthias Gaida: None; Elizabeth D Thompson: None; Ralph Hruban: None; Laura Wood: None

Background: Advances in tissue clearing and in microscopy have opened human pathologies to study in 3-dimensions (3D). It has been previously shown that even densely fibrotic human pancreatic pathology can be studied in 3D using these techniques and labeling with a single antibody. Here we defined the expression of multiple markers in 3D cleared human pancreas pathology.

Design: Thick slabs (up to 7 mm) of tissue from 22 normal pancreata and 6 ductal adenocarcinomas were harvested from surgically resected human pancreata and then cleared and immunolabeled with antibodies, from different species, against cytokeratin 19, p53, and desmin. To facilitate the penetration of antibodies into dense pancreatic parenchyma, gradually increasing antibody concentrations, centrifugal flow and/or sonication were used. Immunolabeled 3D tissues were visualized using both light sheet and confocal laser scanning microscopies.

Results: Co-labeling with cytoskeleton 19 and p53 overcame the problem of definitively identifying neoplastic cells, as the cells of the invasive carcinoma, when *TP53* mutated, co-expressed p53 (nuclear) and cytoskeleton 19 (cytoplasmic), while non-neoplastic epithelial cells only expressed cytokeratin 19. Previous studies utilizing only a single antibody relied on autofluorescence to identify vessels. Here, the combination of labeling for CK19 and desmin lead to the easy identification of venous invasion. These foci were characterized in 3D as cords of neoplastic cells that tracked along and then penetrated into the lumina of the veins. Once inside of the lumina the neoplastic cells formed tubes that lined the vascular wall and extended further along the vein.

Conclusions: Simultaneous 3D visualization of multiple markers provides new insight into pathologies that cannot be visualized with conventional 2D hematoxylin and eosin stained or 3D single color images. Incorporation of these new techniques (tissue clearing, advanced microscopies, and multiple antibody labeling), will provide better insights into the understanding of pancreas pathology and will be widely applicable to other diseases.

1684 IgA+ Tumor-Infiltrating Plasma Cells Are Associated with Lower Recurrence Rate of Pancreatic Ductal Adenocarcinoma

Shaomin Hu[1], Matthew Gabrielson[2], Linlin Yang[1], Joseph Albanese[1], Dale Small[1], Yanhua Wang[3], Qiang Liu[4]
[1]Montefiore Medical Center, Bronx, NY, [2]Albert Einstein College of Medicine, Glen Arm, MD, [3]Bronx, NY, [4]Montefiore Medical Center, Princeton Junction, NJ

Disclosures: Shaomin Hu: None; Matthew Gabrielson: None; Linlin Yang: None; Joseph Albanese: None; Dale Small: None; Yanhua Wang: None; Qiang Liu: None

Background: Tumor-infiltrating lymphocytes (TILs) and its various components including CD8+ and CD4+ T cells have been associated with clinical outcome of pancreatic ductal adenocarcinoma (PDAC). However, rare studies have focused on the role of IgA+ tumor-infiltrating plasma cells (TIPCs). A few recent studies suggested that IgA+ TIPCs can promote progression of chemotherapy-resistant prostate and hepatocellular carcinomas. We also found that IgA+ plasma cells can help delivery of regulatory T cells (Tregs) to target tissue in a mouse model, thus may possess immunosuppressive function. Here we aim to explore the correlation of IgA+ TIPCs with Tregs and its association with PDAC prognosis.

Design: Nineteen patients with primary PDAC were identified; none of them received neoadjuvant therapy. The patients were followed up for a mean period of 41 months (range from 1 to 168 months), and 11 of them (57%) had recurrence. Representative sections of the primary resection specimens were stained for IgA, CD8 and Foxp3 (for Treg); positive cells were blindly recorded as cell counts per 10 representative high power fields (HPFs). Corresponding H&E slides were evaluated for stromal TILs. Fisher's exact test was used for analysis.

Results: The patients were arbitrarily divided into IgA+TIPC low (n=9) and high (n=10) groups based on the median IgA+TIPC count. There is no significant difference in age (71 vs 67 years in low and high groups), follow-up interval (38 vs 40 months) or stage between the two groups. As we expected, high IgA+TIPC correlated with high Treg count (p=0.02) in tumor stroma. However, further analysis revealed a strong association of high IgA+TIPC count with less recurrence (89% recurrence in IgA+TIPC low group vs 30% in high group, p=0.02). Even when we normalized the absolute IgA+TIPC count to IgA+ TIPC/CD8+ T cell ratio, this association is still fairly present (80% recurrence in IgA+TIPC low group vs 50% in high group, p=0.07). There was no significant correlation of IgA+TIPC count with CD8+ T cell count or TILs.

Conclusions: Our results in this small cohort suggested that IgA+ TIPC count positively correlates with Tregs and is associated with lower recurrence rate of PDAC. A large cohort will be further studied to understand more the roles of IgA+ TIPC in PDAC prognosis.

1685 Peripheral Nerve Sheath Tumors of the Pancreas: A Clinicopathologic Study of Nine Cases

Danielle Hutchings[1], Peter Illei[2]
[1]Johns Hopkins Pathology, Baltimore, MD, [2]Johns Hopkins University School of Medicine, Baltimore, MD

Disclosures: Danielle Hutchings: None; Peter Illei: None

Background: Peripheral nerve sheath tumors, including schwannoma and malignant peripheral nerve sheath tumor (MPNST), are exceedingly rare in the pancreas. In this study, we report the clinical, radiographic and pathologic features of these neoplasms in a series of nine surgically resected pancreata.

Design: Nine patients with schwannoma or MPNST of the pancreas were included and the available pathology was reviewed for each. Clinical and radiographic findings were obtained from the electronic medical records.

Results: Among all patients, the median age was 59 years (range 43-81 years) and 56% were female. There were seven patients with pancreatic schwannoma and schwannoma was the primary pathologic diagnosis on surgical resection in six of these seven patients. One

patient with pancreatic ductal adenocarcinoma (PDAC) had an incidental intrapancreatic schwannoma on resection. The median tumor size was 2.1 cm (range 0.5-9.5 cm). Three tumors were located in the neck, two in the head, one in the body and one in the uncinate process. Fine needle aspiration (FNA) of the pancreas was performed in five cases and showed spindle cell morphology diagnostic of schwannoma in one case, an atypical epithelioid and spindled cell proliferation in two cases and was non-diagnostic in one case. FNA showed ductal adenocarcinoma in the one case with PDAC on resection. Clinical and radiographic findings were available in five patients with schwannoma as the primary diagnosis. Four were asymptomatic and one presented with persistent abdominal pain. Computed tomography (CT) showed cystic lesions in three patients and solid, hypodense masses in two patients. All five patients were alive and without evidence of recurrence after resection with median follow-up time of 20 months (range 5-104 months). Two patients had MPNST arising in the pancreas. One tumor measured 2.5 cm and the other 13 cm; both tumors were located in the head of the pancreas. Follow-up was available for one patient who was alive with no evidence of recurrence at 200 months. No other clinical or radiographic information was available for either patient.

Conclusions: The clinicopathologic features of pancreatic schwannoma and MPNST are diverse and the diagnosis can be challenging of FNA. They may present as solid or cystic lesions of variable size and location within the pancreas. Although rare, these neoplasms are important for pathologists to consider in the differential diagnosis of pancreatic spindle cell lesions, particularly on cytology or small biopsy.

1686 SPINK1-Associated Pancreatitis is Characterized by Progressive Pancreatic Parenchymal Fibrosis and Differs from Other Genetically Associated Etiologies of Chronic Pancreatitis

Terrell Jones[1], Melena Bellin[2], Dhiraj Yadav[1], Aatur Singhi[3]
[1]University of Pittsburgh Medical Center, Pittsburgh, PA, [2]University of Minnesota Medical Center, Minneapolis, MN, [3]University of Pittsburgh Medical Center, Sewickley, PA

Disclosures: Terrell Jones: None; Melena Bellin: *Advisory Board Member*, ARIEL precision medicine; Dhiraj Yadav: None; Aatur Singhi: None

Background: Chronic pancreatitis is a heterogenous group of disorders with protean clinical and pathologic findings. The identification of germline alterations associated with pancreatitis, such as in *PRSS1*, *CFTR*, *SPINK1* and *CTRC*, provides the opportunity to define the pathologic hallmarks of pancreatitis and etiologic-specific changes. For example, the pancreata in *PRSS1* and *CFTR* patients exhibit progressive lipomatous atrophy without significant fibrosis. To date, the histologic features of *SPINK1*-associated pancreatitis have not been described and, therefore, we collected a series of *SPINK1* patients that underwent total pancreatectomy with islet autotransplantation (TPIAT).

Design: Representative pancreatic sections after TPIAT and associated clinicopathologic data were collected from 21 patients with a *SPINK1* germline mutation. Pathologic findings were correlated with patient demographics, onset and duration of pancreatitis, germline genetics and pancreatic duct anatomy.

Results: Patients at the time of TPIAT ranged in age from 4 to 41 years (median, 18 years) with a slight female predominance (n=13, 61%). Age at disease onset was from birth to 32 years (median, 8 years) with a duration of 2 to 25 years (median, 7 years). Most patients were heterozygous for *SPINK1* and 13 (62%) had co-occurring *CFTR* (n=10), *CTRC* (n=2) and *PRSS1* (n=1) mutations. Homozygous *SPINK1* mutations and pancreatic divisum were found in 2 and 4 patients, respectively. Overall, 17 (81%) patients had co-occurring pancreatitis-associated germline alterations, *SPINK1* homozygosity and/or anomalous ductal anatomy. Examination of patient pancreata revealed a sequential pattern of histologic changes with increasing duration of pancreatitis. For patients with a ≤3-year pancreatitis history, the pancreas exhibited mild lobular atrophy and mild interlobular fibrosis. Moderate lobular atrophy, moderate interlobular fibrosis and mild ductal dilatation were seen with pancreatitis of >3 years to 15 years. A >15-year history of pancreatitis was associated with marked lobular atrophy, scattered islets of Langerhans, moderate intralobular and interlobular fibrosis, mild-to-moderate perilobular lipomatous atrophy and moderate ductal dilatation with intraductal concretions.

Conclusions: In contrast to *PRSS1* and *CFTR*, patients with *SPINK1* germline alterations develop progressive pancreatic parenchymal fibrosis. Further, *SPINK1* pancreatitis patients frequently harbor other predisposing germline alterations and/or anomalous ductal anatomy.

1687 MMR-Deficiency is Rare in Cholangiocarcinomas, Associated with a Distinct Morphology, and Not Associated with PD-L1 Expression

Jennifer Ju[1], Megan Dibbern[2], Mani Mahadevan[2], Jinbo Fan[1], Paul Kunk[1], Edward Stelow[1]
[1]University of Virginia Health System, Charlottesville, VA, [2]University of Virginia, Charlottesville, VA

Disclosures: Jennifer Ju: None; Megan Dibbern: None; Mani Mahadevan: None; Jinbo Fan: None; Paul Kunk: None; Edward Stelow: None

Background: Patients with cholangiocarcinomas that are mismatch repair deficient (MMR-d) may benefit from immunotherapy targeting programmed cell death protein-1 (PD-1) and its ligand (PD-L1). Here, we investigate MMR status in a large cohort of cholangiocarcinomas and compare results with tumor morphology and PD-L1 expression.

Design: Tissue microarrays (TMA) were made with 96 cases of cholangiocarcinomas. These were evaluated for MLH1, PMS2, MSH2, and MSH6 by immunohistochemistry (IHC). Cases that showed loss on microarray were re-evaluated on full section recuts. Cases that continued to show loss were evaluated using microsatellite instability (MSI) molecular testing. The TMA was stained and scored for PD-L1 expression in the tumor cells and surrounding inflammatory cells. Morphology and tumor site were recorded and compared to results.

Results: Eight of 96 (8%) cholangiocarcinomas showed possible MMR loss by IHC. Of these, 5 (63%, 5% overall) were MSI-low (-L) or -high (-H) (considered true MMR-d). Thirty cases of cholangiocarcinomas originated in the liver (including 2 MMR-d) and 66 were extra-hepatic. Location was not correlated with MMR status (p=1.0). All 5 MMR-d cases showed a pure pancreatobiliary phenotype, though this was not significantly different than for MMR-intact (MMR-i) cases (p=0.6). However, MMR-d cases were overwhelming more likely to show solid (Figure 1) or mucinous (Figure 2) morphology as opposed to a typical infiltrating tubular pattern (p=0.00005). MMR status did not correlate with tumor expression of PD-L1, with all 16 cases (17%) of >1% tumor cell staining occurring in MMR-i cancers (p=0.6). PD-L1 expression in tumor associated immune cells was more frequent, found in 53 (55%) of cases, including 4 of the MMR-d (p=0.4).

Figure 1 - 1687

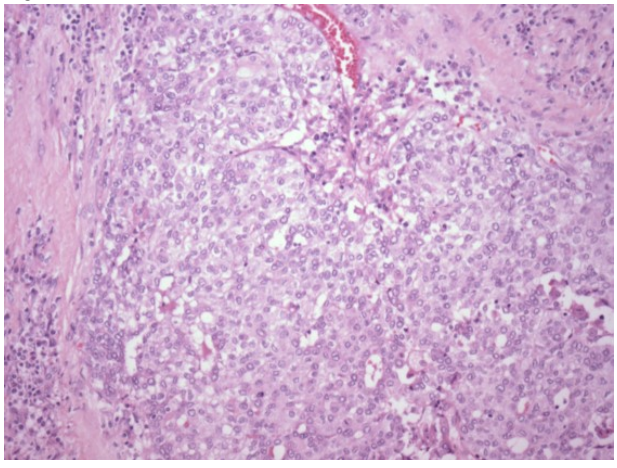

Figure 2 - 1687

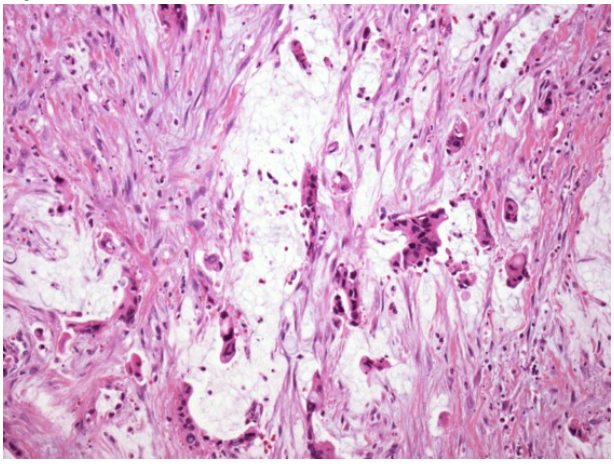

Conclusions: Our study found that 5% of cholangiocarcinomas showed MMR-d. The best predictive factor of MMR-d was a solid or mucinous morphology, regardless of whether the tumor was intestinal or pancreatobiliary phenotype. MMR status may not be the best way to test for cholangiocarcinoma response to anti-PD-L1 therapy given its infrequency compared to direct PD-L1 staining.

1688 Staging Differences between Pancreatic Adenocarcinoma Arising in Intraductal Papillary Mucinous Neoplasm Versus Conventional Pancreatic Ductal Adenocarcinoma Using the 8th Edition AJCC System

Ari Kassardjian[1], Hanlin Wang[2]
[1]University of California, Los Angeles, West Hollywood, CA, [2]David Geffen School of Medicine at UCLA, Los Angeles, CA

Disclosures: Ari Kassardjian: None; Hanlin Wang: None

Background: Intraductal papillary mucinous neoplasm (IPMN) is a precursor lesion of invasive pancreatic ductal adenocarcinoma (PDAC). There has been controversy regarding the outcome of surgically-resected PDAC arising in IPMN when compared with conventional PDAC. The goal of this study was to evaluate the differences of staging and pathologic characteristics between PDAC arising in IPMN versus conventional PDAC.

Design: Pathology and clinical follow-up database was retrospectively queried at our institution for patients who had undergone pancreaticoduodenectomy or distal pancreatectomy between 2007-2018 for PDAC and IPMN. Patient survival data was analyzed and the tumors were staged according to the 8th edition AJCC Cancer Staging Manual.

Results: A total of 377 patients were included in this study. As shown in Table 1, 91 cases had PDAC arising in IPMN and 287 had conventional PDAC. Patients with PDAC arising in IPMN were 4 years older on average (70.5 vs 66.4). Although the mean size of the invasive tumors between the two groups were similar (3 and 3.1cm), patients with PDAC arising in IPMN had a higher proportion of lower T-stage (T1 a,b,c) tumors (33% vs 21.3%). Similarly, PDAC arising in IPMN was associated with a lower incidence of lymph node metastasis (56% vs 71%), average number of positive lymph nodes (1.7 vs 2.6), lymphovascular invasion (46.2% vs 60.8%), and perineural invasion (79.1% vs 86.8%). SMAD4 was retained in higher percentage of cases in PDAC arising in IPMN (65% vs 36%). There was a small survival difference in PDAC arising in IPMN in T1 tumors (42.3 vs 36.5 months), however this difference disappeared in higher stage tumors.

	PDAC arising from IPMN (%)	**Conventional PDAC (%)**
	N=91	N=286
Gender		
Female	39 (42.9)	134 (46.7)
Male	52 (57.1)	153 (53.3)
Age, mean	70.5	66.4
Tumor size (cm), mean	3	3.1
Nodes assessed, mean	22.5	21.7
Positive nodes, mean	1.7	2.6
Positive for PNI	72 (79.1)	249 (86.8)
Positive for LVI	42 (46.2)	174 (60.8)
Retained SMAD4	13/20 (65)	36/100 (36)
Histologic Grade		
G1	19 (20.9)	37 (12.9)
G2	56 (61.5)	180 (63)
G3	16 (17.6)	59 (20.6)
Gx	0	10 (3.5)
T-stage		
T1 (a,b,c)	30 (33)	61 (21.3)
T2	39 (42.9)	162 (56.7)
T3	22 (24.1)	54 (18.9)
T4	0	3 (1)
TX	0	6 (2.1)
N-stage		
N0	40 (44)	83 (29)
N1	38 (41.8)	127 (44.4)
N2	13 (14.2)	76 (26.6)
Overall stage		
IA	18 (19.8)	29 (10.4)
IB	14 (15.4)	36 (12.6)
IIA	9 (9.9)	11 (3.9)
IIB	37 (40.6)	128 (45.7)
III	13 (14.3)	76 (27.1)
Survival in months		
T1 (a,b,c)	42.3	36.5
T2	25.4	24.1
T3	20.2	18.1

Conclusions: PDAC arising in IPMN has a lower rate of advanced T stage, lymph node metastasis, perineural and lymphovascular invasion. However, survival outcomes following resection appear similar specially in the higher stage tumors.

1689 Pancreatic Intraepithelial Neoplasia (PanIN) As A Morphologic Marker Of Pancreatobiliary Type Of Ampullary Carcinoma

Kritika Krishnamurthy[1], Vathany Sriganeshan[1]
[1]Mount Sinai Medical Center, Miami Beach, FL

Disclosures: Kritika Krishnamurthy: None; Vathany Sriganeshan: None

Background: In 1994, Kimura reported two main histological subtypes of ampullary adenocarcinoma, the intestinal and the pancreatobiliary (PB). This classification was later found to be important in predicting the prognosis as well as determining the therapeutic strategy. Isolated histological analysis is hindered by inherent subjectivity and considerable interobserver variability. Additionally, undifferentiated or poorly differentiated tumors cannot be classified based purely on tumor morphology. PanIN is a well recognised precursor to pancreatic adenocarcinoma. Three studies have shown concurrent PanIN in patients with ampullary carcinoma, but their association with the two subtypes has not yet been reported. Reports of similar molecular alterations in pancreatic adenocarcinoma and PB type of ampullary adnocarcinoma hint at a common carcinogenic pathway.

Design: Fourteen cases of segmental resection for ampullary adenocarcinoma were retreived from the archives. The cases were classified into two groups based on the presence of concomitant PanIN. All the cases were stained for CK7, CK 20 and CDX 2 and were classified as intestinal or PB types based on the staining pattern.

Results: All the 10 cases with PanIN stained negative for CDX2 and were classified as PB type (p=0.01). Of the cases without PanIN, 3 were classified as intestinal subtype based on CDX2 positivity and 1 was classified as PB type. Concomitant PanIn was present in 91% of PB type of ampullary adenocarcinoma. The grade of PanIN did not influence the grade or stage of the adenocarcinoma (p>0.05). CK 7 was positive in 13 cases and CK 20 was positive in 12 cases (p>0.05).

Conclusions: The histologic subtying of ampullary adenocarcioma appears to have significant prognostic and therapeutic implications. But due to the considerable variablity in isolated morphology based subtyping, higher frequency of poorly differentiated cancers and low incidence of the disease, the histomorphologic classification of ampullary adenocarcinomas remains one of the grey zones in surgical pathology. In this scenario, the co-occurence of PanIN in a high percentage of the PB subtype and its complete absence in the intestinal subtype may serve as a strong differentiator between the two subtypes.

This is supported by the establishment of PanIN as a definite precursor of pancreatic adenocarcinoma and the identical molecular lanscape of pancreatic adenocarcinoma and PB type ampullary adenocarcinoma.

1690 Identification of racial-specific novel mutations in pancreatic ductal adenocarcinoma by whole-exome sequencing: comparison of African American patients to Caucasian patients

Jinping Lai[1], Srikar Chamala[1], Feng Yin[1], Miles Cameron[2], Xiuli Liu[1], Petr Starostik[1], Jose Trevino[2]
[1]University of Florida, Gainesville, FL, [2]University of Florida College of Medicine, Gainesville, FL

Disclosures: Jinping Lai: None; Srikar Chamala: None; Feng Yin: None; Miles Cameron: None; Xiuli Liu: None; Petr Starostik: None; Jose Trevino: None

Background: African American (AA) patients have 50-90% higher incidence of pancreatic ductal carcinoma (PDAC) and worst prognosis among all of the racial groups in the USA. The aim of the present study was to compare the genomic alterations in PDACs from AA patients and the PDACs from age, gender and tumor grade matched Caucasian (CA) patients and to identify racial-specific mutations.

Design: We performed whole-exome sequencing on DNA from 18 paired PDAC and adjacent benign pancreatic parenchyma tissues from five AA patients and four CA patients matched for age, gender and tumor grade.

Results: As expected, Kras, P53, Smad4 mutations were present in the PDCAs in both AA and CA patients. 22 gene mutations including ABCF1, ANAPC1, ANK3, ANKRD65, ARHGEF11, ARV1, C4B-AS1, CCDC135, COPZ2, CYP21A2, CYP2A7, HCAR2, KIAA2026, KLHL18, MYL1, OR11H12, PHACTR4, PPP1R12B, SARM1, TBC1D3G, TTC39A, and ZNF687 were only present in the PDAC from all of the AA patients. While 7 gene mutations including ARHGEF10, IGSF10, KCMF1, SENP6, WRN, EFCAB2, EML3, IQSEC3, and SCN2A were only present in the PDACs from all of the CA patients. 27 out of the 29 mutations (except ARHGEF10 and KCMF1) have not been previously reported in PDAC. Among the mutations exclusively present in the AA patients, ABCF1 and ANAPC1 were previously reported to be associated with chemotherapy response and survival in colorectal and lung adenocarcinomas, respectively. Cytochrome P450 family member CYP2A7 mutation was associated with peritoneal cancer seeding and CYP21A2 was induced by chemotherapy through P53 signaling. Additionally, PHACTR4 mutations were associated with Stat3 signaling activation and IL-6 mediated phosphorylation in hepatocellular carcinoma. Among the mutations exclusively present in CA patients, ARHGEF10, SENP6, IGSF10, and KCMF1 were reported to be potentially important tumor treatment targets in PDAC and other malignancies. In addition, ARHGEF10 was also reported to be associated with chemotherapy-induced neuropathy.

Conclusions: In this pilot study, we identified 29 racial-specific novel PDAC-associated gene mutations among AA and CA patients through whole-exome sequencing. Some of them are potentially important prdictors of response and side effects of chemotherapy as well as therapeutic targets of PDACs in AA or CA patients in the era of personalized medicine.

1691 The Prognostic Value of Lymph Node Metastasis Number, Size and Extracapsular Extension in Distal and Perihilar Bile Duct Cancers

Yangkyu Lee[1], Hyunjin Park[2], Kyoungbun Lee[3], Soomin Ahn[4], Haeryoung Kim[5]
[1]Seoul National University Bundang Hospital, Gyeonggi-Do(Seoul), Korea, Republic of South Korea, [2]Seoul National University Bundang Hospital, Seongnam, Korea, Republic of South Korea, [3]Seoul National University Hospital, Seoul, Korea, Republic of South Korea, [4]Seoung-Nam, Korea, Republic of South Korea, [5]Seoul, Korea, Republic of South Korea

Disclosures: Yangkyu Lee: None; Hyunjin Park: None; Soomin Ahn: None; Haeryoung Kim: None

Background: The concept of N stage was changed from the location of lymph nodes (LNs) to the number of metastasized LNs in the 8th edition of the AJCC TNM staging systems for distal bile duct cancer (D-BC) and perihilar bile duct cancer (P-BC). We evaluated the prognostic significance of the revised nodal staging system for D-BC and P-BC, and the additional prognostic significance of metastastic tumor burden and extranodal soft tissue extension (ENE).

Design: A retrospective analysis was performed on two independent cohorts of surgically resected D-BCs and P-BCs. Cohort 1 (Seoul National University Bundang Hospital) consisted of 93 D-BCs and 90 P-BCs, and cohort 2 (Seoul National University Hospital) consisted of 84 D-BCs and 99 P-BCs. The number of total and metastasized LNs, the size of the largest LN metastases, and the presence of ENE were recorded, and correlated with the overall survival (OS) and progression-free survival (PFS).

Results: For cohort 1 D-BCs, the revised N stage was significantly associated with decreased OS ($p=0.002$) and PFS ($p<0.001$); however, the difference between N1 and N2 stages were not significant. Metastasis size≥1cm and the presence of ENE were associated with decreased OS ($p<0.001$ and $p=0.001$, respectively) and PFS ($p<0.001$, both). In cohort 2, metastasis size≥1cm and ENE were associated with decreased PFS ($p<0.001$, both), but not with OS. For P-BCs, no significant associations were found between the nodal parameters and survival in both cohorts.

Conclusions: LN metastasis size and the presence of ENE were significantly associated with decreased survival in D-BCs in both cohorts. Neither the current N staging system nor the additional nodal factors were correlated with survival for P-BCs. Including LN metastasis size and ENE in the pathology reports may provide valuable prognostic information for D-BCs in addition to the number-based pN stage.

1692 Epstein-Barr Virus Infection in Carcinomas of the Biliary Tract

Michael Lee[1], Susan Hsiao[2], Helen Remotti[3], Stephen Lagana[4]
[1]Long Island City, NY, [2]New York-Presbyterian/Columbia University Medical Center, Flushing, NY, [3]Columbia University Medical Center, Dobbs Ferry, NY, [4]New York, NY

Disclosures: Michael Lee: None; Susan Hsiao: None; Helen Remotti: None; Stephen Lagana: None

Background: Epstein-Barr virus is a ubiquitous DNA virus. Infection or reactivation is associated with mononucleosis, lymphomas, nasopharyngeal carcinoma and gastric carcinoma (typically with a lymphoepithelioma pattern). Some EBV associated cancers have a better prognosis than their non-viral counterparts in a particular organ. High mutational burdens may also contribute to selection of treatment modality. We evaluated EBV infection in carcinomas of the biliary tract (cholangiocarcinomas, ChCa) by performing RNA in-situ hybridization (ISH) for Epstein-Barr encoding region (EBER).

Design: 102 cases of cholangiocarcinoma in the biliary tract (intrahepatic, perihilar and distal common bile duct) from our institution (all formalin fixed paraffin embedded (FFPE)) were evaluated for EBER by ISH. The ISH results were graded as either positive or negative based on nuclear staining within tumor cells which represent a labeled probe for a specific EBER RNA sequence in EBV.

Results: 3 of 29 cholangiocarcinomas in the extrahepatic distal biliary tract showed positive EBER staining, consistent with EBV infection. All three cases were poorly differentiated. Two cases involved the common bile duct and showed signet ring cell morphology. One case involved the common bile duct with extension to the ampulla of Vater and showed tumor cells arranged in a syncytial pattern with numerous tumor infiltrating and peri-tumoral lymphocytes (Figures 1 and 2). All cases of intrahepatic (n=38) and hilar ChCa (n=35) were negative for EBER.

Figure 1 - 1692

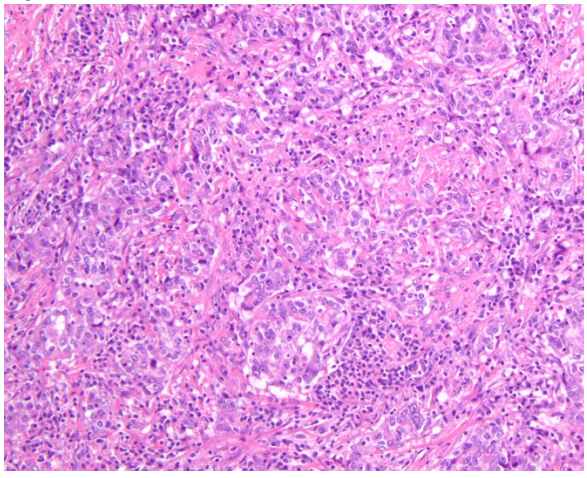

Figure 2 - 1692

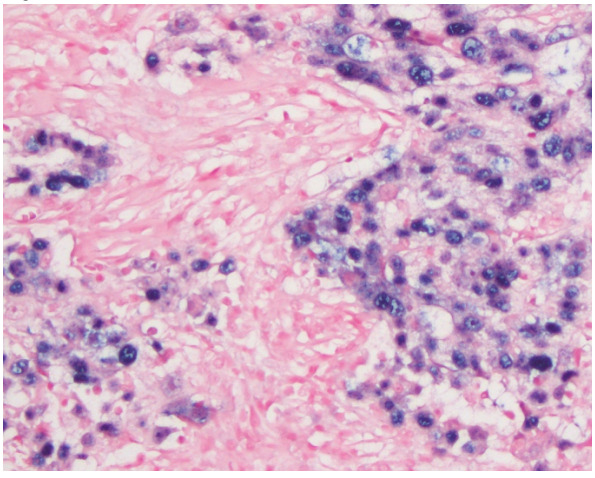

Conclusions: EBV infection by EBER ISH is occasionally seen in ChCa. Though one case resembled lymphoepithelioma-like carcinomas of other organs, the other cases did not. Additional studies will be needed to determine if there is a difference in clinical prognosis and outcome.

1693 Mismatch Repair Protein Expression Analysis in Pancreatic Ductal Adenocarcinoma Shows Reduced Expression of MSH6

Anna Lee[1], Helen Remotti[2], Alina Iuga[1]
[1]Columbia University Medical Center, New York, NY, [2]Columbia University Medical Center, Dobbs Ferry, NY

Disclosures: Anna Lee: None; Helen Remotti: None; Alina Iuga: None

Background: Microsatellite instability (MSI) has been shown to predict susceptibility to immunotherapy. This led to implementation of mismatch repair protein (MMR) expression and MSI screening for a variety of solid tumors, including pancreatic ductal adenocarcinoma (PDA). MMR deficiency and MSI have been reported in less than 1% of PDAs. However, MMR expression pattern has not been extensively studied in PDAs. MMR immunohistochemistry (IHC) interpretation shows considerable interobserver variability and reduced expression is a pitfall in diagnosing MMR deficiency by IHC.

Design: We identified the PDAs with MMR expression status reported in the past year, since screening was implemented. We compared MMR expression and MSI status in neoadjuvant chemotherapy-treated and untreated PDAs. We further randomly selected 10 cases for each group and quantified the IHC expression for MLH1, PMS2, MSH2 and MSH6. MSI testing was performed using multiplexed PCR amplification of tumor and normal DNA with primers specific for 5 mononucleotide and 2 pentanucleotide markers using the Promega MSI Analysis System. MSI-H was defined as alteration of > 20% of loci tested. MMR testing was performed using antibodies for MLH1 (clone G168-15), MSH2 (clone FE11), MSH6 (clone 44) and PMS2 (clone MRQ-28).

Results: We identified 65 PDA cases with MMR IHC performed (43 untreated, 22 treated) out of which 49 were tested for MSI. All cases were MSS and none showed complete loss of MMR expression. MSH6 expression was decreased compared to the other MMR proteins in both scored groups (paired t-test, $p<0.05$). Nuclear expression was high for MLH1 (mean of 82.0% in treated, 85.5% in untreated), PMS2 (mean of 88.0% in treated, 85.0% in untreated) and MSH2 (mean of 70.0% for both treated and untreated), with no significant differences between groups. In contrast, MSH6 showed decreased expression in the treated PDAs, with mean nuclear expression of 21.6% in treated and 45.0% in untreated cases (t-test, $p=0.0295$).

Conclusions: PDAs showed lower expression of MSH6 compared to MLH1, PMS2 and MSH2, with more reduction in neoadjuvant therapy setting. Isolated loss of MSH6 expression has been reported in microsatellite-stable (MSS) colorectal carcinoma after chemotherapy. The pathophysiology is not well understood. One hypothesis is that loss of MSH6 expression may develop as a drug resistance mechanism. It is our hope that awareness of the MSH6 expression pattern in PDAs will help pathologists interpret more accurately the MMR status in PDAs.

1694 Loss of HES1 Expression Indicates Worse Prognosis in Lymph Node Negative Pancreatic Ductal Adenocarcinoma

Yuan Li[1], Zhenjian Cai[2], Amad Awadallah[3], Lan Zhou[4], Wei Xin[5]
[1]Peking Union Medical College Hospital, Redondo Beach, CA, [2]The University of Texas Health Science Center at Houston, Houston, TX, [3]University Hospitals Cleveland Medical Center, Cleveland, OH, [4]Cleveland Medical Center, Case Western Reserve University, Solon, OH, [5]Case Western Reserve University, Cleveland, OH

Disclosures: Yuan Li: None; Zhenjian Cai: None; Amad Awadallah: None; Lan Zhou: None; Wei Xin: None

Background: HES1 is a critical downstream target of Notch pathway and can be used as an indicator of Notch pathway activity. In a normal pancreas, Notch signaling pathway regulates pancreatic ductal differentiation, and it has been shown that dysregulated Notch pathway is involved in pancreatic carcinogenesis. Additionally, 50-60% of pancreatic ductal carcinomas (PDACs) express loss of SMAD4 (DPC4), a component of TGF-? signaling pathway. In this study, we explored the relationship between SMAD4 and HES1 in PDACs, and investigated whether it can be used as a prognostic indicator.

Design: Formalin-fixed paraffin embedded blocks from surgically resected PDACs were extracted from our surgical pathology archive, totaling 209 consecutive cases with demographic data. Among them, 68.9% (144/209) had regional lymph node metastasis. Immunohistochemical stains of HES1 (Abcam) and SMAD4 (Cell Signaling) were performed in the hospital diagnostic lab. Kaplan-Meier survival curves and Fisher's Exact test were used for statistical analysis.

Results: Among the 209 cases, 37 (17.7%) showed complete nuclear loss of HES1 while 127 (59.8%) had loss of SMAD4 expression. HES1 loss was more common in SMAD4 negative cases (75.7%, 28/37) than in SMAD4 positive cases (24.3%, 9/37) ($p<0.05$). There is no statistical difference between HES1 positive and negative groups with age, lymph nodes metastasis, angiolymphatic invasion, and perineural invasion. Survival averaged 988 days in the group with lymph node negative PDAC, with worse prognosis for those with loss of HES1 expression, who averaged 606 survival days compared to 1052 days for HES1 positive patients ($p<0.05$). Loss of SMAD4 and lymph nodes metastasis were also two independent negative prognostic indicators in multivariate analysis.

Figure 1 - 1694

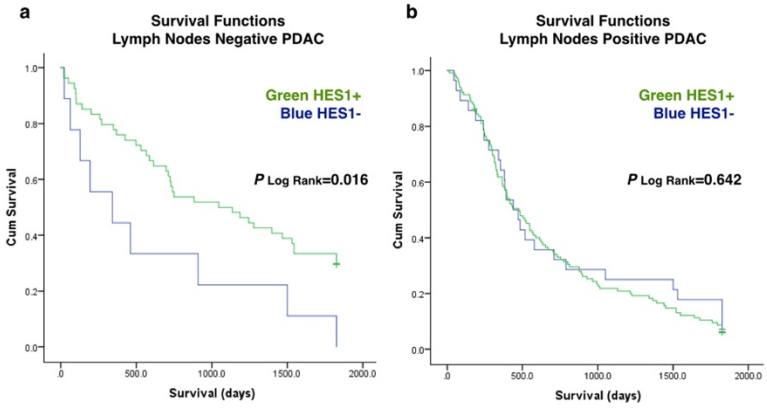

Figure 1: Overall survival using the Kaplan-Meier method. (a) Lymph Nodes Negative PDACs; (b) Lymph Nodes Positive PDACs.

Conclusions: Our results suggest that loss of expression of HES1 is associated with the loss of SMAD4 in some PDACs, which implies dysregulated Notch interacts with mutated TGF-? pathway in pancreatic carcinogenesis. Loss of Hes1 is an independent prognostic marker to indicate worse prognosis in lymph node negative PDACs but not in lymph node positive PDACs.

1695 Interobserver Agreement in Pathologic Evaluation of Bile Duct Biopsies

Yongjun Liu[1], Jessica Rogers[2], Lisa Koch[3], Camtu Truong[3], Florencia Jalikis[4], Paul Swanson[5], Matthew Yeh[1]
[1]University of Washington Medical Center, Seattle, WA, [2]University of Washington Medical Center, Woodway, WA, [3]University of Washington, Seattle, WA, [4]Seattle, WA, [5]University of Washington, Bainbridge Island, WA

Disclosures: Yongjun Liu: None; Jessica Rogers: None; Camtu Truong: None; Paul Swanson: None

Background: Evaluation of biliary stricture etiologies frequently necessitates bile duct biopsies. Pathologic diagnosis of dysplasia in bile duct biopsies is clinically important as it often dictates a potentially morbid surgery. Interpretation of these biopsies is challenging and in addition to small sizes of specimens and technical factors, the diagnosis suffers from interobserver disagreement. Current literature lacks studies that evaluate interobserver variation in diagnosis of dysplasia in bile duct biopsies.

Design: Eighty five bile duct biopsies performed from 2004 to 2018 were retrieved at our institution, falling into five diagnostic categories: negative for dysplasia (ND), indefinite for dysplasia (IND), low grade dysplasia (LGD), high grade dysplasia (HGD), and carcinoma (CA), with a roughly equal number of cases in each category. Among them, 40 biopsies were processed using Hollande's fixative, and the rest 45 were processed using formalin fixative. Five pathologists practicing in gastrointestinal/liver pathology subspecialty blindly reviewed all slides. Agreement among pathologists was analyzed by kappa statistics.

Results: The results of interobserver agreement are shown in Table 1. In the entire biopsies (n = 85), the overall agreement was moderate (kappa= 0.47). Interobserver agreement was nearly perfect for CA (kappa = 0.87), substantial for HGD (kappa = 0.68), moderate for ND (kappa = 0.56), and fair for LGD (kappa = 0.38) and IND (kappa = 0.23). When CA and HGD were grouped into 1 category as the end of the spectrum, interobserver agreement was substantial (kappa = 0.68). When IND and ND were grouped into 1 category as the other end of the spectrum, interobserver agreement was substantial (kappa = 0.70). When IND and LGD were grouped in 1 category, interobserver agreement was fair (kappa = 0.33). Statistical analysis was also performed on biopsies using Hollande's fixative and formalin fixative, respectively. Interobserver agreement improved in almost all diagnostic categories (particularly IND and LGD) in biopsies using formalin fixative as compared to those of Hollande's fixative.

Table 1. Interobserver Agreement in the Diagnosis of Dysplasia in Bile Duct Biopsies

Diagnostic Category	Kappa [95% CI] (Entire, n=85)	Kappa [95% CI] (Hollande's fixative, n=40)	Kappa [95% CI] (Formalin fixative, n=45)
Overall	0.47 [0.38, 0.55]	0.36 [0.23, 0.49]	0.56 [0.44, 0.68]
ND	0.56 [0.45, 0.68]	0.43 [0.25, 0.61]	0.68 [0.53, 0.83]
IND	0.23 [0.02, 0.44]	0.11 [-0.12, 0.34]	0.67 [0.52, 0.83]
LGD	0.38 [0.24, 0.52]	0.12 [-0.13, 0.38]	0.65 [0.49, 0.82]
HGD	0.68 [0.57, 0.80]	0.68 [0.52, 0.85]	0.68 [0.52, 0.84]
CA	0.87 [0.79, 0.96]	0.83 [0.71, 0.96]	0.90 [0.81, 1.00]
Two groups (CA and HGD *vs* ND, IND, LGD)	0.68 [0.56, 0.80]	0.60 [0.43, 0.77]	0.76 [0.62, 0.90]
Two groups (CA, HGD, LGD *vs* IND and ND)	0.70 [0.59, 0.81]	0.57 [0.39, 0.75]	0.81 [0.69, 0.94]
Group IND and LGD in 1 category	0.33 [0.21, 0.45]	0.20 [0.03, 0.37]	0.44 [0.27, 0.62]

Abbreviation: Negative for dysplasia (ND), indefinite for dysplasia (IND), low grade dysplasia (LGD), high grade dysplasia (HGD), and carcinoma (CA).

The level of interobserver agreement was graded based on the Landis and Koch scale (<0, poor agreement; 0.01 – 0.20, slight agreement; 0.21 – 0.40, fair agreement; 0.41 – 0.60, moderate agreement; 0.61 – 0.80, substantial agreement; and > 0.80, nearly perfect agreement).

Conclusions: This is the first study assessing interobserver concordance in diagnosis of bile duct biopsies. Interobserver reproducibility was substantial at the ends of the diagnostic spectrum (CA/HGD/ND) but fair for IND and LGD. Interobserver variation improved overall after the application of formalin fixative.

1696 A Comparison of Whipple Grossing Methods: Whole Mount Versus Conventional

Valerie Lockhart[1], Zongming Eric Chen[2], Haiyan Liu[2], Jinhong Li[1], Joseph Blansfield[1], Tania Arora[1], David Diehl[1], Fan Lin[2]
[1]Geisinger, Danville, PA, [2]Geisinger Medical Center, Danville, PA

Disclosures: Valerie Lockhart: None; Zongming Eric Chen: None; Haiyan Liu: None; Jinhong Li: None; Joseph Blansfield: None; Tania Arora: None; David Diehl: None; Fan Lin: None

Background: The exocrine pancreas staging in the 8th edition of the *AJCC Cancer Staging Manual* places more emphasis on tumor size and number of positive lymph nodes (LNs) than previous versions. In August 2017, our institution began using a whole mount (WM) method to gross Whipple specimens using axial slicing techniques, cutting from superior to inferior, in hopes of better visualizing and measuring the tumor with key anatomic relationships, assessing margins, quantifying LNs, and correlating the pathologic findings with CT/MRI findings (see Figure 1).

Design: Using CoPath surgical pathology reports, data were collected from all Whipple specimens grossed at our institution using the WM technique (8/2017 to 9/2018). Data were also collected from an equal number of consecutive prior cases (grossed using the conventional technique, 6/2016 to 8/2017) for comparison. Cases where pre-operative chemotherapy was administered were excluded. T-test and chi-square test were used for statistical analysis.

Results: Results are shown in Table 1.

Table 1. Data from Whipple specimens grossed with whole mount and conventional methods.

Case Characteristics	WM (43)	Conv (43)	
Age (average)	67.2	68.3	
Gender			
Female	22	24	
Male	21	19	
Benign Cases	4	4	
Neoplastic Cases	39	39	
Invasive ductal adenocarcinoma	28	31	
Intraductal papillary mucinous neoplasm	5	3	
Invasive adenocarcinoma duodenum	3	1	
Invasive adenocarcinoma ampulla	2	3	
Neuroendocrine tumor (NET)	1	1	
Adenocarcinomas + NET	**WM (34)**	**Conv (36)**	**P-value**
Tumor size (average)	3.32	3.15	0.67
Margin status (positive)			
Uncinate	6	7	0.85
Pancreatic (circumferential)	6	1	0.04
Common bile duct	1	2	0.59
Lymph Nodes (LNs)			
Average number per case	23.62	12.78	<0.01
Number of cases with positive LNs	27 (79%)	18 (50%)	0.01
Number of cases with ≤ 3 positive LNs	18 (53%)	7 (19%)	<0.01
Number of cases with > 3 positive LNs	9 (26%)	11 (31%)	0.71
Average positive LNs per LN-positive case	5.11	4.72	0.82

Figure 1 - 1696

Conclusions: This study shows that the greatest benefit of the WM grossing method is the ability to identify more LNs. Not only were more total LNs identified, but more *positive* LNs were identified using the WM method. The most profound improvement over the conventional grossing method was the number of cases where 1-3 positive LNs were identified. The ability to identify more positive LNs allows for more accurate staging, which in turn qualifies patients for the most appropriate subsequent treatment and clinical trials. The pancreatic margin was also positive at a significantly higher rate in the WM cohort, allowing for a more accurate assessment of curative resection rate. The WM technique provides more accurate measurement of tumor size (pT staging), because intact tumor can be demonstrated on a WM slide and viewed under a microscope. This is important because precise tumor size measured on the gross specimen may be unreliable due to an infiltrative tumor border. The WM technique is a superior grossing technique that allows for more accurate staging of pancreatic tumors and more appropriate patient care.

1697 Acute Pancreatitis in Autopsies Associated with Surgeries and Severe Inflammatory Diseases

Yoko Matsuda[1], Yuko Kinowaki[2], Yuki Fukumura[3], Junko Aida[4], Kaiyo Takubo[5], Toshiyuki Ishiwata[6], Tomio Arai[7]
[1]Tokyo Metropolitan Geriatric Hospital, Tokyo, Japan, [2]Tokyo Medical and Dental University, Bunkyo-ku, Japan, [3]Juntendo University, Tokyo, Tokyo, Japan, [4]Tokyo Metropolitan Institute of Gerontology, Tokyo, Tokyo, Japan, [5]Tokyo Metropolitan Institute of Gerontology, Tokyo, Japan, [6]Tokyo Metropolitan Institute of Gerontology, Itabashi-ku, Japan, [7]Tokyo Metropolitan Geriatric Hospital, Itabashi-ku, Japan

Disclosures: Yoko Matsuda: None; Yuko Kinowaki: None; Yuki Fukumura: None; Junko Aida: None; Kaiyo Takubo: None; Toshiyuki Ishiwata: None; Tomio Arai: None

Background: The commonest causes of acute pancreatitis are mechanical obstruction and heavy alcohol consumption, but in shock severe hypoperfusion also lead to ischemia-related pancreatitis. Acute pancreatitis is classified into interstitial edematous pancreatitis and necrotizing pancreatitis. However, little is known about the pathological characteristics of acute pancreatitis. In the present study, we evaluated pathologic changes in the whole pancreas from autopsy patients to provide useful information for diagnosis and treatment of acute pancreatitis.

Design: The pancreas obtained from 183 serial autopsies was cut into 5 mm sections vertical to the main pancreatic duct. We evaluated pathological changes associated with acute pancreatitis according to presence or absence of necrosis and the size range and divided the lesions into the following three categories: focal neutrophil infiltration, focal necrotizing pancreatitis, and diffuse necrotizing pancreatitis. Focal neutrophil infiltration comprised neutrophil infiltration without necrosis, localized in one zone of the pancreas (head, body, or tail). Focal necrotizing pancreatitis consisted of necrosis and neutrophil infiltration localized in one zone. Diffuse necrotizing pancreatitis comprised necrosis and neutrophil infiltration extended into two or more zones.

Results: We observed pathologically acute pancreatitis in 45 patients (25%), and no patients were diagnosed with acute pancreatitis prior to autopsy. Focal neutrophil infiltration was present in 22 cases (12%), focal necrotizing pancreatitis in 18 cases (10%), and diffuse necrotizing pancreatitis in 5 cases (3%). Age, body mass index, sex, drinking and smoking habits, diabetes mellitus, and malignant neoplasm were not associated with acute pancreatitis. Severe inflammatory disease confirmed by autopsy and surgery within 6 months was associated with acute pancreatitis ($P < 0.05$). The cause of acute pancreatitis was determined pathologically in only 9 of 45 patients

and viral or bacterial infection was the most common. Patients with pancreatitis showed decrease of white blood cell and platelet counts. Amylase levels were not increased in cases of acute pancreatitis.

Conclusions: We demonstrated that acute pancreatitis was frequently detected in autopsy samples without typical clinical signs. Multiorgan failure in terminal patients might mask clinical signs of pancreatitis. It is necessary to be alert to the signs of acute pancreatitis because it often causes severe complications and death.

1698 Carbohydrate Sulfotransferase 15 in Pancreatic Cancer Associated with Mature Fibrosis and Prognosis

Yoko Matsuda[1], Yuko Fujii[1], Miho Matsukawa[1], Makoto Nishimura[1], Toshiyuki Ishiwata[2], Tomio Arai[3]
[1]Tokyo Metropolitan Geriatric Hospital, Tokyo, Japan, [2]Tokyo Metropolitan Institute of Gerontology, Itabashi-ku, Japan, [3]Tokyo Metropolitan Geriatric Hospital, Itabashi-ku, Japan

Disclosures: Yoko Matsuda: None; Yuko Fujii: None; Makoto Nishimura: None; Toshiyuki Ishiwata: None; Tomio Arai: None

Background: Carbohydrate sulfotransferase 15 (CHST15) synthesizes matrix proteoglycan that regulates various pathogenic mediators and contributes to tissue remodeling and fibrosis during injury. CHST15 has been reported to promote tumor growth and invasion in various cancers. Previously, we reported the safety and efficacy of EUS-guided fine-needle injection (EUS-FNI) of STNM01, the double-stranded RNA oligonucleotide that specifically represses CHST15, for use in patients with pancreatic cancer. The present study aimed to determine the expression and clinicopathological characteristics of CHST15 in pancreatic cancer.

Design: We performed immunohistochemical staining for CHST15 using pancreatic tissues from 64 pancreatic cancer patients who underwent surgery (28 males and 36 females; 69.0 ± 9.6 years old). We quantified the positive percentages of CHST15, divided the patients into two groups according to high and low CHST15 expression in both cancer and stroma to determine whether CHST15 expression in stroma might play an important role in cancer progression. For the evaluation of fibrosis, there were two categories defined (mature and immature), based on the existence of collagen, myxoid stroma, and fibroblasts, using H&E specimens.

Results: The expression of CHST15 was detected in the cytoplasm of pancreatic cancer cells and fibroblasts in the cancer stroma. In noncancerous tissue, centroacinar cells, pancreatic duct epithelium, and islets expressed CHST15. CHST15 expression in cancer cells was not associated with overall survival (P=0.52). However, high CHST15 expression in stroma showed worse overall survival than low CHST15 (P=0.02). CHST15 expression in stroma showed a positive correlation to that in cancer cells (P=0.01). High CHST15 in the stroma group was associated with a higher incidence of immature fibrosis (P=0.02) than mature fibrosis. CHST15 expression in cancer cells was associated with UICC stage (P=0.02) and invasive front. Age and gender were not associated with CHST15 expression.

Conclusions: The present study revealed that overexpression of CHST15 in stroma was associated with worse overall survival and immature fibrosis. Overexpression of CHST15 in cancer cells was associated with tumor stage. These results suggest that targeting therapy for CHST15 might be useful for stroma fibroblasts and cancer cells.

1699 Frequency of Dysplasia/Carcinoma and Foveolar Atypia Associated with Gallbladder Cancer Risk: Comparative Analysis in Mapped/Totally Sampled Gallbladders from High-Risk versus Low-Risk Regions

Bahar Memis[1], Juan Carlos Roa[2], Juan Araya[3], Enrique Bellolio[4], Miguel Villaseca[4], Hector Losada[4], Juan Sarmiento[5], Jill Koshiol[6], Burcin Pehlivanoglu[7], Serdar Balci[8], Yue Xue[9], Gokce Askan[10], Olca Basturk[10], Michelle Reid[9], N. Volkan Adsay[11]
[1]TC.SBU. Sanliurfa Mehmet Akif Inan Training and Research Hospital, Sanliurfa, Turkey, [2]Pontificia Universidad Catolica de Chile, Santiago, Santiago, Chile, [3]Temuco, Chile, [4]Universidad de La Frontera, Temuco, Chile, [5]Emory University, Atlanta, GA, [6]National Cancer Institute, Rockville, MD, [7]Adiyaman University Training and Research Hospital, Adiyaman, Turkey, [8]Ankara, Turkey, [9]Emory University Hospital, Atlanta, GA, [10]Memorial Sloan Kettering Cancer Center, New York, NY, [11]Koç University Hospital, Istanbul, Turkey

Disclosures: Bahar Memis: None; Juan Carlos Roa: None; Juan Araya: None; Enrique Bellolio: None; Miguel Villaseca: None; Hector Losada: None; Juan Sarmiento: None; Jill Koshiol: None; Burcin Pehlivanoglu: None; Serdar Balci: None; Yue Xue: None; Gokce Askan: None; Olca Basturk: None; Michelle Reid: None; N. Volkan Adsay: None

Background: The data on the frequency of dysplasia and carcinoma in the gallbladder (GB) are highly conflicting. The association of different epithelial alterations with GB cancer risk has also not been established.

Design: 203 mapped and totally-sampled GBs from a low-cancer risk region (LR; USA; obesity rate, 2nd in the world) were compared with 140 from a very high-cancer risk region (HR, Chile; obesity rate, 4th). Findings were reviewed in a consensus format, including a meeting in Santiago, Chile, 2017.

Results: Dysplasia, carcinoma, goblet cells and a distinctive type of mucinous epithelial change on the surface mucosa (similar to foveolar epithelium, with a spectrum of atypia including frank dysplasia) were significantly more common in the HR (See Table). All lesions were significantly more prominent in the fundus. HGD/CIS was extensive (involving the majority of the intact epithelium) in 5 cases (2 non-invasive, 3 invasive) and was also present in the initial (random) section. LGD, goblet cells and foveolar atypia/dysplasia were typically focal and subtle (involving <5% surface area) and were often not detected on initial sections. Incidentally, the frequency (and amount) of lipogranulomas in lymph nodes was significantly higher in the US (40% vs 3%, p<0.001).

	US 203 totally mapped/sampled GBs	Chile 140 totally mapped/sampled GBs	p-value (US vs Chile)	Location	Estimated surface area involved	Present in the first (random) section
Low-grade dysplasia	**2%**	**10%**	**0.002**	**Fundus dominant**	**<5%**	**50%**
HGD/CIS without invasion	**1% (2/203)**	**0%**	**1.0**	**Fundus dominant**	**>95%**	**100%**
Invasive carcinoma associated with HGD/CIS	**0%**	**2% (3/140)**	**0.07**	**Fundus dominant**	**Invasion and/or HGD >95%**	**100%**
Goblet cells (IM)	**7%**	**28%**	**<0.001**	**Fundus dominant**	**<5%**	**33%**
Surface foveolar (mucinous) atypia/dysplasia	**5%**	**33%**	**<0.001**	**Fundus dominant**	**<5%**	**75%**
Lipogranulomas in lymph nodes	**40%**	**3%**	**<0.001**	**-**	**-**	**-**

Figure 1 - 1699

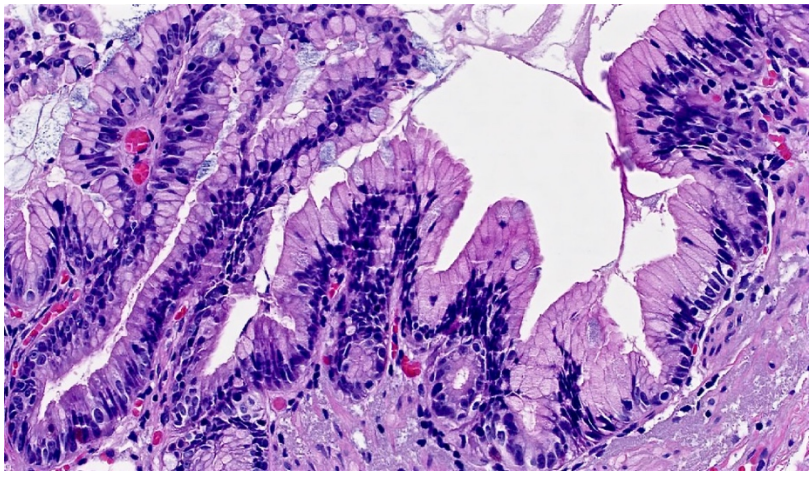

1. Invasive carcinoma associated with HGD/CIS is detected in 2% of clinically/grossly unsuspected cholecystectomies in the HR, and in-situ carcinoma (without invasion) in 1% in the LR. These findings refute the notion that “grossly unremarkable” GBs do not need histologic examination.
2. HGD/CIS is a wild-fire phenomenon, involving most of the intact epithelium at diagnosis, and is therefore more typically captured in the initial (random) section.
3. LGD and intestinal metaplasia are more common in the HR but are focal and subtle fundic lesions that may be missed in random sections.
4. This study elucidates the previously unrecognized connection between a distinctive epithelial alteration and cancer risk: i.e. foveolar change with spectrum of atypia including frank dysplasia, similar to that in PanINs, and foveolar/gastric-type dysplasia in the GI tract. This connection requires further analysis and molecular scrutiny to establish its true nature.
5. The frequency of lipogranulomas in lymph nodes is incomparably lower in the HR, suggesting a selective precipitation in the GBs in this population, and may be a manifestation of differences in cholesterol metabolism associated with carcinogenesis.

1700 Morphology predicts known molecular subtypes and survival in pancreatic ductal adenocarcinoma

Sangeetha N Kalimuthu[1], Gavin Wilson[2], Rajkumar Vajpeyi[1], Runjan Chetty[1]
[1]University Health Network, Toronto, ON, [2]Princess Margaret Cancer Centre, Toronto, ON

Disclosures: Sangeetha N Kalimuthu: None; Gavin Wilson: None; Rajkumar Vajpeyi: None; Runjan Chetty: None

Background: Recently, transcriptional analyses have identified several distinct molecular subtypes in pancreatic ductal adenocarcinoma (PDAC) that are prognostically and therapeutically significant. However, to date, an in depth morphological analysis of these different molecular subtypes has not been performed. Herein, we sought to identify specific morphological patterns that could be associated with known molecular subtypes and interrogate its biological significance.

Design: In the University Health Network (UHN), Toronto, we had 89 primary, chemotherapy naive PDAC specimens with paired RNA-seq data. Gene expression was correlated with morphological features. The histology from all cases were reviewed and immunohistochemistry (IHC) panel incorporating genes enriched in the basal molecular subtype was performed (CK5, p63, p40, CK14). IHC was quantified based on proportion of positive tumour cells and scored as 0%, <25% 25-49%, 50-75% and >75%. Overall survival (OS) was calculated from time of surgical resection to death.

Results: Five distinct morphological patterns were identified and were designated as 1/conventional, 2/IPMN-like, 3/IPMN, 4/squamous and 5/basal. The basal subtype collectively represented an array features traditionally associated with poor differentiation. Each morphological subtype aligned with a different gene expression module, substantiating these to be distinct patterns. Tumours that had >40% of the basal component and/squamous morphology were grouped as the basal subtype, which also overlapped with the basal transcriptional subtype. The morphologically identified “basal group” had a significantly poorer OS compared to “classical group” (p value=0.008). Additionally, the basal subgroup could be further subdivided into 2 groups based on the % of staining (Group 1=<50% in <3 basal IHC; Group 2= >50% in 3/> basal IHC). Interestingly, a subset of basal cases with high *KRT14* expression showed a unique CK14 staining pattern, selectively staining cells at the leading edge of tumour clusters, suggesting a potential role for “collective invasion” in PDAC. All classical cases were negative for basal markers.

Conclusions: This is a first study of its kind to show that morphology accurately predicts distinct molecular subtypes of PDAC with clear prognostic implications. This may provide the basis for an improved taxonomy of PDAC and may lend itself to the development of deep learning techniques in the future.

1701 The utility of immunohistochemistry aids diagnosis of colonization of duodenal mucosa by invasive ampullary adenocarcinoma

Rebecca Obeng[1], Burcin Pehlivanoglu[2], Frank Schneider[1], Jessica Tracht[3], Alyssa Krasinskas[1], Michelle Reid[4], Yue Xue[4]
[1]Emory University, Atlanta, GA, [2]Adiyaman University Training and Research Hospital, Adiyaman, Turkey, [3]The University of Alabama at Birmingham, Birmingham, AL, [4]Emory University Hospital, Atlanta, GA

Disclosures: Rebecca Obeng: None; Burcin Pehlivanoglu: None; Frank Schneider: None; Jessica Tracht: None; Alyssa Krasinskas: None; Michelle Reid: None; Yue Xue: None

Background: Histologically colonization of duodenal mucosa by invasive ampullary carcinoma cells can mimic high-grade precursor lesions of this region, causing a diagnostic challenge particularly in the evaluation of limited biopsy specimens. The added value of immunohistochemistry to routine hematoxylin and eosin (H&E) evaluation has not been evaluated.

Design: We reviewed 125 invasive ampullary carcinoma resections for histologic features of colonization, which included adjacent histologically similar invasive ampullary carcinoma and an abrupt transition between markedly atypical epithelium and normal duodenal epithelium (PMID: PMID:30212393). Thirty-eight cases (30%) were found to meet these criteria. Immunohistochemical stains for p53, SMAD4, MUC1 and MUC5AC were performed on the tissue blocks with both colonization and invasive carcinoma components. Four cases with tubular adenoma were used as controls.

Results: Aberrant p53 immunostaining was found in 30 (78%) cases including overexpression in 25 (65%) and lack of expression in 5 (13%) in these areas of colonization. Loss of SMAD4 staining was in 18 (47%). Sixteen (42%) cases showed both aberrant p53 and loss of SMAD4 expression. Diffuse and strong MUC1 staining was seen in all except one case (97%). Seven (18%) cases showed strong and diffuse MUC5AC staining, while 21 (55%) had strong, but patchy staining. Among 6 cases (16%) with normal p53 and intact SMAD4 expression, 3 cases had strong MUC5AC staining and all had MUC1 staining. Overall, thirty-seven cases had at least two positive immunomarkers in these areas of colonization. Interestingly, all 4 tubular adenomas showed intact SMAD4 and negative MUC5AC staining; only one had positive p53 and one had weak MUC1 staining compared to areas of colonization and invasive carcinoma within the same case. More importantly, the immunoprofile of all these markers showed concordance between areas of colonization and invasive carcinoma.

Figure 1 - 1701

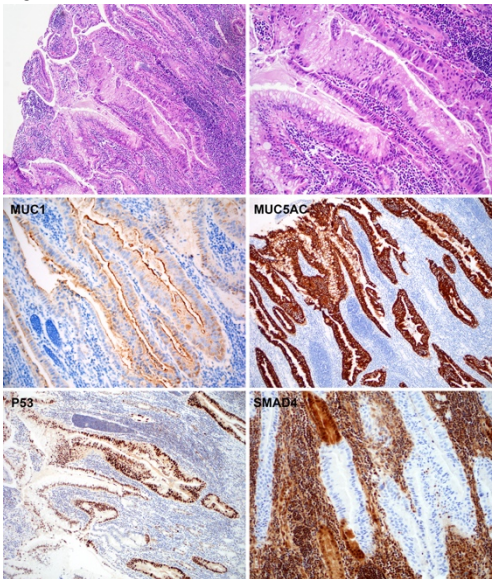

Conclusions: In summary, colonization is not an uncommon phenomenon and shows high concordance with invasive ampullary carcinoma. In combination with evaluation of morphology, an IHC panel including p53, SMAD4, MUC1 and MUC5AC may aid the diagnosis of surface mucosal colonization by adenocarcinoma in limited tissue samples.

1702 Area of residual tumor (ART) measurement has a prognostic value in post neoadjuvant resections for pancreatic ductal adenocarcinoma (PDAC).

Satoshi Okubo[1], Yoko Matsuda[2], Shinichiro Takahashi[1], Naoto Gotohda[1], Mari Mino-Kenudson[3], Motohiro Kojima[4]
[1]National Cancer Center Hospital East, Kashiwa, Japan, [2]Tokyo Metropolitan Geriatric Hospital, Tokyo, Japan, [3]Massachusetts General Hospital, Boston, MA, [4]National Cancer Center Hospital, Kashiwa, Chiba, Japan

Disclosures: Satoshi Okubo: None; Yoko Matsuda: None; Shinichiro Takahashi: None; Mari Mino-Kenudson: None; Motohiro Kojima: None

Background: Increasing numbers of PDACs are treated with neoadjuvant therapy in the hopes of achieving curative resection. However, an objective pathological assessment of tumor regression, and its prognostic role has not been well established. We have reported ART as a potential prognostic marker in multiple cancer types (rectal, lung, and gastric cancer) and proposed a practical assessment of tumor regression based on ART. Here we evaluated and correlated ART with clinicopathological features and prognosis in post neoadjuvant resections for PDAC.

Design: 107 patients with PDAC who had undergone post neoadjuvant resection at 5 institutions from 2006 – 2016 formed our study cohort. The measurement of ART was as follows: 1) The H.E slide with the largest slice of tumor was digitally scanned in each case. 2) The largest, viable residual tumor area was outlined and calculated using morphometric software. 3) Isolated, viable tumor foci more than > 2mm apart from the largest tumor area were also calculated individually. The sum of the tumor areas was defined as ART. 4) In situ lesions and acellular mucous lake were not included in this study. Cut-off value of ART was determined by usig ROC curve. Marked pathological response (PR) was defined as Evans grading system IIb ~ IV (destruction of more than 50% of tumor cells).

Results: Of 107 cases, resectable, borderline resectable, locally advanced and metastatic disease were 31 (29%), 52 (49%), 15 (14%), 9 (7%), respectively. 44 (41%) patients received chemoradiation therapy and 63 (59%) received chemotherapy before resection. The median value of ART was 162 mm^2 (range: 0 – 1062 mm^2). Cases with ART ≤ 63 mm^2 (22%) were less likely to have perineural invasion, vascular invasion and nodal metastasis compared to those with ART > 63mm^2. Median overall survival (OS) was 30.3 months in the entire cohort, 24.6 months in patients with ART > 63mm^2, and not reached in those with ART ≤ 63 mm^2. The recurrence rate was 78% in patients with ART > 63mm^2 and 32% in those with ART ≤ 63 mm^2 ($P < 0.01$). By multivariable analysis, ART $\leq$ 63 mm^2 was an independent predictor of longer OS and recurrence free survival, while PR was not. ART could predict patient outcomes regardless of pre-neoadjuvant tumor extent/resectability or therapeutic regimens (preoperative chemo- vs chemoradiation).

Figure 1 - 1702

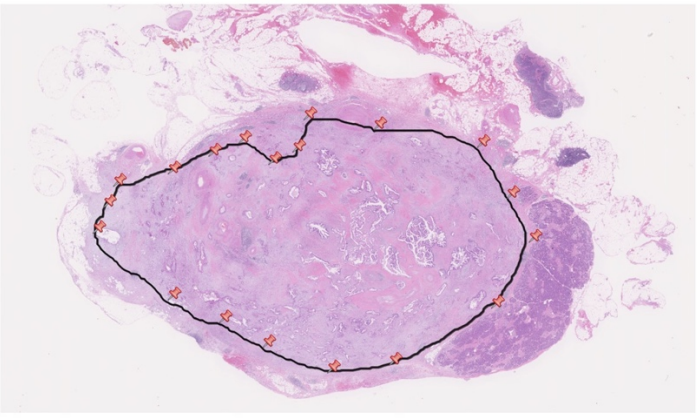

Figure 2 - 1702

Figure. Survival curves of patients classified by the degree of area of resident tumor.
A) Overall survival time, B) Relapse-free survival time

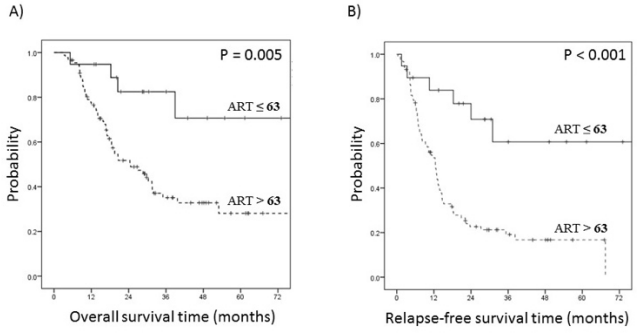

Conclusions: ART that is designed to be a more objective assessment of tumor regression may have a prognostic value in post neoadjuvant resections for PDAC.

1703 A Revised Model of Clonal Evolution of Intraductal Papillary Mucinous Neoplasm-related Pancreatic Carcinogenesis

Yuko Omori[1], Yusuke Ono[2], Mishie Tanino[3], Hidenori Karasaki[2], Hiroshi Yamaguchi[4], Yusuke Mizukami[5], Hiroyuki Maguchi[6], Toru Furukawa[1], Shinya Tanaka[7]

[1]Tohoku University Graduate School of Medicine, Sendai, Japan, [2]Institute of Biomedical Research, Sapporo Higashi Tokushukai Hospital, Sapporo, Japan, [3]Sapporo, Japan, [4]Tokyo Medical University, Tokyo, Japan, [5]Asahikawa Medical University, Asahikawa, Japan, [6]Center for Gastroenterology, Teine-Keijinkai Hospital, Sapporo, Japan, [7]Hokkaido University, Sapporo, Japan

Disclosures: Yuko Omori: None; Hidenori Karasaki: None; Hiroyuki Maguchi: None; Toru Furukawa: None; Shinya Tanaka: None

Background: Intraductal papillary mucinous neoplasms (IPMNs) are regarded as precursors of pancreatic ductal adenocarcinomas (PDACs), however, the mechanism of the progression is not well understood, which may intervene precise assessment of a cancer risk in patients with IPMNs. We investigated associations of IPMNs with concurrent PDACs by histologic and genetic analyses.

Design: In 30 pancreatectomy specimens concurrently with PDAs and IPMNs, 168 lesions of PDAs and IPMNs, including incipient foci, were mapped, microdissected, and examined for mutations in 18 PDAC-associated genes and protein expression of tumor suppressors.

Results: By clonal relatedness determined by shared driver mutations between PDAC and concurrent IPMN, the examined cases were classifiable into three distinct subtypes of molecular progression of IPMN toward PDAC. 12 PDACs harbored driver mutations shared by concurrent IPMNs, which was coined as sequential subtype. This subtype was characterized by less *KRAS* diversity in incipient foci with frequent *GNAS* mutations. 11 PDACs harbored driver mutations partially shared by concurrent IPMNs, which was coined as branch-off subtype. In this subtype, PDAC and concurrent IPMN harbored identical *KRAS* mutations but different *GNAS* profile although they are closely located. Additional whole-exome sequencing and methylation analysis for these lesions indicated clonal with divergent progression, i.e., fork-like relatedness. 10 PDACs harbored distinct driver mutations compared to concurrent IPMNs, which was coined as de novo subtype. Notably, the branch-off and the de novo subtype were related to the substantial heterogeneity in early clones marked by various *KRAS* mutations. Furthermore, patients with PDACs of the branch-off subtype were found to have longer disease-free survival than patients with PDACs of the de novo or the sequential subtypes.

Conclusions: Detailed histologic and genetic analysis of PDACs and concurrent IPMNs uncovered three different ways of molecular progression of IPMNs toward PDAs, namely, sequential, branch-off, and de novo subtypes. This subtype classification may be associated with clinicopathological features and serve for designing an efficient surveillance program of patients with IPMN.

1704 Increased rRNA Synthesis Activity in Pancreatic Intraepithelial Neoplasia

Busra Ozbek[1], Qizhi Zheng[1], Laura Wood[2], Ralph Hruban[3], Marikki Laiho[1], Angelo De Marzo[1]
[1]Johns Hopkins University, Baltimore, MD, [2]Johns Hopkins Hospital, Baltimore, MD, [3]Johns Hopkins Medical Institutions, Baltimore, MD

Disclosures: Busra Ozbek: *Grant or Research Support*, BlueOne Bioscience; Qizhi Zheng: None; Laura Wood: None; Ralph Hruban: None; Marikki Laiho: *Grant or Research Support*, Blueone Biosciences; Angelo De Marzo: *Grant or Research Support*, Blueone Biosciences

Background: Ribosome biogenesis is required for cell growth and division, and is often increased in cancer cells and their precursors . The rate-limiting step of ribosome biogenesis is transcription of the 45S precursor rRNA by RNA polymerase I (Pol I). We developed a quantitative chromogenic *in situ* hybridization assay to the 5′ external transcribed spacer (5'ETS) of the 45S rRNA that is a surrogate for RNA Pol I activity *in vivo* (PMID: 28119429). We reported a marked increase in 5′ ETS/45S CISH signal in human high-grade PIN and prostatic adenocarcinomas, although other cancers have not been tested. Given that RNA Pol I inhibitors are in development as potential anti-neoplastic agents (PMID: 24434211), it is important to determine the range of cancer types and precursors that have elevated RNA Pol I activity. Pancreatic intraepithelial neoplasia (PanIN) lesions are microscopic precursors of invasive pancreatic ductal adenocarcinoma. In this study we examined expression of 5′ ETS/45S rRNA in human PanINs.

Design: FFPE blocks were obtained from patients undergoing partial or complete pancreatectomy at a single institution. Cases without invasive carcinoma were preferentially selected to avoid cancerization of the ducts. 5′ETS/45S CISH was performed as described (PMID: 28119429) on 14 FFPE blocks from 10 patients. For each patient, H&E slides and 5′ETS/45S CISH slides were subjected to whole slide scanning. PanINs and regions containing normal appearing ducts were separately annotated and quantified using HALO image analysis software (Indica Labs). We used a nuclear area fraction quantification algorithm and optical density measurements to examine differences. Additional cases are being analyzed.

Results: Hybridization signals were consistent with nucleolar localization in all cell types. There was a significant increase in nuclear area fraction (median normal duct = 0.055, median PanIN = 0.16; p =0.0001 by paired t-test) and optical density (median normal duct = 0.49, median PanIN =0.56, p = 0.0005 by paired t-test) in PanIN lesions compared to normal ductal cells.

Figure 1 - 1704

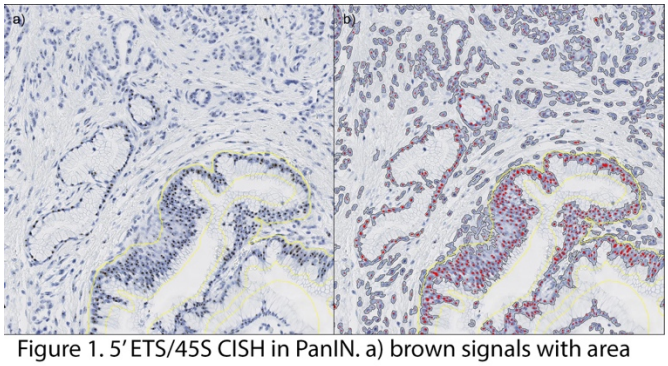

Figure 1. 5′ ETS/45S CISH in PanIN. a) brown signals with area of epithelium outlined. b) Red represents positive signals. Black outlines nuclear area.

Figure 2 - 1704

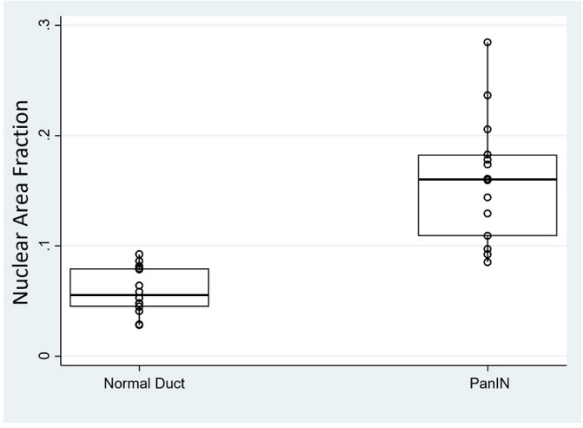

Conclusions: In situ hybridization signals for the 45S rRNA were significantly elevated in PanINs as compared to matched normal pancreatic ductal epithelium from the same patients. As pharmacological inhibition of RNA Pol I is a potentially important therapeutic strategy in cancer treatment, these results suggest that PanIN precursors to pancreatic ductal adenocarcinomas may be important targets for such an approach.

1705 M2 Tumor-Associated Macrophages in Pancreatic Neuroendocrine Tumors and Solid Pseudopapillary Neoplasms

Hyunjin Park[1], Yangkyu Lee[2], Hyejung Lee[3], Soomin Ahn[4], Haeryoung Kim[5]
[1]Seoul National University Bundang Hospital, Seongnam, Korea, Republic of South Korea, [2]Seoul National University Bundang Hospital, Gyeonggi-Do(Seoul), Korea, Republic of South Korea, [3]Seoul National University Hospital, Seoul, Korea, Republic of South Korea, [4]Seoung-Nam, Korea, Republic of South Korea, [5]Seoul, Korea, Republic of South Korea

Disclosures: Hyunjin Park: None; Yangkyu Lee: None; Hyejung Lee: None; Soomin Ahn: None; Haeryoung Kim: None

Background: Tumor-associated macrophages have been shown to play a protumorigenic role in pancreatic adenocarcinomas; however, the significance of M2 macrophage infiltration in pancreatic neuroendocrine tumors (PanNETs) and solid pseudopapillary neoplasms (SPN) is not clear. We performed a quantitative analysis of two M2 macrophage-related markers, CD163 and CD206, in PanNETs and SPNs, and correlated the results with microvascular density, proliferative activity and other clinicopathological factors.

Design: Immunohistochemistry for CD163 and CD206 was performed on surgically resected whole tissue sections from PanNETs (n=27) and SPNs (n=29). CD163 and CD206-positive macrophages were manually counted at ten high-power fields (HPF) under the microscope in the tumor, the peritumoral parenchyme and remote non-neoplastic parenchyma. CD34-positive microvascular density was counted in ten HPFs and tumoral Ki-67 indices were calculated in 200-300 cells using an automated algorithm with Aperio Imagescope.

Results: Intratumoral and peritumoral CD163-positive macrophage counts were positively correlated with each other, for both PanNETs (p=0.012) and SPNs (p=0.001). CD206-positive macrophages were more abundant in peritumoral stroma than remote parenchyma (p=0.004) in PanNET while intratumoral CD163-positive macrophages were more abundant than remote parenchyma (p=0.003) in SPN. Peritumoral CD163-positive macrophage counts in PanNETs showed significant positive correlations with tumor size (p=0.003), mitotic activity (p=0.005 and higher pathologic tumor stage (p=0.047). Similarly, in SPNs, higher intratumoral- and peritumoral CD163-positive macrophage counts were both associated with higher Ki-67 labeling index (intratumoral: p= p<0.001, peritumoral: p=0.000). No significant associations were found between CD206-positive macrophage counts and any clinicopathological factors for PanNETs and SPNs, and no associations were seen between M2 macrophage count and microvascular density.

Conclusions: M2 tumor-associated macrophages are frequently seen in PanNETs and SPNs and high CD163-positive macrophage counts are associated with increased proliferative activity, tumor size and stage, suggesting that CD163-positive macrophages may play important roles in promoting the aggressive behavior of these tumors.

1706 Molecular Mechanisms of Transcription Factor E3 (TFE3) Upregulation in Solid Pseudopapillary Neoplasm of Pancreas using FISH

Rugved Pattarkine[1], Christopher Gault[2], John Fallon[3], Chitra Kumar[1], Minghao Zhong[1]
[1]Westchester Medical Center, Valhalla, NY, [2]Westchester Medical Center/Mid-Hudson Regional Hospital, New York, NY, [3]New York Medical College and Westchester Medical Center, Valhalla, NY

Disclosures: Rugved Pattarkine: None; Christopher Gault: None; John Fallon: None; Minghao Zhong: None

Background: Solid Psudopapillary neoplasm (SPN) is a rare and distinctive tumor of the pancreas. The pathogenesis and genetic alterations are far from being well understood. TFE3 has recently been identified as a diagnostic marker for SPN. TFE3 is a MiTF family transcription factor thought to promote tumorigenesis through activation of the Wnt pathway. TFE3 overexpression most notably occurs in other tumors (translocation renal cell carcinoma, alveolar soft parts sarcoma) through a specific translocation event. The molecular mechanism by which TFE3 amplification occurs in SPN is not known. Here we use TFE3 specific FISH probes to determine if TFE3 overexpression in SPN occurs through an amplification or translocation mechanism.

Design: We performed a comprehensive and retrospective review (clinical, demographic and pathologic features) of all solid psudopapillary neoplasm cases at our institute from 2011-2018 and identified 50 cases. All the cases were stained with IHC for TFE3. 10 of these cases were strong nuclear positive for TFE3(Figure 1) and were selected for FISH processing based on this criterion. A LSI TFE3 (Xp11.23) Dual Color Break Apart Rearrangement Probe, orange color probe binding 5” end and green color probe binding 3” end of the TFE3 gene was added to the blnk slides of parafin embeded tissue , after a standardized proteolysis pretreatment protocol.

Results: FISH probes for TFE3 were used on the 10 SPN cases which were positive for TFE3 by immunohistochemistry. FISH signal (red and green) was normal in all the selected tumor cells in metaphases showed single loccus of signal for male patients and 2 sets of signals for female patients(Figure 2); highlighting that the TFE3 gene located on chromosome X is intact and not amplified. No evidence of a translocation, genetic breakage event, or evidence of gene amplification in10 out of 10 (100%) cases.

Figure 1 - 1706

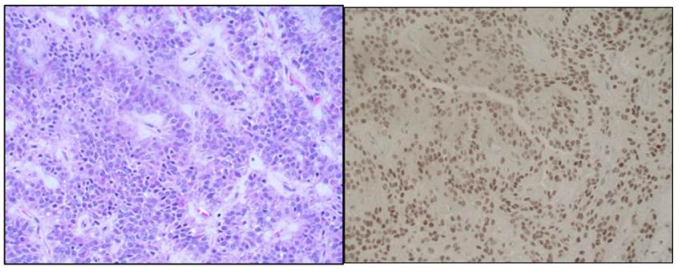

Figure 1. A) H&E stained slide of the SPN
B) Immunostaining with TFE3 of the SPN

Figure 2 - 1706

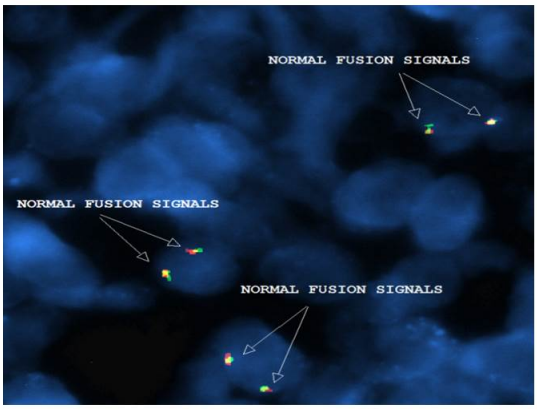

Figure 2. A) LSI TFE3 (Xp11.23) Dual Color Break Apart Rearrangement
Probe showing two fusion signals which represent two intact TFE3 gene in tumor cells of a female patient (hence two sets of genes).

Conclusions: We conclude that the neoplastic cells of SPN do not show any evidence of gene amplification, translocation, or other TFE3 chromosomal breakage event. Hence the upregulation of TFE3 gene associated with SPN likely occurs through a distinct mechanism unrelated to TFE3 translocation. Although we did not detect any abnormal FISH signal the possibility of presence of such mutations cannot be completely ruled out (requiring a larger sample size) and a continuation of this study on a larger level is being done at our department.

1707 Pancreatic Invasive Ductal Adenocarcinomas (PDACs) Arising in Association with Intraductal Papillary Mucinous Neoplasms (IPMNs) versus "Pseudo-IPMNs": Clinicopathologic Analysis and the Importance of the Distinction

Burcin Pehlivanoglu[1], Takashi Muraki[2], Michelle Reid[3], Bahar Memis[4], Yue Xue[3], Serdar Balci[5], Ipek Erbarut Seven[6], Juan Sarmiento[7], David Kooby[7], Shishir Maithel[7], Susan Tsai[8], Kathleen Christians[8], Douglas Evans[8], N. Volkan Adsay[9]
[1]Adiyaman University Training and Research Hospital, Adiyaman, Turkey, [2]Matsumoto, Japan, [3]Emory University Hospital, Atlanta, GA, [4]TC.SBU. Sanliurfa Mehmet Akif Inan Training and Research Hospital, Sanliurfa, Turkey, [5]Ankara, Turkey,[6]Marmara University, Istanbul, Turkey, [7]Emory University, Atlanta, GA, [8]Medical College of Wisconsin, Milwaukee, WI, [9]Koç University Hospital, Istanbul, Turkey

Disclosures: Burcin Pehlivanoglu: None; Takashi Muraki: None; Michelle Reid: None; Bahar Memis: None; Yue Xue: None; Serdar Balci: None; Ipek Erbarut Seven: None; Juan Sarmiento: None; David Kooby: None; Shishir Maithel: None; Susan Tsai: None; Kathleen Christians: None; Douglas Evans: None; N. Volkan Adsay: None

Background: The literature is highly conflicting regarding the clinicopathologic characteristics of PDACs arising in association with IPMNs.

Design: All cases in the authors' files that have PDAC (tubular, pancreatobiliary-type adenocarcinomas) associated with a classical IPMN or with any cyst >1 cm were assessed. In identification of IPMN and its distinction from mimickers, recently proposed criteria (PMID: 26559377; 25775066) were used and a purist's approach was utilized (clinically/grossly diagnosable and >1 cm cystic/intraductal component revealing clear-cut papillae formation of the IPMN type). Cases qualified as "incipient IPMNs" were excluded. Separately, to determine the relative frequencies, 424 consecutive PDACs were analyzed systematically for the presence of a >1 cm cystic component.

Results: There were 59 bona-fide IPMN-associated PDACs and another 40 cases were PDACs with a >1 cm cyst that we re-classified as "pseudo-IPMN"-associated PDACs. These included 15 retention cysts, 6 large duct-type PDACs; 5 with pseudocysts; 5 cystic tumor necrosis partially lined by carcinomatous epithelium; 4 "simple mucinous cysts" (PMID:27740966); 3 paraduodenal wall cyst of groove pancreatitis (PMID: 28795998), and 2 congenital cysts. About third of these 40 cases had been diagnosed as IPMN preoperatively. Detailed clinicopathologic characteristics are documented in the table. IPMN-associated PDACs had a significantly better prognosis compared to pseudo-IPMN-associated PDACs as well as conventional (non-cystic) PDACs. This survival advantage of IPMN-associated PDACs appeared to persist even when stage-matched for T1 cases (p=0.03); however, the numerical differences did not reach statistical significance for T2 and T3 cases due to small numbers in these stage categories.

	Conventional (non-cystic) PDACs (Control group)	IPMN-associated PDACs	Pseudo-IPMN-associated PDACs	P-value
Number of the cases (all cases including consultations)	377	59	40	
Frequency in 424 systematically evaluated cases	89% (n=377)	6.1% (n=26)	4.9% (n=21)	
Mean age (years) **Range (years)**	65 (29-89)	68 (35-82)	67 (50-87)	
Gender, male (%)	48%	59%	44%	
Cysts localized in body/tail	N/A	22%	50%	
Mean size of PDAC (cm) **Range (cm)**	3 (0.1-10.6)	2.7 (0.1-7.0)	3.8 (1.2-7.0)	**< 0.001**
Mean size of cystic component (cm) **Range (cm)**	N/A N/A	4.2 (1.0-8.7)	1.9 (1.0-11.0)	**< 0.001**
T-stage (AJCC-8) T1 T2 T3	22% 63% 15%	66% 24% 10%	69% 21% 10%	**< 0.001**
Preoperative diagnosis of "IPMN"	N/A	63%	33%	
Overall survival Median survival (months) 1-year survival rate (%) 3-year survival rate (%) 5-year survival rate (%)	24 70% 34% 18%	44 88% 55% 32%	23 77% 22% 0%	**IPMN-associated vs Pseudo-IPMN-associated: p=0.004** **IPMN-associated vs conventional (non-cystic): p=0.019**

Conclusions: 6% of PDACs arise in association with IPMN, but another 5% is accompanied by pseudo-IPMNs. IPMN-associated PDACs seem to be slightly more common in men, have significantly larger mean cyst size (4.2 cm) than the pseudo-IPMN-associated PDACs (1.9 cm) but their size of invasive carcinoma is smaller (2.7 cm vs 3.8 cm). Most importantly, IPMN-associated PDACs appear to have a significantly better clinical outcome compared with conventional (non-cystic) PDACs. In contrast, pseudo-IPMN-associated PDACs are highly aggressive as a group, perhaps even more so than non-cystic PDACs, although it should be remembered that this is a heterogenous group (including necrotic PDACs) and there may be variations in the subset.

1708 BAP1 and SMAD4 Immunohistochemistry in 218 Pancreatobiliary Adenocarcinomas Stratified by Anatomic Site

Daniel Pelletier[1], Isabelle Cui[1], Jason Hornick[2], Craig Dunseth[3], Andrew Bellizzi[1]
[1]University of Iowa Hospitals and Clinics, Iowa City, IA, [2]Brigham and Women's Hospital, Harvard Medical School, Boston, MA, [3]Coralville, IA

Disclosures: Daniel Pelletier: None; Isabelle Cui: None; Jason Hornick: None; Craig Dunseth: None; Andrew Bellizzi: None

Background: Germline mutations in the deubiquitylase *BAP1* predispose to uveal (and to a lesser extent cutaneous) melanoma and mesothelioma. Biallelic BAP1 inactivation typically leads to loss of nuclear immunohistochemical expression. Somatic BAP1 inactivation is frequent in mesothelioma, and BAP1 immunohistochemistry (IHC) has become a mainstream "mesothelioma marker." Recent studies of the mutational landscape of cholangiocarcinoma (CC) have reported frequent somatic inactivation (~25%) in intrahepatic (i) tumors; inactivation in extrahepatic (e) CC appears less frequent (though fewer eCCs have been studied). SMAD4 inactivation, also leading to IHC loss, is frequent in pancreas cancer (PDAC), though it is also reported throughout the biliary tree. We sought to explore the reciprocal relationship between BAP1 and SMAD4 expression in a large cohort of pancreatobiliary adenocarcinomas stratified by anatomic site.

Design: BAP1 and SMAD4 IHC was performed on tissue microarrays of 131 CCs (97 primary, 34 metastatic) and 87 metastatic PDACs. Primary CCs included 27 intrahepatic, 8 perihilar, 3 cystic duct, 46 gallbladder, 12 distal, and 1 unspecified tumors. BAP1 was assessed as intact (any nuclear staining) or lost (no nuclear staining in the presence of intact internal control); SMAD4 was similarly assessed as intact (any nuclear and/or cytoplasmic staining) or lost (no staining in the presence of intact internal control). Fisher's exact test was used with $p<0.05$ considered significant.

Results: BAP1 inactivation was seen in 11% of CCs and 2.6% of PDACs (p=0.056). SMAD4 inactivation was seen in 35% of CCs and 37% of PDACs (p=0.88). BAP1 inactivation was most frequent in iCC (22%; p=0.027 compared to all other CCs). SMAD4 inactivation was least frequent in iCC (16%; p=0.027 compared to all other CCs). In 3 BAP1-inactivated primary CCs with matched metastases, inactivation was also seen in the metastasis. BAP1 and SMAD4 inactivation were mutually exclusive (of 15 BAP1-inactivated samples, only 1 showed SMAD4 inactivation). BAP1 and SMAD4 results by anatomic site are presented in the Table.

Tumor Type	BAP1 inactivation	SMAD4 inactivation
Intrahepatic	22% (6/27)	16% (4/25)
Perihilar	13% (1/8)	43% (3/7)
Cystic duct	0% (0/3)	33% (1/3)
Gallbladder	7% (3/46)	37% (16/43)
Distal	0% (0/12)	60% (6/10)
Pancreatic	3% (2/77)	37% (31/84)

Conclusions: BAP1 inactivation is common in iCC, though it is occasionally seen throughout the pancreatobiliary tree. We observed similar rates of SMAD4 inactivation in PDAC and eCC. These results have implications for our interpretation of BAP1 and SMAD4 clinical IHC (i.e., BAP1 loss implies iCC; SMAD4 loss does not reliably distinguish PDAC from eCC and does not exclude iCC).

1709 Pancreatic Acinar Cell Carcinoma Demonstrates an Active Tumor Immune Microenvironment

David Peske[1], Elizabeth Engle[2], Laura Wood[2], Ralph Hruban[3], Elizabeth Jaffee[3], Elizabeth D Thompson[2]
[1]Baltimore, MD, [2]Johns Hopkins Hospital, Baltimore, MD, [3]Johns Hopkins Medical Institutions, Baltimore, MD

Disclosures: David Peske: None; Elizabeth Engle: None; Laura Wood: None; Ralph Hruban: None; Elizabeth Jaffee: *Primary Investigator*, Aduro Biotech; *Advisory Board Member*, Genocea, Adaptive Biotech, DragonFly, CSTONE; *Grant or Research Support*, Aduro Biotech, Amgen, Bristol-Myer Squibb, Hertix, Corvus; Elizabeth D Thompson: None

Background: Pancreatic acinar cell carcinoma (ACC) is a rare and aggressive malignancy with limited treatment options. While characterization of the tumor immune microenvironment (TME) of pancreatic ductal adenocarcinoma shows domination by immunosuppressive and immunoregulatory molecules, no studies have evaluated the TME in ACC and addressed the possibility of immune-based therapeutic intervention in this tumor type. Here we describe the TME a cohort of primary ACC surgical resection specimens.

Design: Whole slides from 23 ACC resection specimens were labeled by immunohistochemistry for CD4, CD8, CD20, FoxP3, CD68, Myeloperoxidase, PD-L1, PD-1 and IDO. Density of tumor infiltrating immune cells (TIL) was scored as none (0), rare (1, <5% of tumor area), mild (2, 5-10%), moderate (3, 11-50%), or brisk (4, >50%) and the pattern of TIL was recorded. Expression of PD-L1 or IDO on tumor cells was scored based on membranous or cytoplasmic staining, respectively, with >1% labeling considered positive. PD-L1 or IDO expression on TIL was scored as none (0, 0%), focal (1, <5%), moderate (2, 5-50%), or diffuse (3, >50%).

Results: All ACC showed some degree of immune infiltration (39% focal, 52% moderate, 9% brisk). 65% of ACC showed an “interface” pattern, with TIL predominantly located at the interface between invasive tumor and normal pancreas and 22% showed more “diffuse” TIL within tumor nests. TIL were comprised of a mix of T cells, B cells and myeloid cells. 13% of cases showed B-cell rich lymphoid aggregates at the tumor periphery suggestive of tertiary lymphoid structures. 48% of ACC showed tumor cell labeling for PDL1 and all cases contained PDL1+ TIL. While overall, PDL1+ ACC and ACC with PD-L1+ TIL were more likely to have higher immune cell density (73% vs 50%, p=0.4 and 735 vs 42%, p=0.2, respectively) these were statistically non-significant trends and multiple tumors with high levels of PDL1 labeling on tumor cells had very low TIL density. 17% of ACC showed IDO expression.

Conclusions: Pancreatic ACC show an active TME characterized by robust lymphocytic and myeloid infiltration with expression of PDL1 on both tumor cells and TIL. High levels of PDL1 in ACC with both high and low TIL density suggests the presence of both adaptive and innate expression PDL1. These results indicate that immunomodulatory therapies may be effective in the treatment of ACC, and support further studies to characterize the mechanisms of PDL1 expression and the presence of other immunosuppressive factors in ACC.

1710 Adenosquamous Carcinoma of the Pancreas Shows an Active Tumor Immune Microenvironment with Expression of Multiple Immunosuppressive and Immunoregulatory Molecules

David Peske[1], Michael Noe[2], Elizabeth Engle[3], Ralph Hruban[4], Elizabeth Jaffee[4], Robert Anders[5], Elizabeth D Thompson[3]
[1]Baltimore, MD, [2]Johns Hopkins School of Medicine, Baltimore, MD, [3]Johns Hopkins Hospital, Baltimore, MD, [4]Johns Hopkins Medical Institutions, Baltimore, MD, [5]Johns Hopkins, Baltimore, MD

Disclosures: David Peske: None; Michael Noe: None; Elizabeth Engle: None; Ralph Hruban: None; Elizabeth Jaffee: *Primary Investigator*, Aduro Biotech; *Advisory Board Member*, Genocea, Adaptive Biotech, DragonFly, CSTONE; *Grant or Research Support*, Aduro Biotech, Amgen, Bristol-Myer Squibb, Hertix, Corvus ; Robert Anders: *Advisory Board Member*, Bristol-Myers Squibb; *Advisory Board Member*, Merck SD; *Advisory Board Member*, Astra Zeneca; *Grant or Research Support*, Five Prime Therapeutics; *Grant or Research Support*, FLX Bio; Elizabeth D Thompson: None

Background: Adenosquamous carcinoma of the pancreas (ASQ) is an aggressive malignancy with a poor response to standard therapies. Targeting immunosuppressive molecules has shown promise in other tumors, particularly those with an active tumor immune microenvironment (TME), mutations in DNA mismatch repair (MMR) proteins, and/or expression of the immunusuppressive molecules. We previously documented an active TME in ASQ with high levels of PDL1 expression and now characterize additional immunosuppressive molecules and MMR proteins status.

Design: Tissue microarrays with 34 ASQs (2 cores per tumor), previously labeled for PDL1, PD1, CD8, CD68 and FoxP3 were labeled for IDO, LAG3, TIM3, VISTA, and MMR proteins (MLH1, PMS2, MSH2 and MSH6). Tumor infiltrating immune cell (TIL) density, PD-L1 expression, CD8 and FoxP3 counts and density of CD68+ cells were previously evaluated. IDO labeling on ASQ tumor cells was scored (>1% positive), and percentage of IDO, LAG-3, TIM-3, and VISTA expression by TIL was scored as negative (0, 0%), focal (1 <5%), moderate (2, 5-50%), or diffuse (3, >50%). Nuclear MMR protein expression was scored as intact/lost.

Results: 71% of ASQ expressed IDO on tumor cells and 53% had the combined presence of PDL1+ and IDO+ tumor cells. PDL1+ tumors were more likely to also express IDO than PD-L1- tumors (81% vs. 50%, p=0.14). IDO+ ASQ were more likely to have moderate/diffuse PD-L1+ TIL (p=0.005). 58% of ASQ had the combined presence of PDL1+TIL, IDO+TIL, LAG3+TIL and VISTA+TIL. 76% of ASQ showed populations of TIL with labeling for at least 3 immunosuppressive molecules, while 6% of ASQ showed no TIL labeling for all of the immunosuppressive molecules tested and all cases were negative for TIM3. ASQ with tumor cell labeling for PD-L1, IDO, or both were more likely to have TIL with the combined presence of PDL1, IDO, LAG3 and VISTA (p=0.03, 0.05 and 0.03, respectively). ASQ with IDO+TIL, LAG3+TIL or VISTA+TIL showed higher average CD8 and FoxP3 cell counts than negative tumors (CD8: p=<0.001, 0.1 and 0.05, FoxP3: p=<0.001, p=0.01, and p=0.005, respectively), with increased CD8/FoxP3 ratios in tumors.

Conclusions: ASQ have an active TME with robust TIL that is balanced by adaptive immune resistance and the expression of multiple inhibitory signaling molecules. These results provide further support for the development of immune-based interventions in ASQ and suggest that targeting multiple immunoregulatory pathways may be most beneficial in this patient population.

1711 Paraganglia of the Gallbladder: A Potential Diagnostic Pitfall That May Lead to a Misdiagnosis of Neuroendocrine Neoplasm

Bharat Ramlal[1], Theresa Voytek[1], Saverio Ligato[2]
[1]Hartford Hospital, Hartford, CT, [2]Hartford Hospital, Canton, CT

Disclosures: Bharat Ramlal: None; Theresa Voytek: None; Saverio Ligato: None

Background: Paraganglias (PGs) of the gallbladder are rarely seen, and due to their close resemblance to neuro-endocrine cells may cause an erroneous interpretation as low-grade neuroendocrine tumors. The aim of this study was to evaluate the incidence and histological features of PGs of the gallbladder and discuss potential interpretative pitfalls.

Design: A retrospective review of cholecystectomies resected in our hospital from March 2017 to August 2017 was performed. Routine H&E sections from the body and cystic duct margin (1 to 3 blocks) were reviewed. Immunohistochemistry (IHC) for Chromogranin, Synaptophysin and S100 were performed in selected cases, and presence of paraganglionic tissue and its association with other pathologies was recorded.

Results: A total of 365 gallbladders were reviewed, and in 16 cases (4.4%) PGs were identified within the sub-serosal connective tissue of gallbladder wall (15) or cystic duct (1). Histologically, they were well-demarcated, ovoid structures, ranging in size from 0.2 cm to 0.5 cm, usually in proximity to small capillaries, nerve, and ganglia. The dominant cell type was composed of polygonal cells with round to oval vesicular nuclei and granular, amphophilic cytoplasm. Strong, cytoplasmic expression for Synaptophysin and Chromogranin was identified. In 15 cases the gallbladder showed cholecystitis and in 1 case the cholecystectomy was incidental with a pancreaticoduodenectomy for pancreatic adenocarcinoma and showed no histopathologic abnormalities. Interestingly, 1 of 16 cases, positive for chromogranin and synaptophysin, was initially misinterpreted as a neuroendocrine neoplasm involving the lymphatic spaces of the gallbladder wall, (Fig. 1) prompting a diagnostic work-up to identify a primary tumor. However, subsequent IHC stain for S100 was

performed highlighting a minor component of S100 positive sustentacular cells with scant cytoplasm (Fig. 2) confirming the diagnosis of paraganglia.

Figure 1 - 1711

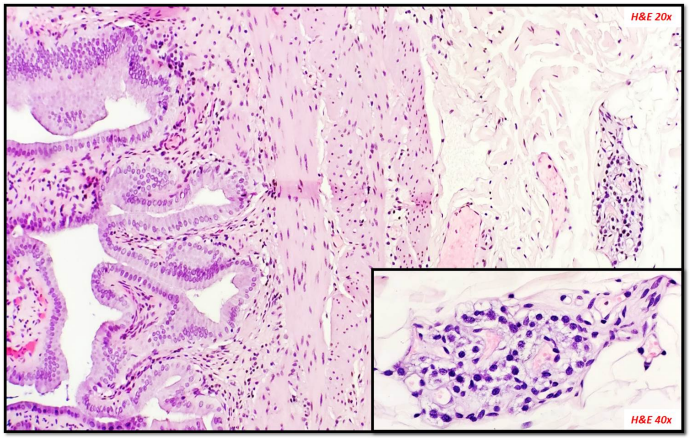

Figure 2 - 1711

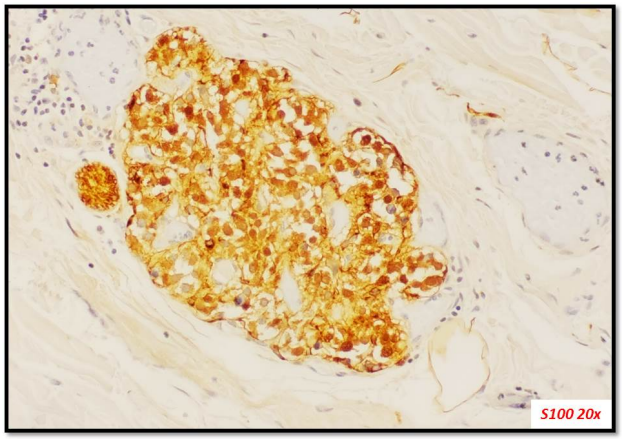

Conclusions: Our study confirms that, although uncommon, PGs can be identified in the gallbladder. Awareness of the features of PGs and their presence in the gallbladder can avoid misinterpretation of these benign incidental findings as neoplastic; thereby preventing additional testing and unnecessary diagnostic work-ups.

1712 Axial Standardized Protocol Versus "Traditional" Protocol for Prosection of Pancreatoduodenectomies: Which Method is Better? A Ten Year Experience in a Tertiary Care Center

Bharat Ramlal[1], Ali Kazerouni Timsar[2], Saverio Ligato[3]
[1]Hartford Hospital, Hartford, CT, [2]Montefiore Medical Center, Bronx, NY, [3]Hartford Hospital, Canton, CT

Disclosures: Bharat Ramlal: None; Ali Kazerouni Timsar: None; Saverio Ligato: None

Background: The Pancreatobiliary Pathology Society (PPS) is currently debating the best method for prosecting pancreaticoduodenectomy (PD) performed for pancreatic ductal adenocarcinoma (PDAC). In Europe, studies have shown that the implementation of an axial standardized protocol (ASP) may lead to a more accurate examination with statistically significant differences with respect to margin status, number of lymph nodes (LNs) retrieved, identification of lymphovascular (LVI) and perineural invasion (PNI) compared to the “traditional” protocol (TP) currently used in many institutions in the U.S. The goal of our study was to assess the ASP and compare the results to the TP.

Design: In this retrospective study, 53 PDs performed for PDAC over a ten-year period were reviewed. 30 PDs (2000-2005), prosected by conventional bivalving or multivalving (TP), underwent selective margins submissions taken closest to the tumor, and “orange-peeling” of the peripancreatic soft tissue for the harvesting of LNs. Instead, 23 cases (2006-2010) prosected by ASP, were differentially inked prior to axial sectioning perpendicular to the duodenal axis and the surgical margins were completely submitted. The peripancreatic LNs were directly obtained from the examination of the peripancreatic soft tissue. All cases were evaluated for – marginal status, positive / total # of LNs, LVI, and PNI.

Results: The 30 PDs prosected by TP had a positive microscopic margin (R1) rate of 53%, an average number of positive vs harvested LNs of 2.1/14.3, LVI of 25% and PNI rate of 65%. The 23 PDs grossed using the ASP, demonstrated a positive R1 rate of 83%, an average number of positive vs harvested LNs of 4.6/21.7, LVI rate of 65% and PNI rate of 100%. The difference between these two groups was statistically significant with a $p<0.5$. (Table 1).

Figure 1 - 1712

	Traditional Protocol	Axial Standardized Protocol	P-Value
Average # of Lymph Nodes Harvested	14.3	21.7	0.003
Average # of Positive Lymph Nodes	2.3	4.6	0.035
Lymphovascular Invasion (%)	30	70	0.003
Peri-neural Invasion (%)	73	96	0.032
R1 Resection Rates (%)	57	83	0.046

Conclusions: Similar to other studies, ours confirms that ASP for PDAC identifies higher rates of R1 resection, LVI and PNI, suggesting that the ASP may be a better method for the pathological evaluation and accurate staging of these specimens. Although a greater number of both positive and harvested LNs were apparently identified in our cohort, due to the lack of documentation of a structured sequential submission of the slices of tissue examined by ASP, it is possible that we overestimated the number of LNs obtained by ASP. Additional studies addressing this issue are necessary, a topic currently being addressed by the PPS.

1713 Histologic Types of Ampullary Carcinoma: Frequency and Clinicopathologic Associations in 367 Cases

Michelle Reid[1], Yue Xue[1], Serdar Balci[2], Burcin Pehlivanoglu[3], Ipek Erbarut Seven[4], Takuma Tajiri[5], Nobuyuki Ohike[6], Keetaek Jang[7], Grace Kim[8], Juan Sarmiento[9], David Kooby[9], Shishir Maithel[9], N. Volkan Adsay[10]
[1]Emory University Hospital, Atlanta, GA, [2]Ankara, Turkey, [3]Adiyaman University Training and Research Hospital, Adiyaman, Turkey, [4]Marmara University, Istanbul, Turkey, [5]Tokai University Hachioji Hospital, Hachioji, Japan, [6]Showa University Fujigaoka Hospital, Yokohama, Japan, [7]Samsung Medical Center, Seoul, Korea, Republic of South Korea, [8]University of California, San Francisco, San Francisco, CA, [9]Emory University, Atlanta, GA, [10]Koç University Hospital, Istanbul, Turkey

Disclosures: Michelle Reid: None; Yue Xue: None; Serdar Balci: None; Burcin Pehlivanoglu: None; Ipek Erbarut Seven: None; Takuma Tajiri: None; Nobuyuki Ohike: None; Keetaek Jang: None; Grace Kim: None; Juan Sarmiento: None; David Kooby: None; Shishir Maithel: None; N. Volkan Adsay: None

Background: The relative rarity and highly variable definition of what constitutes ampullary cancer has resulted in highly conflicting literature on the frequency and the clinicopathologic associations of different histologic carcinoma types occurring in the ampulla.

Design: All pathology material and clinical data on 367 ACs that were stringently defined using recently revised classification guidelines were reviewed.

Results: TABLE 1. (Detailed clinicopathologic characteristics are documented in the table). While the majority of ACs were conventional tubular-type adenocarcinomas (pancreatobiliary (PB), intestinal (INT) or mixed phenotypes), ~ 20% of cases were non-glandular carcinoma types. Noteworthy associations included: Non-glandular carcinomas, especially medullary and mucinous, occurred more frequently in men; Medullary AC occurred in slightly younger patients; Poorly-cohesive (signet-ring; PCC/SR) and PB-patterned tubular carcinomas showed propensity for PNI; LVI was low in INT but high in mucinous and PB-type; LN metastasis was low in INT but high in mucinous; medullary and PB presented at higher T-stage (T3/T4) ; 5-year survival was low in PCC/SR cases, while medullary seemed more indolent despite being advanced tumors. MSI was seen in 23/127 (18%), including 9/11 medullary carcinomas but rare in mixed-mucinous cases. Of 145 ACs tested PB tended to be MUC1 (+), INT MUC2/CDX2 (+) and almost all PCC/SRs were MUC5AC (+).

	N	Glandular-Intestinal (n=24) %	Glandular-Mixed, Intestinal Predominant (n=53) %	Glandular-PB (n=133) %	Glandular-Mixed, PB Predominant (n=76) %	Glandular-Other (n=3) %	Nonglandular-Poorly Cohesive (n=9) %	Nonglandular Mucinous (n=33) %	Nonglandular-Medullary (n=11) %	Nonglandular-Adenosquamous (n=3) %	Nonglandular-Other (n=22) %	p value
Gender: Male	360	58.3	53.8	48.8	48.8	66.7	66.7	71.9	81.2	100	76.2	0.078
Age	359	54.7	60.7	58.7	55.7	66.8	57.7	55.7	43.7	56.8	61.8	0.112
Overall Tumor Size (mm)	353	24.5	19.5	13.2	15.2	18.3	20.3	21.4	20.5	12.2	17.2	<0.001
Size of Invasion (mm)	365	5.3	10.2	10.2	10.2	18.2	20.2	15.3	18.4	11.2	16.2	<0.001
Perineural Invasion: Present	367	12.5	20.7	36.8	31.6	66.7	77.8	45.4	27.2	66.7	45.4	0.005
LVI: Present	367	16.7	45.3	69.9	72.3	33.3	66.7	66.7	63.6	33.3	90.9	<0.001
Surgical Margin: Positive	359	0	7.5	3.9	2.6	0	11.1	6.2	9.1	0	15.8	0.403
Metastatic Lymph Nodes: Present	329	15.8	37.5	46.2	41.8	66.7	44.4	62.5	40	66.7	68.4	0.043
T AJCC	365											0.027
T1		25	20.7	13.6	14.5	0	0	6.1	9.1	0	14.3	
T2		50	52.8	37.9	46	0	0	42.4	27.3	33.3	38.1	
T3		16.7	18.9	34.8	32.9	100	66.7	33.3	63.6	33.3	38.1	
T4		8.3	7.5	13.6	6.6	0	33.3	18.2	0	33.3	9.5	
Site Specific Classification	367											<0.001
Ampullary Ductal		0	0	42.1	9.2	66.7	22.2	9	0	66.7	13.6	
Ampullary NOS		54.2	43.4	42.8	59.2	33.3	77.8	48.5	72.3	33.3	72.7	
IAPN Associated		29.2	43.4	12.8	28.9	0	0	12.1	9.1	0	9	
Ampullary Duodenal		16.7	13.2	2.2	2.6	0	0	30.3	18.2	0	4.5	
Outcome: Dead	390	29.2	55.8	48.4	54	66.7	88.9	48.5	40	0	57.9	0.087

Conclusions: A substantial proportion (20%) of ACs are non-glandular histologic types (unlike ductal pancreatic cancers where non-glandular phenotypes accounted for < 5%). This illustrates the morphologic versatility of the ampulla, which presumably corresponds to the multiple epithelial cell types that converge in this small region. ACs like medullary, mucinous and poorly-cohesive/signet-ring occur with regularity are otherwise exceedingly rare in the pancreas or common bile duct (once tumor origin is precisely confirmed with careful grossing). Recognition of these different types is important because of their different clinical, IHC and behavioral characteristics, and potentially different therapeutic targets.

1714 Field Risk ("Field-Effect"/"Field-Defect") in the Gallbladder and Biliary Tree: An Under-Recognized Phenomenon with Major Implications for Management and Carcinogenesis

Michelle Reid[1], Hector Losada[2], Takashi Muraki[3], Burcin Pehlivanoglu[4], Bahar Memis[5], Jill Koshiol[6], Pelin Bagci[7], Ipek Erbarut Seven[7], Serdar Balci[8], Burcu Saka[9], Nevra Dursun[10], Keetaek Jang[11], Nobuyuki Ohike[12], Takuma Tajiri[13], Michael Goodman[14], Juan Carlos Roa[15], Juan Araya[16], Enrique Bellolio[2], Juan Sarmiento[14], Yue Xue[1], Olca Basturk[17], N. Volkan Adsay[18]
[1]Emory University Hospital, Atlanta, GA, [2]Universidad de La Frontera, Temuco, Chile, [3]Matsumoto, Japan, [4]Adiyaman University Training and Research Hospital, Adiyaman, Turkey, [5]TC.SBU. Sanliurfa Mehmet Akif Inan Training and Research Hospital, Sanliurfa, Turkey, [6]National Cancer Institute, Rockville, MD, [7]Marmara University, Istanbul, Turkey, [8]Ankara, Turkey, [9]Medipol Mega University Hastanesi, Istanbul, Turkey, [10]University of Health Sciences, Istanbul, Turkey, [11]Samsung Medical Center, Seoul, Korea, Republic of South Korea, [12]Showa University Fujigaoka Hospital, Yokohama, Japan, [13]Tokai University Hachioji Hospital, Hachioji, Japan, [14]Emory University, Atlanta, GA, [15]Pontificia Universidad Catolica de Chile, Santiago, Santiago, Chile, [16]Temuco, Chile, [17]Memorial Sloan Kettering Cancer Center, New York, NY, [18]Koç University Hospital, Istanbul, Turkey

Disclosures: Michelle Reid: None; Hector Losada: None; Takashi Muraki: None; Burcin Pehlivanoglu: None; Bahar Memis: None; Jill Koshiol: None; Pelin Bagci: None; Ipek Erbarut Seven: None; Serdar Balci: None; Burcu Saka: None; Nevra Dursun: None; Keetaek Jang: None; Nobuyuki Ohike: None; Takuma Tajiri: None; Michael Goodman: None; Juan Carlos Roa: None; Juan Araya: None; Enrique Bellolio: None; Juan Sarmiento: None; Yue Xue: None; Olca Basturk: None; N. Volkan Adsay: None

Background: Field risk (field-effect/field-defect) phenomenon (FR) is established in the oral cavity, where development of multiple independent cancers due to smoking, HPV or inherent mutations is well documented. Similarly, in the urothelial organs synchronous or metachronous cancers can develop in different compartments. In the pancreatobiliary tract, this occurrence is not appreciated.

Design: Four separate cohorts were analyzed for evidence for FR in the biliary tract. Long-term follow-up (f/u) (>3 years) information of patients with gallbladder (GB) high grade dysplasia/CIS (HGD/CIS) was investigated for emergence of new biliary tract cancer on f/u: 1) Our cohort (n=125), 2) NCI SEER (Surveillance Epidemiology End Results) database cases (n=686), 3) GB cancer (GBC) patients in whom concurrent distal bile duct brushings (BDB) were taken during curative cholecystectomy (n=7), 4) Patients who showed synchronous or metachronous GB and biliary tree cancers (n=5).

Results: 1. An estimated 3% of patients with GB HGD/CIS developed biliary tract cancers on long-term f/u (> 3 years) in our and SEER cohorts (Table).

2. Synchronous adenocarcinoma was found in 2/7 distal bile duct brushings (BDB; Figure) obtained from GBC patients undergoing radical cholecystectomy.

3. Five patients with independent carcinomas occurring in different compartments of the GB and biliary tree were encountered in daily practice. Mean age of these patients was 70, interestingly 3 of these were men, 2 of whom had pancreatobiliary maljunction (PBM). Separately, a patient with margin-negative HGD/CIS of GB underwent bile duct brushing after cholecystectomy and revealed HGD.

	SEER database ("CIS")	**Our cohort (HGD/CIS)**
Number of cases	686	125
1-yr	94	96
3-yr	**89**	**93**
5-yr	87	90
10-yr	**79**	**86**
% deaths documented to be due to GB/biliary tree cancers	6.8	7.2

Figure 1 - 1714

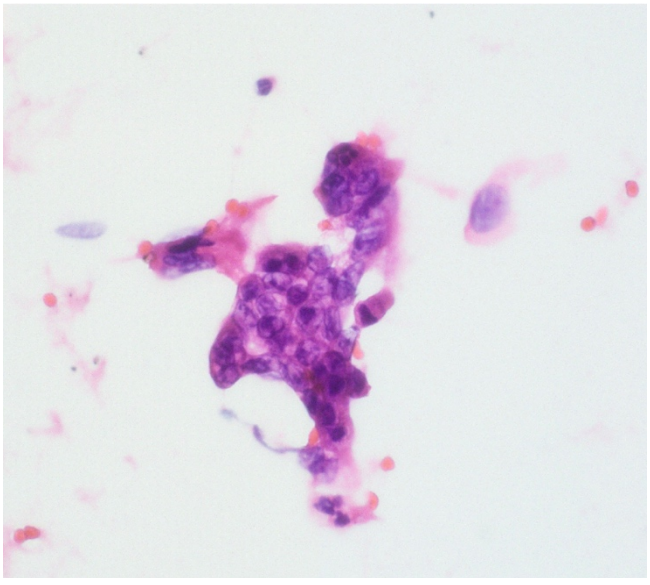

Conclusions: Field risk phenomenon appears to be valid for GB/biliary tree. Whether this is due to (1) field-effect of a specific carcinogenetic factor (PBM, where pancreatic enzymes reflux into entire biliary system including GB), (2) a field-defect in which inherent (genetic) abnormality predisposes to multifocal cancers, or (3) pagetoid spread of dysplastic/CIS cells to sites in biliary tract ("homage phenomenon") or a combination thereof requires further scrutiny and may provide invaluable insights into the etiopathogenesis and mechanisms of carcinogenesis in cancers arising in these sites. Patients with early GB/BD cancers should be investigated for concurrent flat/tumoral lesions (perhaps with baseline brushings) and followed long-term to ensure early identification of cancers in the biliary tract.

1715 Assessing the contribution of mutation analysis to improved diagnosis of pancreatic cysts

Rongqin Ren[1], Somashekar Krishna[2], Weiqiang Zhao[2], Sean Caruthers[2], Dan Jones[2]
[1]The Ohio State University Wexner Medical Center, Westerville, OH, [2]The Ohio State University, Columbus, OH

Disclosures: Rongqin Ren: None; Somashekar Krishna: None; Weiqiang Zhao: None; Sean Caruthers: None; Dan Jones: None

Background: Diagnostic testing of cyst fluid obtained by endoscopic ultrasound-guided fine needle aspiration (EUS-FNA) has traditionally utilized elevated CEA (≥ 192 ng/ml) and cytomorphologic examination to differentiate premalignant mucinous from benign pancreatic cystic lesions (PCLs). Molecular testing for *KRAS/GNAS* mutations has been shown to improve accuracy of detecting mucinous PCLs. Using a small next-generation sequencing (NGS) panel, we assess the status of PCL-associated mutations to improve understanding of the key diagnostic variables.

Design: Molecular analysis of cyst fluid was performed on 30 PCLs as part of a clinical study (NCT02516488) that had concurrent CEA and cytological analysis. Total nucleic acid was extracted using the QIAamp UltraSens Virus Kit. A 50-gene Ion Chef-S5 NGS assay was performed, which included genes commonly mutated in mucinous PCLs such as *GNAS*, *KRAS, CDKN2A*, *PIK3CA*, *SMAD4* and *TP53,* in serous cystadenomas (*VHL),* and solid pseudopapillary neoplasms (*CTNNB1)*. At an average of 1150 reads/sample, *KRAS* and *GNAS* hotspots were validated down to 1% mutant variant allele frequency (VAF). Correlations were made with the clinical, imaging, and histopathological diagnosis.

Results: All the tested samples yield sufficient DNA for NGS testing with at least 250 reads/amplicon for target hotspots. *KRAS* and/or *GNAS* mutations were seen in 18 of 22 (81.8%) cases with the clinical/radiologic impression of a mucinous-PCL. Positive cytology was found in only 8 of these cases (36.4%), with fluid CEA elevated in 10 of 18 cases (55.6%). Multiple *KRAS* mutations at different VAFs were seen in 4 cases favoring multiclonal patterns, with 3 of these cases showing at least two separately located PCLs by imaging. Mutant VAFs for *KRAS* and *GNAS* varied from 3.2-61.3% (median 13.5%). No *KRAS* or *GNAS* mutations were seen in the 8 samples with other clinical diagnoses indicating a sensitivity of 81.8%, specificity of 100%, and accuracy of 86.7%, for the NGS assay. Other genes mutated included *ATM, CDKN2A* and *TP53* in 1 case each.

Conclusions: In this series, we confirm the high sensitivity and sensitivity of *KRAS* and *GNAS* mutations for detection of mucinous-PCLs, as compared to CEA and cytological examination. A nucleic acid extraction method that collects cell-associated and cell-free DNA led to informative results for all mucinous PCL cases. Even within few tested samples, there was an observed correlation between multiple *KRAS* mutations and multifocal PCL radiologic characters.

1716 AJCC 8th pT Stage Based Risk Stratification of Pancreatic Ductal Adenocarcinoma Arising in Neoplastic Cystic Lesions

Neda Rezaee[1], Greg Williams[1], Deyali Chatterjee[1]
[1]*Washington University, St. Louis, MO*

Disclosures: Neda Rezaee: None; Greg Williams: None; Deyali Chatterjee: None

Background: By the time a pancreatic ductal adenocarcinoma (PDAC) comes to clinical attention, the tumor is almost always greater than 1 cm. Encountering PDAC T-stages 1a and 1b in resection specimens are rare. They usually arise in a neoplastic cystic lesion such as intraductal papillary mucinous neoplasm (IPMN) or mucinous cystic neoplasm (MCN), unless they are residual foci of PDAC after a good response to neoadjuvant treatment (NAT). The aim of this study was to evaluate the prognostic significance of PDAC arising in cystic lesions and how the AJCC 8th edition T-stage system risk stratifies them.

Design: Our cohort consisted of a total of 316 patients who underwent a pancreatic resection for an IPMN (222, 70.3%) or MCN (94, 29.7%) between years of 1994 and 2017, without prior NAT, and who had archival resection slides and follow-up information available for review. All cases were reviewed by a GI pathologist to confirm the diagnosis, grade of dysplasia, and presence, type and size of invasive carcinoma. Non-invasive cystic lesions that were not submitted entirely for histologic evaluation were excluded. Kaplan-Meier survival estimates were used to evaluate the overall survival.

Results: Tumors were classified per AJCC 8th edition as pT0 in 194 (62%), pTis in 21 (6.7%), pT1a in 11 (3.5%), pT1b in 3 (1%), pT1c in 26 (8.3%), pT2 in 32 (10.2%), and pT3 in 26 (8.3%). Amongst patients with IPMN, low-grade dysplasia was diagnosed in 116 (52.2%, pT0), high-grade dysplasia in 19 (8.6%, pTis), and IPMN-associated invasive carcinoma in 87 (39.2%). Among patients with MCN, low-grade dysplasia was diagnosed in 79 (84.1%, pT0), high-grade dysplasia in 2 (2.1%, pTis), and invasive carcinoma in 13 (13.8%). The estimated 5-year overall survival after resection of non-invasive tumors (pT0/pTis, 88%) was not statistically different to that of patients with pT1a/pT1b invasive carcinoma (76%, p-value=0.079, 95% CI: 0.85-9.42). The estimated 5-year overall survival was 53% in patients with pT1c tumors, which was superior to those patients who had a pT2/pT3 tumor resection (42%, p-value=0.054, 95% CI: 0.97-4.37), (figure).

Figure 1 - 1716

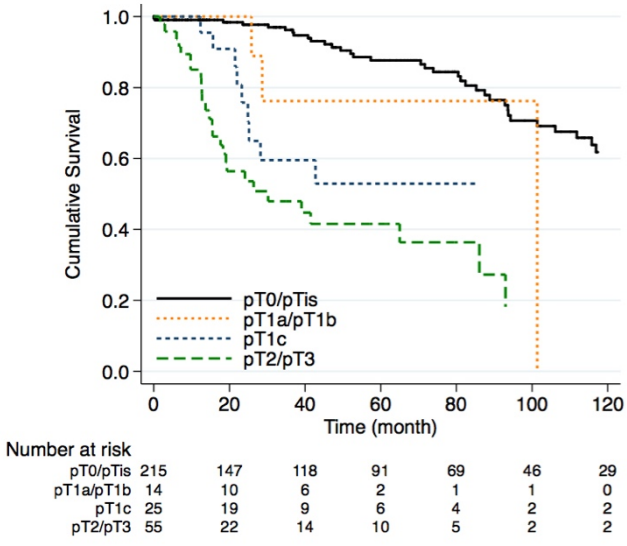

Conclusions: PDAC arising in association with IPMN or MCN can be prognostically stratified by the AJCC 8th edition staging system. The survival of patients with small invasive component (<1cm; pT1a/pT1b) is comparable to those with non-invasive disease. The survival of patients after resection of pT1c tumors is superior compared to patients with a pT2/pT3 tumor resection.

1717 Targeted Next-Generation Sequencing (NGS) of Intracholecystic Papillary-Tubular Neoplasms (ICPNs) Identifies Two Distinct Subtypes and Their Relationship to Gallbladder Carcinomas

Somak Roy[1], Dora Lam-Himlin[2], Elizabeth Montgomery[3], Raja Seethala[4], Aatur Singhi[5]
[1]University of Pittsburgh Medical Center, Pittsburgh, PA, [2]Mayo Clinic, Scottsdale, AZ, [3]Johns Hopkins Medical Institutions, Baltimore, MD, [4]University of Pittsburgh School of Medicine, Pittsburgh, PA, [5]University of Pittsburgh Medical Center, Sewickley, PA

Disclosures: Somak Roy: None; Dora Lam-Himlin: None; Elizabeth Montgomery: None; Raja Seethala: None; Aatur Singhi: None

Background: ICPNs are mass-forming, preinvasive neoplasms of the gallbladder with multiple histologic subtypes. Although largely limited to gastric-type ICPNs, studies have shown these neoplasms harbor *CTNNB1* mutations and lack *TP53*mutations. In contrast, gallbladder carcinomas are characterized by alterations in *TP53* and genes within the ErbB/HER signaling pathway. As a result, malignant transformation of ICPNs is regarded as a minor pathway in gallbladder tumorigenesis. However, a comprehensive genomic analysis of various ICPN histologic subtypes is lacking.

Design: Eighteen ICPNs were collected from three medical institutions. Patients ranged in age from 50 to 85 years (mean, 70 years) with a slight female preponderance (n=12, 67%). The ICPNs measured 1.0 to 4.7 cm (mean, 1.9 cm) and the majority were found within the gallbladder body (n=14, 78%). Based on the histologic subtype, 10 (56%) cases were classified as biliary-type, 5 as gastric and 3 as intestinal. High-grade dysplasia was present in 15 (83%) cases. Surrounding flat dysplasia and an invasive component were present in 13 (72%) and 5 (28%) ICPNs, respectively. Targeted NGS was performed using the TruSight 170 (Illumina) for 170 cancer-associated genes on a NextSeq 550 (Illumina) with >90% amplicons at ≥500X coverage and correlated with various clinicopathologic features.

Results: A total of 63 genomic alterations were identified in 21 genes that included *TP53* (n=10, 56%), *CTNNB1* (n=7, 39%), *ERBB2* (n=5, 28%), *SMAD4* (n=4, 22%), *ERBB3* (n=3, 17%), *KRAS* (n=3, 17%), *PIK3CA* (n=3, 17%) and others. Overall, ErbB/HER signaling (*ERBB2*, *ERBB3*, *KRAS*, *PIK3CA* and *EGFR*) was the most extensively mutated pathway and affected 12 (67%) cases. Correlating clinicopathologic features revealed *TP53* alterations were more frequently found in biliary-type ICPNs as compared to non-biliary type ICPNs (80% vs. 25%). In contrast, non-biliary type ICPNs were more likely to harbor mutations in *CTNNB1* or *APC* (88% vs. 20%). No significant associations were found between individual gene mutations/pathway alterations and patient age, gender, anatomic location, grade of dysplasia, surrounding flat dysplasia or the presence of an invasive component.

Conclusions: Based on targeted NGS and histologic correlation, ICPNs can be stratified into two distinct subtypes: biliary and non-biliary. Further, the frequent presence of ErbB/HER signaling alterations in both types suggests a closer relationship between ICPNs and gallbladder carcinomas than previously appreciated.

1718 Tumour Budding in Pancreatic Ductal and Periampullary Adenocarcinomas – Validation of the ITBCC Scoring Method

Paromita Roy[1], Rohit Tapadia[1], Sudeep Banerjee[1], Lateef Zameer[1], Deep Lamichhane[1]
[1]Tata Medical Center, Kolkata, India

Disclosures: Paromita Roy: None; Rohit Tapadia: None; Sudeep Banerjee: None; Lateef Zameer: None; Deep Lamichhane: None

Background: The International Tumour Budding Consensus Conference (ITBCC) method is now accepted as the standardized reporting system for budding (TB) in colon cancer. In pancreatic ductal (PDAC) and periampullary carcinomas (PAC) there has been very few studies, which have all shown prognostic significance of TB, but varied in the criteria used for reporting. We aimed to evaluate whether ITBCC method could be adopted for PDAC and PAC.

Design: Hematoxylin-eosin stained slides of all tumour sections of 154 consecutive cases of Whipple's specimen were reviewed by 2 pathologists. Only PDAC, invasive PAC, distal bile duct and peri-ampullary duodenal adenocarcinomas were included. TB (defined as single or < 5 tumour cell clusters) was recorded on the single worst 20X high power field (HPF) with an area of 0.95mm^2 (hotspot) and scored into 3 groups – 0-5 buds (low), 6-11 (intermediate) and ≥12buds/HPF (high).

Results: After excluding other histologies, there were 122 cases (71 PACs, 35 PDACs, 13 bile duct and 3 perimapullary duodenal adenocarcinomas). TB was present in 93.5% cases and ranged from 0 to 70 buds per HPF. Interobserver concordance for absolute TB count was high. As per ITBCC scoring, 41.8% cases showed high, 24.5% intermediate and 33.6% low budding. High budding was more common in PDAC (53%) than PAC (33.8%). ITBCC score groups showed no significance with recurrence free survival (DFS) (p=0.553), even when analysed separately for PDAC(p=0.671) and PAC(p=0.506), but presence (≥ 2 buds/HPF) or absence (0-1buds/HPF) of TB was significant (p=0.043). TB also correlated significantly with tumour site, histologic subtype, grade, LVI, PNI, AJCC8 T and N stage and lymph node ratio (p<0.05).

Other histopathological parameters showing prognostic significance on univariate analysis were tumour site (p=0.027), grade (well versus moderate to poor; p=0.044), LVI (p=0.000), PNI (p=0.000), AJCC8 T stage (p=0.004), N stage (p=0.000) and lymph node ratio using a cut-off of 0.10 (p=0.000), while margin status and tumour size showed no significance.

Conclusions: Hotspot method of bud counting is simple and reliable for adoption in routine reporting, though ITBCC scoring did not show prognostic significance in our cohort. Presence of TB(≥2buds/HPF) is a significant marker of poor prognosis in PDAC and PAC and should be reported routinely.

1719 Immunohistochemical Characterization of Intraductal Oncocytic Papillary Neoplasms of the Pancreas.

Anthony Rubino[1], Ladan Fazlollahi[1], Helen Remotti[2]
[1]New York-Presbyterian/Columbia University Medical Center, New York, NY, [2]Columbia University Medical Center, Dobbs Ferry, NY

Disclosures: Anthony Rubino: None; Ladan Fazlollahi: None; Helen Remotti: None

Background: Intraductal oncocytic papillary neoplasms of the pancreas (IOPN) are distinct neoplasms arising in the pancreatic ductal system, composed of a proliferation of oncocytic cells with granular eosinophilic cytoplasm (Figure 1). Recent studies have shown these lesions are genetically and immunohistochemically distinct from other intraductal papillary mucinous neoplasms (IPMN) of the pancreas. The clinical behavior is dependent on the presence and extent of invasive tumor associated with these lesions. IOPNs have been shown to express Hepatocyte-Paraffin 1 (HepPar 1), a marker of hepatocellular differentiation. The goal of this study is to attempt to establish an immunohistochemical (IHC) profile for IOPMs and to specifically characterize the expression of additional hepatocellular markers in these lesions.

Design: A search of the intradepartmental archives (from 01/01/2001 to 06/30/2018) identified nine IOPN cases. H&E slides were reviewed, and FFPE blocks retrieved. The associated medical records were reviewed to collect data on patient demographics, treatment and pathologic presentation. Tissue microarrays (TMA) of 2mm tissue cores (2-4 cores per tumor) were created. IHC staining for HepPar 1, Bile Salt Exporter Pump (BSEP), Arginase 1 (Arg1), MUC1, MUC2, MUC5, MUC6, CK7, CK20 and albumin ISH, was performed on the TMAs.

Results: Patients ranged from 41 to 83 years of age and consisted of 6 males and 3 females. In 55% of cases an associated invasive adenocarcinoma was identified, with no lymph node metastases identified in any of the cases. 77% of IOPNs were Hep Par1 positive. All cases were negative for BSEP (bile salt export protein), Arg1(Arginase1) and Albumin ISH. All cases were negative for chymotrypsin. All tumors were positive for CK7 and 1 case was also positive for CK20. MUC profile showed co-expression and heterogeneity in staining of various markers with 89% MUC1 positivity, 33% MUC2 positivity, 78% MUC5 positivity, and 78% MUC6 positivity (Table 1).

Table 1. IHC Profile of IOPN

Case	Hep Par1	BSEP	Arg1	Albumin ISH	MUC1	MUC2	MUC5	MUC6	CK7	CK20
1	-	-	-	-	+	-	-	-	+	-
2	+	-	-	-	+	-	+	+	+	-
3	+	-	-	-	+	-	+	+	+	-
4	+	-	-	-	+	-	+	+	+	-
5	-	-	-	-	+	-	+	+	+	-
6	+	-	-	-	+	+	+	+	+	+
7	+	-	-	-	+	+	+	+	+	-
8	-	-	-	-	-	-	-	-	+	-
9	+	-	-	-	+	+	+	+	+	-

Figure 1 - 1719

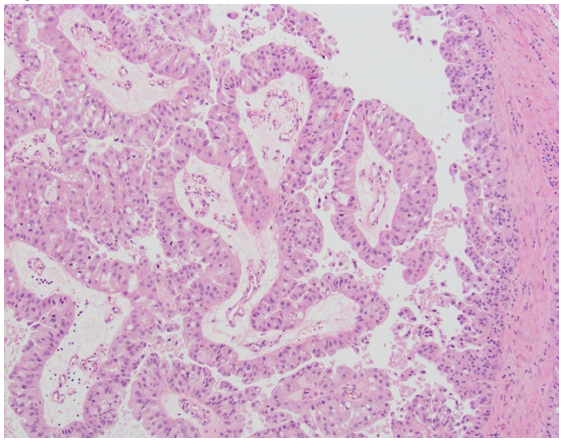

Figure 2 - 1719

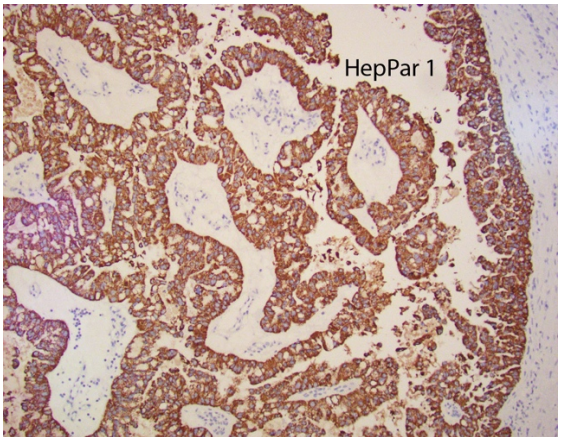

Conclusions: Hep Par1 was expressed in 77% of IOPNs however all cases were negative for additional markers of hepatocellular differentiation (BSEP, Arg1 and Albumin ISH). We identified (CK7, Hep Par1, MUC1, MUC5, MUC6) positivity and (CK20, BSEP, Arg1, Albumin ISH, and MUC2) negativity as the most common IOPN immunoprofile among our cases.

1720 Comparison and Validation of AJCC 7th and 8th Editions of TNM Staging in Resectable Distal Pancreatic Cancer

Mohammed Saad[1], Feng Yin[2], Jingmei Lin[3], Christopher Jackson[4], Bing Ren[4], Cynthia Lawson[5], Dipti Karamchandani[6], Belen Quereda Bernabeu[7], Teena Dhir[8], Richard Zheng[7], Christopher Schultz[8], Wei Jiang[9], Dongwei Zhang[10], Courtney Thomas[11], Xuchen Zhang[12], Jinping Lai[2], Hao Xie[13], Xiuli Liu[2]

[1]Indiana University School of Medicine, Indianapolis, IN, [2]University of Florida, Gainesville, FL, [3]Indiana University, Indianapolis, IN, [4]Dartmouth-Hitchcock Medical Center, Lebanon, NH, [5]Penn State Health, Hershey, PA, [6]Penn State Health Milton S. Hershey Medical Center, Hershey, PA, [7]Thomas Jefferson University Hospital, Philadelphia, PA, [8]Thomas Jefferson University, Philadelphia, PA, [9]Philadelphia, PA, [10]University of Rochester Medical Center, Rochester, NY, [11]Yale New Haven Hospital, Orange, CT, [12]Yale University School of Medicine, Orange, CT, [13]Mayo Clinic, Rochester, MN

Disclosures: Mohammed Saad: None; Feng Yin: None; Jingmei Lin: None; Christopher Jackson: None; Bing Ren: None; Cynthia Lawson: None; Dipti Karamchandani: None; Belen Quereda Bernabeu: None; Teena Dhir: None; Richard Zheng: None; Christopher Schultz: None; Wei Jiang: None; Dongwei Zhang: None; Courtney Thomas: None; Xuchen Zhang: None; Jinping Lai: None; Hao Xie: None; Xiuli Liu: None

Background: The recent AJCC 8th edition has adopted major changes in pancreatic adenocarcinoma (PADC) staging. So far most of the validation studies have examined Whipple specimens where the tumors are located in the head of pancreas. Large-scale study to compare staging between AJCC 7th and 8th editions with a focus on distal PADC has not been reported.

Design: Pathology databases of 5 academic medical centers were search for patients who underwent oncological distal pancreatectomy between 2005 and 2018. Patients who had neoadjuvant therapy, non-invasive intraductal mucinous neoplasm (IPMN), non-invasive mucinous neoplasm, and neuroendocrine neoplasm were excluded. Clinicopathological data were collected through reviewing pathology reports, glass slides, and medical charts. All cases were staged by using both the AJCC 7th and 8th criteria. Univariate analysis was performed to compare prognosis in terms of progression-free survival (PFS) and overall survival (OS).

Results: A retrospective cohort of 396 patients (188 males and 208 females) with a mean age of 66.7 years were included in the study. 297 patients had PADC including mucinous and adenosquamous variants, and 99 had IPMN with associated invasive carcinoma. The total cohort was predominantly categorized as stage 3 according to AJCC 7th edition (T1: 7.3%; T2: 10.9%; T3: 76.8%), and it was more evenly distributed based on 8th edition (T1: 16.9%; T2: 44.4%; T3: 38.6%). T and N staging of both 7th and 8th systems sufficiently stratified PFS and OS in the entire cohort, although dividing into N1 and N2 according to the 8th edition did not provide additional advantage. For PDAC arising in IPMN, T staging of the 7thsystem and N1/N2 staging of the 8th edition appeared to further stratify PFS and OS. For PADC without IPMN component, T staging from both versions failed to stratify PFS and OS; N staging of both systems worked, although dividing N category into N1 and N2 as in the 8th edition did not add further value in this group.

Conclusions: T staging of the 7th edition and N1/N2 of the 8th edition stratify prognosis better for patients with invasive PADC arising in IPMN in distal pancreatectomy, but not for those who have PADC without associated IPMN. Large studies are needed to confirm the current findings.

1721 Molecular Profiling of Intraductal Tubulopapillary Neoplasm

Atif Saleem[1], Henning Stehr[2], James Zehnder[3], Christian Kunder[3], Chieh-Yu Lin[4]
[1]Stanford University, San Jose, CA, [2]Stanford University, Stanford, CA, [3]Stanford University School of Medicine, Stanford, CA, [4]Washington University School of Medicine in St. Louis, St. Louis, MO

Disclosures: Atif Saleem: None; Henning Stehr: None; James Zehnder: None; Christian Kunder: None; Chieh-Yu Lin: None

Background: Intraductal tubulopapillary neoplasm of the pancreas (ITPN-P) and intraductal tubulopapillary neoplasm of the bile duct (ITPN-B) are emerging disease entities that share similar features, characterized by a tubulopapillary growth pattern, high-grade nuclear atypia, variable tumor necrosis, and absent to minimal mucin production. While ITPN-P and ITPN-B are considered pre-invasive, invasive carcinomas are occasionally found from the same patient. It is unclear whether ITPN-P and ITPN-B share molecular signatures, and whether they are bona fide precursor lesions to the associated malignancies. Studying the molecular landscape could provide important insights into the pathogenesis and clinical implications for ITPN-P and ITPN-B.

Design: The pathology database was searched for ITPN-P and ITPN-B cases and clinicopathologic data were collected. A clinically validated targeted exon-sequencing assay with a 130 cancer-associated gene panel was performed using archival tissue. In addition, we reviewed the molecular data of 46 pancreatic adenocarcinomas that underwent the same sequencing assay for clinical indications.

Results: Seven ITPN-P and two ITPN-B cases were included in the study. The average patient age was 61.4 years [48-76]. The average tumor size was 5.8 cm [2.4-10.5 cm]. Both ITPN-B and five ITPN-P cases were associated with invasive carcinoma or metastatic disease. Pathogenic variants were identified in 6 ITPN-P cases and none of the ITPN-B cases. Pathogenic *BRAF* variants were identified in three ITPN-P cases (1 *BRAF* p.V600E, 1 *BRAF-SND1* fusion, and 1 *AKAP9-BRAF*fusion). For ITPN-P cases, pathogenic variants were also identified in *CTNNB1, RB1, CDKN2A, TP53, ARID1A, SMAD4 and PTEN*. In the retrospective review of 46 pancreatic adenocarcinomas, no *BRAF* variants or *BRAF* fusions were identified. In 4 cases (3 ITPN-P and 1 ITPN-B), the associated invasive carcinoma was submitted for molecular study. The ITPN and paired invasive cancer shared the same molecular profile.

Conclusions: Our study demonstrated that ITPN-P exhibits recurrent BRAF pathogenic mutations. This finding might shed some light on the pathogenesis of ITPN-P, and provide possible therapeutic targets. In addition, albeit similar morphologic features, ITPN-P and ITPN-B might not share similar molecular profiles. Finally, the invasive carcinoma associated with ITPN-P or ITPN-B demonstrated the same molecular profile, findings consistent with a clonal process.

1722 A miRNA signature Predicts Grading of Pancreatic Neuroendocrine Tumors.

James Saller[1], Anthony Magliocco[1], Domenico Coppola[1]
[1]Moffitt Cancer Center, Tampa, FL

Disclosures: James Saller: None

Background: Grading of pancreatic neuroendocrine tumors (PNETs) is potentially complicated by interobserver variability. Determination of the Ki-67 proliferative index and mitotic rate is especially challenging when dealing with a tumor that is at the borderline between two grades. Studies have shown the utility of differentially expressed miRNAs (DEM) in predicting tumor progression.

Design: Twelve cases of PNETs of different grades were selected from the Pathology repository at the Moffitt Cancer Center. The H&E slides and report from each case were reviewed by 2 pathologists to confirm the diagnosis. Four patients had grade 1 PNETs and 4 had grade 2 PNETs. Four additional patients had Grade 3 pancreatic neuroendocrine neoplasms (PNENs), two of which were PNETs and the other two were pancreatic neuroendocrine carcinomas (PECAs). The samples were profiled using the miRNA nanoString Assay.

Results: There were 5 statistically significant DEM (miR1285-5p, miR15b-5p, miR155-5p, miR-345-5p, miR548d-5p and miR9-5p) ($p < 0.05$) between different grades of PNENs (G1/2/3). MiR1285-5p was the sole miRNA that had a statistically significant differential expression ($p < 0.05$) between Grade 1 and Grade 2 PNETs. Six statistically significant DEM (miR135a-5p, miR200a-3p, miR3151-5p, miR-345-5p, miR548d-5p and miR9-5p) ($p < 0.05$) were identified between Grade 1 PNETs and Grade 3 PNENs. Finally, 5 miRNAs (miR155-5p, miR15b-5p, miR222-3p, miR548d-5p and miR9-5p) had the highest statistically significant differential expression ($p < 0.05$) between Grade 2 PNET and Grade 3 PNENs.

Figure 1 - 1722

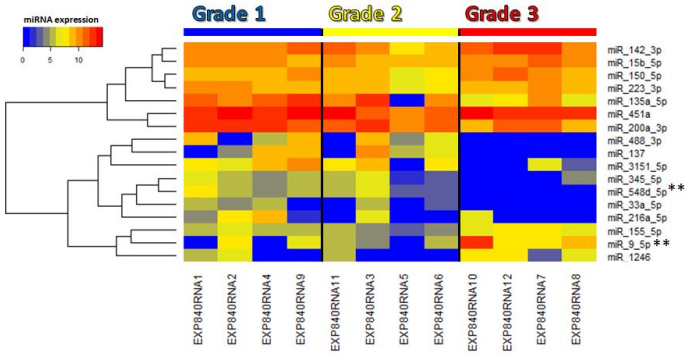

Figure 1: Comparison of miRNAs with statistically significant differential expression between Grade 1, Grade 2 and Grade 3 PNENs.
** miR9-5p and miR548d-5p were the most consistent in statistically significant differential expression ($p < 0.05$) among comparisons across different grades of PNENs.

Figure 2 - 1722

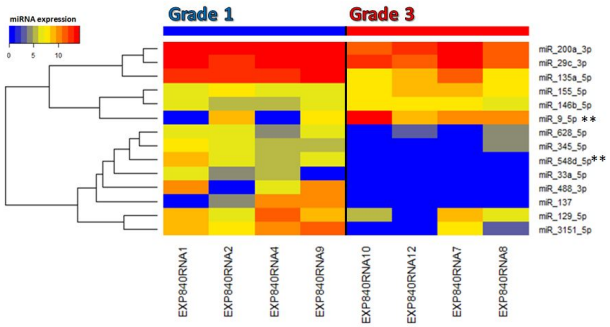

Figure 2: Comparison of miRNAs with statistically significant differential expression between Grade 1 and Grade 3 PNENs.
** miR9-5p and miR548d-5p were the most consistent in statistically significant differential expression ($p < 0.05$) among comparisons across different grades of PNENs.

Conclusions: A review of the literature has corroborated the selected miRNA candidates as being concordant with their patterns of dysregulation in other tumor types. The reliability of these DEM as discriminators of PNEN grades, support further investigation using a larger patient population.

1723 Quantitative Analysis of Viable Tumor to Tumor Bed Ratio as an Approach to Predict Survival in Patients Treated with Neoadjuvant Chemotherapy for Pancreatic Ductal Adenocarcinoma

Elisabeth Tabb[1], Cristina Ferrone[1], Martin Taylor[2], Steffen Rickelt[3], Vikram Deshpande[1]
[1]Massachusetts General Hospital, Boston, MA, [2]Boston, MA, [3]David H. Koch Institute for Integrative Cancer Research, Cambridge, MA

Disclosures: Elisabeth Tabb: None; Martin Taylor: None; Steffen Rickelt: None; Vikram Deshpande: None

Background: The postresection prognosis of a patient with pancreatic adenocarcinoma (PDAC) is primarily determined by the anatomic extent of disease as defined by the TNM stage grouping. FOLFIRINOX (a combination of drugs that includes 5-fluorouracil, oxaliplatin, irinotecan, and leucovorin) has been shown to improve survival for patients with pancreatic adenocarcinoma. It is not currently known whether pathological parameters predict survival in patients treated with FOLFIRINOX. In this study, we evaluate current prognostic parameters and quantitate tumor to tumor-bed ratio in patients treated with FOLFIRINOX in a neoadjuvant setting.

Design: The study comprised of 129 PDAC's resected following FOLFIRINOX therapy. ypTNM stage, CAP tumor regression grade, angiolymphatic invasion and perineural invasion were recorded. In a subset of these patients (n=37) whole slide scanned images were quantitatively assessed to derive a tumor to tumor bed ratio within the tumor bed. A single slide with the highest volume of tumor was assessed in each case.

Results: The mean age of patients was 61 years (range 37-79) with a male:female ratio of 1:1. The ypT stage was as follows: T0-11 (8%), T1-14 (11%), T2-11 (8%) ,T3-91 (71%), T4-2 (2%). Lymph node metastases was identified in 47 individuals (36%), angiolymphatic invasion in 30 (23%), and perineural invasion in 82 (65%).15 patients had an R1 resection (12%). 21 (16%) patients showed a complete response. Based on a univariate analysis, there was no correlation between the following parameters and survival although lymphatic invasion and tumor to tumor bed ratio show a trend: CAP regression grade (p=0.627), ypT stage (p=0.316),ypN stage (p=0.116), lymph node metastasis (p=0.116), lymphatic invasion (p=0.093), perineural invasion (0.59). Patients with a tumor to tumor bed ratio of less than 20% showed median survival of 49 months while patients with a ratio of greater than 20% showed a median survival of 27 months (p=0.095).

Conclusions: Traditional parameters including ypTNM stage and CAP regression grade does not predict survival in PDAC patients treated with neoadjuvant FOLFIRINOX. A quantitative analysis, tumor to tumor bed ratio, shows promise in predicting survival in this cohort of patients.

1724 Correlation of p53 Immunohistochemistry With Histopathological Parameters and Molecular Data in Periampullary and Pancreatic Ductal Carcinomas: Can p53 IHC Be Used As a Surrogate Marker?

Rohit Tapadia[1], Sudeep Banerjee[1], Nilabja Sikdar[2], Deep Lamichhane[1], Gourab Saha[3], Paromita Roy[1]
[1]Tata Medical Center, Kolkata, India, [2]Indian Statistical Institute, Kolkata, India, [3]Indian Statistical Institute, Kolkata, Kolkata, India

Disclosures: Rohit Tapadia: None; Sudeep Banerjee: None; Nilabja Sikdar: None; Deep Lamichhane: None; Gourab Saha: None; Paromita Roy: None

Background: Periampullary region is home to a plethora of tumours. Molecular profiling of these tumours helps assess behaviour, prognosis and treatment. Studies in this context are limited in Indian literature. Mutations in TP53 gene are emerging as important driver mutations in these tumours and surrogate markers to detect these mutations have been studied (p53 immunohistochemistry (IHC) in serous carcinoma). In the present study we aim to highlight the molecular profile of these tumours and to correlate p53 IHC with mutation analysis, histopathology and survival data.

Design: A subset of cases of periampullary (AAC), pancreatic ductal (PDAC) and distal common bile duct (CBD) carcinomas which underwent inhouse Whipple procedure were included. Histopathology was reviewed and survival data was recorded. Tissue microarray was made with a 3mm core per case from the most representative area and stained with p53 antibody (DO7 clone, DAKO) on the BondMAX automated IHC platform. Strong staining in >70% of the cells and complete absence of staining (null type) were taken as positive. A targeted exome sequencing of tumour normal pair tissue was performed for mutations in 10 genes (*KRAS, TP53*, *SMAD 4*, *CTNNB1*, *ERBB2*, *PIK3R1*, *ITGB3*, *BRAF*, *EPHA2* and *ERBB3*).

Results: Of the 49 cases included in the study 63.3% were AAC, 30.6% were PDAC and 6.1% were CBD tumours. Tumour site (p=0.042) and pN stage (p=0.001) showed significant prognostic correlation while lymphovascular invasion (p=0.054) and perineural invasion (p=0.053) showed trends towards significance.

79.6% cases showed strong (55.1%) or null type (24.5%) p53 staining. Mutation analysis was done in 39 cases with the most common genetic abnormality being found in the TP53 gene (35.9%) while the proportion of KRAS mutation was low (7.7%). Of the p53 IHC positive cases, only 10 cases had a corresponding mutation in TP53 gene. p53 IHC correlated significantly with tumour grade (p=0.019) but not with TP53 mutation (0.809). Neither p53 IHC nor TP53 mutation showed significant prognostic correlation (p=0.951 and p=0.689).

Figure 1 - 1724

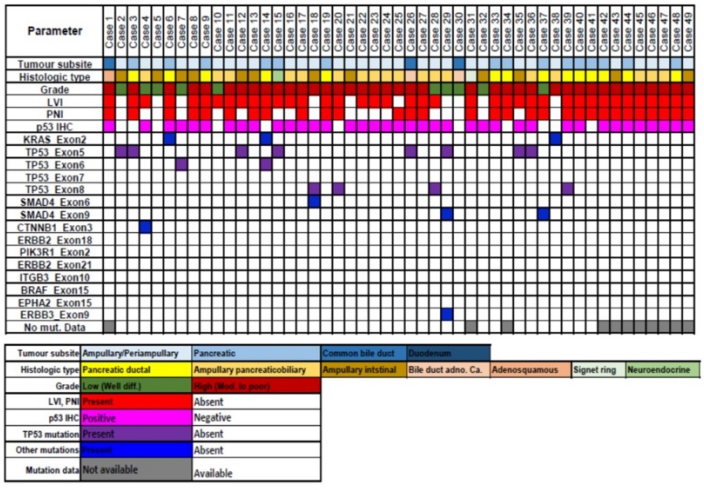

Conclusions: TP53 mutation and p53 IHC did not significantly affect prognosis in our study. The molecular profile of our tumours was different from those defined in Western literature. p53 IHC did not correlate with TP53 mutations in our cohort and cannot be used as a surrogate marker in periampullary cancers. However, due to the small sample size further studies are warranted.

1725 Rosai-Dorfman disease of the pancreas shows significant histologic overlap with IgG4 related disease

Jessica Tracht[1], Michelle Reid[2], Yue Xue[2], Emilio Madrigal[3], Alyssa Krasinskas[4]
[1]The University of Alabama at Birmingham, Birmingham, AL, [2]Emory University Hospital, Atlanta, GA, [3]Boston, MA, [4]Emory University, Atlanta, GA

Disclosures: Jessica Tracht: None; Michelle Reid: None; Yue Xue: None; Emilio Madrigal: None; Alyssa Krasinskas: None

Background: Rosai-Dorfman disease (RDD) is a rare entity characterized by proliferating S100-positive histiocytes. Originally described in lymph nodes, it can involve extra-nodal sites. Pancreatic involvement is rare, with only three cases previously reported. Recent studies demonstrate possible overlap between RDD and the more common IgG4 related disease (IRD), which could create diagnostic difficulty in the pancreas. In this study we identified 5 new cases of pancreatic RDD and describe its characteristics, examine overlapping histologic features with IRD, and compared these findings to nonpancreatic extra-nodal RDD.

Design: Cases of extranodal RDD from 2002 to 2018 were retrospectively examined. Cases were examined for morphologic features of RDD and histologic features of IRD including the presence of: Dense lymphoplasmacytic infiltrate, storiform fibrosis, and obliterative phlebitis. Immunohistochemical staining for S100, CD68 and/or CD163, and IgG4 and special stain for elastin were performed on all available cases.

Results: 5 cases of pancreatic RDD and 13 cases of extranodal, predominately intra-abdominal, RDD from other sites were identified. All cases of RDD were positive for S100 and/or CD68/CD163. The 5 pancreatic RDD (Table 1) were all mass forming and had spindled patterns of elongated histiocytes with smaller areas of more classical appearing RDD with emperipolesis (Figure 1A-C). All had areas of storiform fibrosis and dense lymphoplasmacytic infiltrates (Figure 1D-E). Three cases had obliterative vasculitis (Figure 1F). None had significantly increased IgG4 positive plasma cells. The 13 non-pancreatic extra-nodal RDD cases all had dense lymphoplasmacytic infiltrates, 11 (85%) had fibrosis with 6 (46%) showing storiform fibrosis. 11 (85%) also had at least some degree of vasculitis, with 4 (31%) demonstrating obliterative vasculitis. Two cases, a right breast and para-renal RDD, had increased IgG4 staining (60 and 12 per high power field, respectively).

Table 1. Clinical and pathologic features of pancreatic Rosai-Dorfman disease

Case	Location	Size (cm)	Age	Gender	Race	Presentation	Dense lymphoplasmacytic infiltrate	Fibrosis	Obliterative phlebitis/ vasculitis	IgG4/HPF	Treatment	Spindled histiocytes	Recurrence
1	Distal pancreas	2.1	65	F	AA	Incidental	Y	Focal Storiform	Y	2	Surgical	Y	N
2	Distal pancreas	2.9	51	F	AA	Incidental	Y	Extensive storiform	N	10	Surgical	Y	N
3	Distal pancreas	4.2	47	M	NA	Abdominal pain	Y	Storiform	Y	Rare cells	Surgical	Y	NA
4	Distal Pancreas	2.3	69	F	AA	Abdominal pain	Y	Storiform	Y	11	Surgical	Y	N
5	Pancreatic head	4.5	75	F	AA	Weight loss	Y	Storiform	N	5	Radiation	Y	N

Figure 1 - 1725

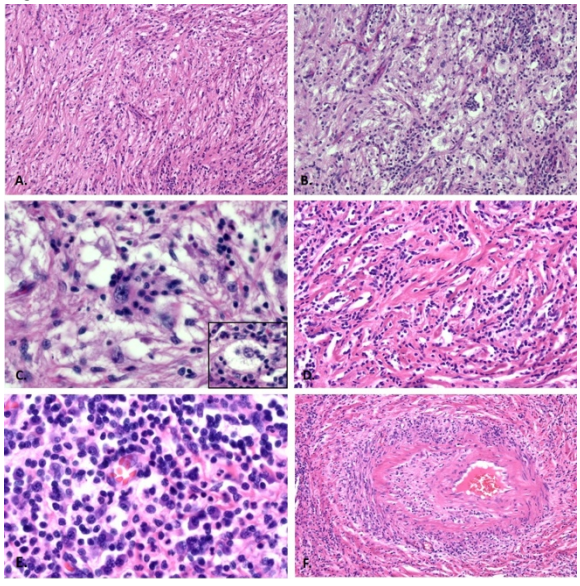

Conclusions: RDD of the pancreas is a mass forming process with areas of storiform fibrosis giving rise to a spindled-appearing S100 positive RDD histiocytes. Extra-nodal (pancreatic and non-pancreatic) RDD often shows overlapping histologic features with IRD. This can create a diagnostic challenge in the pancreas where IRD is more commonly encountered. In any mass forming pancreatic lesion in which morphologic features of IRD are present, pathologists should include RDD in their differential diagnosis and S100 in their workup.

1726 Do We Still Really Need to Count Mitoses for PanNETs?: Proper Ki67 Counting Negates the Need for the Cumbersome and Problematic Mitotic Count Required in the Current WHO-2017 Grading Scheme

Deniz Tuncel[1], Michelle Reid[2], Nobuyuki Ohike[3], Pelin Bagci[4], Serdar Balci[5], Gokce Askan[6], Burcin Pehlivanoglu[7], Olca Basturk[6], N. Volkan Adsay[8]

[1]Saglik Bilimleri Universitesi Istanbul Sisli Hamidiye Etfal SUAM, Istanbul, Turkey, [2]Emory University Hospital, Atlanta, GA, [3]Showa University Fujigaoka Hospital, Yokohama, Japan, [4]Marmara University, Istanbul, Turkey, [5]Ankara, Turkey,[6]Memorial Sloan Kettering Cancer Center, New York, NY, [7]Adiyaman University Training and Research Hospital, Adiyaman, Turkey, [8]Koç University Hospital, Istanbul, Turkey

Disclosures: Deniz Tuncel: None; Michelle Reid: None; Nobuyuki Ohike: None; Pelin Bagci: None; Serdar Balci: None; Gokce Askan: None; Burcin Pehlivanoglu: None; Olca Basturk: None; N. Volkan Adsay: None

Background: Mitotic count (MC) is one of the two requirements along with Ki67-index for grading of PanNETs. WHO-2017 grading scheme requires the case to be assigned to the grade group based on whichever of these 2 parameters gives the higher result. It is not clear whether MC is used compliantly and whether it is truly applicable in daily practice.

Design: The applicability of MC as well as MC's contribution to the grade was investigated in 91 PanNETs with full sections. For MC, 10 areas were counted to achieve an accurate count. Ki67 count was performed on a minimum of 2000 cells from 6 different areas of hot-spots using the manual count of camera-captured/printed image method.

Results: I. In none of the pathology reports of these 91 cases, was the MC result documented numerically, while all reports after 2010 contained Ki67-index. II. While conducting the study, several problematic issues of counting mitoses, some of which are particularly applicable to NETs, were elucidated. *A) Difficulty in finding the "hot spot" for MC by low power screening. Unlike Ki67 count, eye-balling to detect a hot spot for MC is highly challenging; thus, the count necessitates high-power screening without certainty of the "hot spot". This leads to discrepant results with very low MC in a case with relatively high Ki67. B) Subjectivity of what constitutes mitosis and differentiation of a true mitosis from degenerating and apoptotic cells and chromatin disintegration that is common in many NETs (Fig.1). C) Counting field areas (instead of % of cells as is done for Ki67) requires specific determination of the field area of the microscope, which can be >2 fold different between microscopes, and the number of field area counted ranges accordingly, from 20 to 50 fields depending on microscope. D) The stromal dilution phenomenon: The MC of a given tumor could vary several folds between a stroma-poor vs stroma-rich component of the very same tumor (Fig.2), thus leading vastly different MC/HPF count.* **III. Most importantly, the final grade was not driven by MC in any of the cases; Ki67 grade trumped MC negating the value of MC.**

Figure 1 - 1726

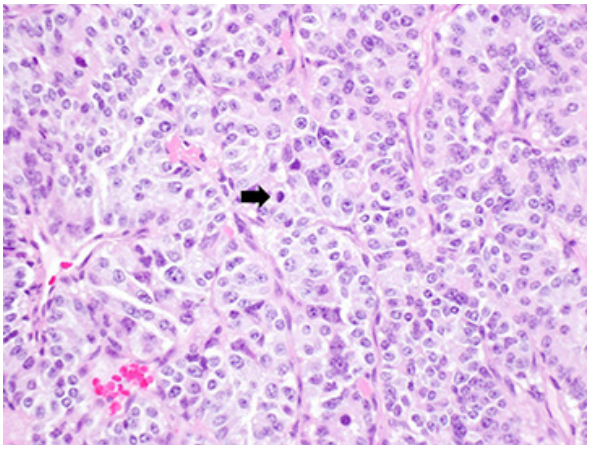

Figure 2 - 1726

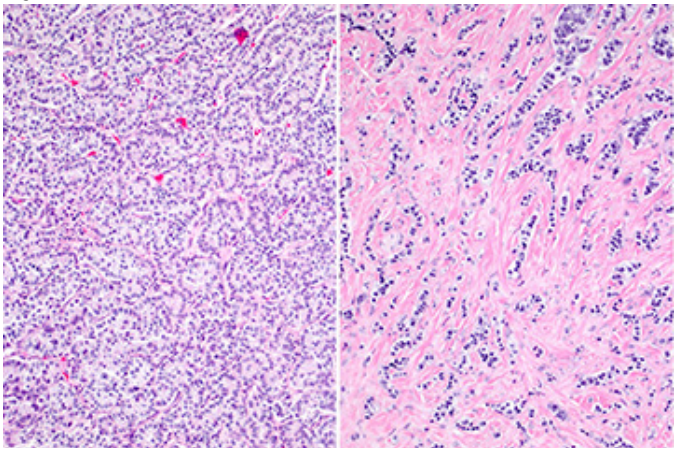

Conclusions: While Ki67 count is also not perfect by any means, it is nevertheless much more performable compared to MC, which is fraught with challenges. In none of our cases did the MC upgrade the tumor; Ki67-index was the main determinant. With the current criteria, MC does not seem to be needed, and it does not seem to be being performed. It may be time to eliminate MC and use only Ki67 for grading.

1727 Post-Neoadjuvant Pancreatic Ductal Adenocarcinoma: Tumor Burden, not Tumor Size, May Predict Outcome.

Rebecca Waters[1], Kelsey McHugh[2], Jiayun Fang[3], Dongmin Gu[4], Haiyan Lu[5], Jiaqi Shi[6], Erinn Downs-Kelly[7], Joanna Roopkumar[7], Davendra Sohal[7], Daniela Allende[8]

[1]Cleveland Clinic, Manvel, TX, [2]Cleveland Clinic, Lakewood, OH, [3]University of Michigan Hospitals, Ann Arbor, MI, [4]Ann Arbor, MI, [5]Cleveland Clinic, Beachwood, OH, [6]University of Michigan, Ann Arbor, MI, [7]Cleveland Clinic, Cleveland, OH,[8]Cleveland Clinic, Avon Lake, OH

Disclosures: Rebecca Waters: None; Kelsey McHugh: None; Jiayun Fang: None; Haiyan Lu: None; Jiaqi Shi: None; Erinn Downs-Kelly: None; Joanna Roopkumar: None; Daniela Allende: None

Background: Based on the latest AJCC 8th edition, pT staging is largely based on tumor size for pancreatic ductal adenocarcinoma (PDA). Neoadjuvant therapy (NT) has become standard of care for PDA, which can interfere with accurate tumor size measurement. Whether tumor size-based pT staging in post-NT PDA remains predictive of outcome is not known. Therefore, this study aims to compare methods of measuring tumor size and tumor burden in relation to outcome.

Design: This is a multi-institutional study including 66 cases identified through retrospective pathology databases' searches for resected PDA with NT from 2013-2018, and staged using AJCC 8th ed. Cases with no residual tumor on resection specimens or available follow up were excluded. Clinical, demographic data and outcomes were obtained from electronic medical records. Tumor size was recorded as follows: imaging pre and post-NT, gross, microscopic assessment of H&E slides (largest single focus linear dimension). Tumor burden was assessed as: number of blocks involved by tumor (B), maximum tumor cellularity per case (MC), average tumor cellularity per case (AC), total positive lymph nodes (LN), largest linear dimension of tumor in positive LN, CAP tumor regression grade (TRG), and residual tumor burden index (TBI, online software, http://www3.mdanderson.org).

Results: Summarized findings are included in Table 1. There are 39 males/27 females, mean 66 years (range 48- 84). All 66 patients had chemotherapy, 44 also had radiation preoperatively. Mean survival was 24.3 months (3-65). Maximum tumor cellularity of >30% is significantly associated with poor survival (p=0.012). There is a trend towards significantly worse survival in patients with positive LN status at resection (p=0.065). After 1-year follow up (n=55), positive LN status and high TBI significantly and negatively impacted survival (p=0.002 and p=0.0025). At 2- year follow-up (n=28), high TBI negatively impacted survival more significantly ($p < 0.0001$). There was no correlation between tumor size (regardless of measurement method), size of LN metastasis, pT stage, TRG and survival.

Table 1. Summary of findings

Variable	Mean	Range
Tumor size (cm)		
Imaging before NT (N=56)	2.98	1.4-6.6
Imaging after NT (N=55)	2.5	1.2-5.9
Gross (N=65)	3.17	0.5-8
Microscopic (largest focus linear) (N=66)	1.39	0.1-5
Tumor Burden		
Blocks involved (N=66)	5.54	2-14
MC (%)	10.63	1-60
AC (%)	5.81	1-48
Positive LN (39/66)	1	0-9
Linear size LN metastasis (mm) (N=66)	1.29	0-9

Conclusions: AJCC 8th ed. pT stage has been proposed as a more reliable predictor of survival in PDA. In the setting of NT, tumor size does not correlate with survival in our cohort. Further, lymph node metastasis and tumor burden assessment methods such as maximum tumor cellularity (30% cut off) and tumor burden index may be better predictors of survival.

1728 Diagnosis, Risk Stratification, and Management of Ampullary Dysplasia by DNA Flow Cytometric Analysis of Paraffin-Embedded Tissue

Kwun Wah Wen[1], Grace Kim[1], Peter Rabinovitch[2], Dongliang Wang[3], Aras Mattis[1], Won-Tak Choi[1]
[1]University of California, San Francisco, San Francisco, CA, [2]University of Washington, Seattle, WA, [3]SUNY Upstate Medical University, Syracuse, NY

Disclosures: Kwun Wah Wen: None; Grace Kim: None; Peter Rabinovitch: None; Dongliang Wang: None; Aras Mattis: None; Won-Tak Choi: None

Background: The diagnosis and grading of ampullary dysplasia (AD) can be challenging, and no ancillary study is available to confirm and/or risk stratify AD. The natural history of AD is also unclear, and there are no clear guidelines on which patients require endoscopic (ampullectomy)/surgical excision (Whipple) versus surveillance endoscopies. This study examines the utility of DNA content analysis in the diagnosis and risk stratification of AD using paraffin-embedded tissue.

Design: DNA flow cytometry was performed on 47 ampullary biopsies with low-grade dysplasia (LGD), 18 high-grade dysplasia (HGD), 11 adenocarcinoma (AC), and 23 negative for dysplasia (NEG).

Results: Abnormal DNA content (aneuploidy or elevated 4N fraction > 6%) was identified in 82% of AC, 72% of HGD, 15% of LGD, and 0% of NEG. The overall 1-, 5-, 9-year detection rates of HGD or AC in all LGD patients were 17%, 26%, and 38%, respectively. More interestingly, 1-, 2-, and 9-year detection rates of HGD or AC for LGD patients in the setting of abnormal DNA content were 57% (p = 0.016), 88% (p = < 0.001), and 88% (p = < 0.001), respectively, whereas LGD patients with normal DNA content had 1-, 2-, and 9-year detection rates of 10%, 10%, and 10%, respectively. The univariate hazard ratio (HR) for subsequent detection of HGD or AC for LGD patients with abnormal DNA content was 16.8 (p = < 0.001). Although older age (HR = 1.1, p = 0.010) and endoscopic appearance of mass (HR = 5.2, p = 0.042) were also associated with an increased risk, DNA content abnormality remained as the only significant risk factor in the multivariate analysis (HR = 9.8, p = 0.002). No other potential risk factors, including gender, ethnicity, familiar adenomatous polyposis, location, and size, were associated with an elevated risk. Among 13 HGD cases with abnormal DNA content, 5 cases (38%) were found to have AC within a mean follow-up time of 3 months, whereas only 1 (20%) of the remaining 5 cases with normal DNA content was found to have AC within a month (HR = 2.6, p = 0.388). The overall 1- and 2-year detection rates of AC in all HGD patients were 34% and 47%, respectively.

Conclusions: The majority of LGD patients with abnormal DNA content developed HGD or AC within two years and thus may benefit from endoscopic/surgical excision, whereas those with normal DNA content may be conservatively followed with surveillance endoscopies (or ampullectomy if symptomatic). The presence of DNA content abnormality can also confirm a morphological suspicion of HGD.

1729 Prognostic Value of PD-L1 expression in Different Pancreatic Neoplasms

Yiqin Xiong[1], Shi Bai[2], Karen Dresser[3], Benjamin Chen[4], Xiaofei Wang[3], Michelle Yang[2]
[1]University of Massachusetts, Worcester, MA, [2]University of Massachusetts Medical School, Worcester, MA, [3]UMass Memorial Health Care, Worcester, MA, [4]UMass Memorial Medical Center, Worcester, MA

Disclosures: Yiqin Xiong: None; Shi Bai: None; Karen Dresser: None; Benjamin Chen: *Grant or Research Support*, TESARO Inc.; Xiaofei Wang: None; Michelle Yang: None

Background: Cancer immunotherapy targeting PD1/PD-L1 pathway has emerged as an effective treatment strategy and PD-L1 expression appears to be a prognostic factor for some tumor types. This study is to characterize PD-L1 expression pattern in various pancreatic neoplasms and evaluate the potential prognostic value of PD-L1 in these entities.

Design: A total of 156 resected pancreatic tumors were selected randomly from 2000 to 2017, including 111 pancreatic ductal adenocarcinomas (PDAC), 19 ampullary adenocarcinomas, 12 pancreatic neuroendocrine tumors (PNET), 5 intraductal papillary mucinous neoplasms (IPMN), 5 mucinous cystic neoplasms (MCN), 1 low grade pancreatic intraepithelial neoplasm (PanIN), 2 undifferentiated carcinomas and 1 solid pseudopapillary tumor. PD-L1 immunohistochemistry was performed and the result was quantitated by the combined positive score (CPS). A CPS ?1 was considered positive. The association of overall survival (OS) as pognostic value with PD-L1 expression was evaluated.

Results: Among the PDAC group, 15 of 111 cases (13.5%) were positive for PD-L1. There was no age difference in positive (64.7 years) and negative groups (64.4 years), although the PD-L1 positivity was slightly higher in females (20%) than males (9%). The median OS for the PDAC patients, regardless of TNM stage, was 16.7 months for PD-L1 positive cases versus 21.4 months for PD-L1 negative cases (p=0.05). Among the ampullary adenocarcinoma group, 2 of 19 cases (10.5%) were PD-L1 positive and the median OS was 13.3 months and 41.2 months for PD-L1 positive and negative cases (p=0.12), respectively. All 12 cases of PNET were negative for PD-L1. Among pancreatic precursors group, only 2 MCN cases were positive for PD-L1. Interestingly, the 2 undifferentiated carcinomas and 1 solid pseudopapillary tumor were all positive for PD-L1. In all positive cases, the CPS score of PD-L1 ranged from 1 to 4.

Conclusions: This study showed PD-L1 expression was generally low in different pancreatic neoplasms. There was a significant association of PD-L1 expression with worse overall survival in patients with PDAC. Our study provides additional information on other pancreatic tumors and similar negative predictive value of PD-L1 expression was observed in ampullary adenocarcinoma but not in PNET. Our preliminary result suggests that PD-L1 expression may be a valuable prognostic factor in predicating worse clinical outcomes in these two entities, and the efficacy of PD1/PD-L1 inhibitors may be evaluated in these patients.

1730 Using a Minimum Set of Prognostic Parameters to Predict Survival of Patients with Well-differentiated Pancreatic Neuroendocrine Tumor

Zhaohai Yang[1], Biyi Shen[2], Ming Wang[2]
[1]Penn State Hershey Medical Center, Hershey, PA, [2]Penn State College of Medicine, Hershey, PA

Disclosures: Zhaohai Yang: None; Biyi Shen: None; Ming Wang: None

Background: The prognostic parameters of well-differentiated pancreatic neuroendocrine tumor (PanNET) include margin status, lymphovascular invasion (LVI), perineural invasion (PNI), WHO grade (by mitosis or Ki67 index), and AJCC stage. Phosphohistone H3 (PHH3) is a mitosis-specific marker and mitotic rate assessed by PHH3 also has prognostic value. Currently WHO separates PanNET into 3 grades using set cutoffs, and the continuous nature of mitotic rate and Ki67 index is largely underutilized. A model using a minimum set of parameters to better predict patient survival is lacking.

Design: 65 cases of PanNETs (G1/G2/G3: 35/28/2) were included in the study. Cox Proportional Hazards models were considered for disease specific survival (DSS) or disease free survival (DFS) analysis using these parameters: age, gender, MEN1 status, tumor location, size, necrosis, LVI, PNI, node status, distant metastasis, margin, and mitotic rate (by H&E, average PHH3 count, single PHH3 hotspot, or PHH3 index in %) or Ki67 index. Univariate analyses were conducted first to select the variables with $p < 0.05$, which were then considered for multiple regressions. To assess predictive accuracy for model selection, the whole data were randomly split into two sets: training data (60%) and testing data (40%). Each candidate model was fitted using the training data and then the parameter estimates were used to compute the area under ROC curve (ROC-AUC) for testing data at 5-year, 10-year, & 15-year (for DSS only). The procedures were repeated 500 times and the average ROC-AUC estimates were reported. The model with the largest ROC-AUC was considered optimal.

Results: Using the whole dataset, the optimal model to predict DSS included these minimum set of parameters: margin, distant metastasis, PNI, and mitosis by H&E, with ROC-AUC of 0.947, 0.995, & 0.629 for 5-year, 10-year, & 15-year survival, respectively. The optimal model to predict DFS included these minimum set of parameters: margin, distant metastasis, LVI, and mitosis (by single PHH3 hotspot), with ROC-AUC of 0.927 & 0.836 for 5-year & 10-year survival, respectively. The hazard ratios (HR), 95% confidence intervals (CI), and p values are shown in the Table.

	DSS			DFS		
Parameters	HR	95% CI	P value	HR	95% CI	P value
Margin	5.94	2.05-17.23	0.001	5.26	1.86-14.90	0.002
Distant Metastasis	4.09	1.31-12.75	0.015	3.05	1.26-7.41	0.014
PNI	3.50	1.12-10.95	0.031			
LVI				6.70	2.03-22.10	0.002
Mitosis (H&E)	2.51	1.68-3.75	<0.001			
Mitosis (PHH3 hotspot)				1.04	1.02-1.06	<0.001

Conclusions: Our data show that it is possible to select a minimum set of parameters to develop a survival prediction model for patients with PanNET, without using any arbitrary cutoff for continuous variables (mitosis and Ki67 index). Further study with a larger patient cohort is needed to validate this model.

1731 Splenic arterial involvement is associated with poor prognosis in resected distal pancreatic cancer

Feng Yin[1], Mohammed Saad[2], Jingmei Lin[3], Christopher Jackson[4], Bing Ren[4], Cynthia Lawson[5], Dipti Karamchandani[6], Belen Quereda Bernabeu[7], Wei Jiang[8], Teena Dhir[9], Richard Zheng[7], Christopher Schultz[9], Dongwei Zhang[10], Courtney Thomas[11], Xuchen Zhang[12], Jinping Lai[13], Hao Xie[14], Xiuli Liu[1]
[1]University of Florida, Gainesville, FL, [2]Indiana University School of Medicine, Indianapolis, IN, [3]Indiana University, Indianapolis, IN, [4]Dartmouth-Hitchcock Medical Center, Lebanon, NH, [5]Penn State Health, Hershey, PA, [6]Penn State Health Milton S. Hershey Medical Center, Hershey, PA, [7]Thomas Jefferson University Hospital, Philadelphia, PA, [8]Philadelphia, PA, [9]Thomas Jefferson University, Philadelphia, PA, [10]University of Rochester Medical Center, Rochester, NY, [11]Yale New Haven Hospital, Orange, CT, [12]Yale University School of Medicine, Orange, CT, [13]University of Florida College of Medicine, Gainesville, FL, [14]Mayo Clinic, Rochester, MN

Disclosures: Feng Yin: None; Mohammed Saad: None; Jingmei Lin: None; Christopher Jackson: None; Bing Ren: None; Cynthia Lawson: None; Dipti Karamchandani: None; Belen Quereda Bernabeu: None; Wei Jiang: None; Teena Dhir: None; Richard Zheng: None; Christopher Schultz: None; Dongwei Zhang: None; Courtney Thomas: None; Xuchen Zhang: None; Jinping Lai: None; Hao Xie: None; Xiuli Liu: None

Background: The American Joint Cancer Committee on Cancer (AJCC) 8th edition made changes to criterion for pT4; it replaced resectability with arterial involvement as evidence of pT4 and specified that pancreatic cancer in the head with involvement of superior mesenteric artery, common hepatic artery, or celiac axis should be staged as pT4. However, splenic arterial involvement/invasion (SAI) for distal pancreatic cancer has not been clearly stated in the AJCC 8th edition. This study aims to assess the prognostic value of splenic vasculature involvement in resected distal pancreatic cancers.

Design: A retrospective study from 5 academic medical centers was performed. Cases of resected distal pancreatic cancers from year 2005 to 2018 were included. Pathology reports and slides were reviewed. Cases received neoadjuvant therapy, non-invasive intraductal mucinous neoplasm, non-invasive mucinous neoplasm, and neuroendocrine neoplasm were excluded. Medical charts were reviewed for recurrence, metastasis, and survival status. Univariate and multivariate analyses were performed to identify factors associated with progression-free survival (PFS) and overall survival (OS).

Results: A total of 396 cases were included. Demographics and major pathologic features are summarized in Table 1. Univariate analysis revealed splenic vascular invasion (histologically or radiographically), splenic parenchymal invasion, higher T stage (per 7th or 8th edition) and N stage (per 7th or 8th edition) correlated with shorter PFS, and splenic vein invasion (either histologically or radiographically), higher T stage and N stage with worse OS. Multivariate analysis confirmed nodal metastasis and SAI as independent predictors of shorter PFS in context of both staging systems, but only nodal metastasis as an independent predictor of shorter OS in both staging systems.

Clinicodemographics and major tumor characteristics		
Feature	**Level**	
Age (in years), mean (SD)		66.7 (10.5)
		N (%)
Male		188 (47)
Type of cancer	Ductal adenocarcinoma Invasive IPMN Others	257 (64.9) 99 (25) 40 (10.1)
Tumor location	Tail Body Tail/body Others	206 (52) 117 (29.5) 67 (16.9) 6 (1.5)
AJCC 7th staging system	T1 T2 T3 Tx	29 (7.3) 43 (10.9) 304 (80.8) 4 (1)
AJCC 8th staging system	T1 T2 T3 Tx	67 (17) 166 (42) 162 (41) 1 (0.25)
Lymph node	Positive Negative	203 (51) 193 (49)
Splenic artery invasion	Present Absent Not examined	22 (5.6) 189 (47.7) 185 (46.7)
Splenic vein invasion	Present Absent Not examined	47 (12) 163 (41) 186 (47)
Splenic parenchymal invasion	Present Absent Not examined	24 (6.1) 367 (82.7) 5 (1.3)
Radiographic Splenic artery invasion	Present Absent Not examined	68 (17) 190 (48) 138 (35)
Radiographic Splenic vein invasion	Present Absent Not examined	86 (22) 178 (45) 132 (33)
Multivariate analysis for PFS and OS		
PFS	**HR (95% CI)**	**P value**
AJCC 7th staging system		
Nodal metastasis Splenic artery invasion	2.05 (1.15-3.65) 2.76 (1.32-5.80)	0.015 0.007
AJCC 8th staging system		
Nodal metastasis Splenic artery invasion	1.75 (0.98-3.13) 2.61 (1.24-5.53)	0.058 0.012
OS		
AJCC 7th staging system		
Nodal metastasis	1.76 (1.07-2.99)	0.026
AJCC 8th staging system		
Nodal metastasis	1.73 (1.05-2.85)	0.03

Conclusions: In resected distal pancreatic cancers, nodal metastasis predicted shorter PFS and OS, and SAI predicted shorter PFS only. SAI should be reported in the pathology report and potentially be incorporated into AJCC staging system for all resected distal pancreatic cancers.

1732 Prognostic significance of stem/progenitor cell markers in biliary tract carcinoma: Association of two markers with better patient survival

Ju-Yoon Yoon[1], Jennifer Knox[2], David Hedley[2], Runjan Chetty[3], Stefano Serra[4]
[1]University of Toronto, Toronto, ON, [2]University Health Network Medical Oncology, Toronto, ON, [3]University Health Network, Toronto, ON, [4]University Health Network, University of Toronto, Toronto, ON

Disclosures: Ju-Yoon Yoon: None; Jennifer Knox: None; David Hedley: None; Runjan Chetty: None; Stefano Serra: None

Background: Hepatobiliary tract is one of the rare examples of a disease where immunophenotypic resemblance to stem cells portends worse survival. We sought to further examine the prognostic significance of stem/progenitor cell markers in biliary tract carcinoma, including intra- and extra-hepatic cases.

Design: Genes of interest were first chosen based on literature search. The list was restricted based on each gene's prognostic significance at the mRNA level in the Cancer Genome Atlas (TCGA) cohort. Final genes of interest were examined at the protein level in our cohort of biliary tract carcinoma by immunohistochemistry (IHC) in our previously characterized cohort of 163 cases. Each core was scored 0-8, combining the IHC intensity and frequency of staining. Survival analyses were performed using the Kaplan-Meier method, examining both disease-free/recurrence-free (RFS) and overall survival (OS).

Results: Six genes, *LGR5*, *THY1* (CD90), *PDGFRB* (CD140b), *MCAM* (CD146), *ITGB1* (CD29) and *SUSD2*, were chosen as genes of interest based on the prognostic values of their gene expression levels (mRNA). These genes were examined at the protein level by IHC, and the prognostic significance of two proteins met statistically significance, namely LGR5 (log-rank $p = 0.0007$ for OS or RFS) and CD90 (log-rank $p = 0.0007$ for OS only). LGR5 and CD90 protein levels correlated positively with one another (Spearman rho = 0.6212, $p < 0.0001$). There were no significant differences in either LGR5 or CD90 protein levels in comparison to disease stage, patient sex or patient age. Interestingly, stronger expression of LGR5 or CD90 portended better survival by both protein and mRNA analyses. Strong LGR5 expression remained statistically significant for OS in a multivariate analysis that included CD90, disease stage (stage I/II *vs.* III/IV) and anatomic site (risk ratio for high LGR5 expression = 0.5506, 95% range 0.3298-0.9085).

Conclusions: Immunophenotypic resemblance to stem/progenitor cells in cholangiocarcinoma, in the form of strong LGR5 or CD90 expression, was associated with better patient survival. The biologic significance of these findings remains to be further explored.

1733 Cancerization of Bile Ducts in Hilar Cholangiocarcinomas: Immunophenotyping Using P53 and SMAD4

Yang Zhang[1], Zainab Alruwaii[2], Tatianna Larman[3], James Miller[3], Robert Anders[4], Kiyoko Oshima[1]
[1]Johns Hopkins Hospital, Baltimore, MD, [2]Johns Hopkins Medical Institutions, Baltimore, MD, [3]Johns Hopkins University School of Medicine, Baltimore, MD, [4]Johns Hopkins, Baltimore, MD

Disclosures: Yang Zhang: None; Zainab Alruwaii: None; Tatianna Larman: None; James Miller: None; Robert Anders: None; Kiyoko Oshima: None

Background: Cancerization of ducts (COD), and has been reported in cases of cholangiocarcinoma, and can histologically mimic high-grade biliary intraepithelial neoplasia (HG-BilIN). In this study, we investigated the prevalence of COD in a series of surgically resected hilar cholangiocarcinomas (HC), and analyzed areas of COD and invasive cholangiocarcinoma using immunolabeling for p53 and SMAD4.

Design: Resections of HC from 105 patients from 1989 to 2018 were identified using our electronic pathology database. The cases were reviewed for the presence of ducts with histologic features of COD, defined as a markedly atypical intraductal lesion with an abrupt transition to normal duct epithelium. Paired invasive cholangiocarcinoma and histologically suspected COD lesions were then immunolabeled with antibodies to p53 and SMAD4. P53 expression was categorized as wild-type (>0% but ?60% staining), null pattern (0% staining), and diffuse pattern (>60% staining).

Results: The mean age of the 105 patients was 62 years, with 65 males (62%) and 40 females (38%). COD was identified in 33 of 105 cases (31%). However, only 26 of these cases had available tissue for performance of p53 and SMAD4 immunolabeling. The study group of 26 cases had a mean age of 63 years, with 15 males (58%) and 11 females (42%). The degree of tumor differentiation was "well" in 3 cases (12%), "moderate" in 18 cases (69%), and "poor" in 5 cases (19%). The area of COD was lost on deeper sectioning in 10 of these cases. In the invasive cholangiocarcinomas, 14 cases were p53 wild-type (54%), 6 cases were p53 null pattern (23%), and 6 cases were p53 diffuse pattern (23%). In 16 cases with concurrent COD lesions analyzed, a matching pattern of p53 expression between the invasive component and COD lesions was seen in 15 of 16 cases (94%). One case showed a null pattern of p53 expression in the COD, but wild-type p53 expression in the invasive component. SMAD4 immunolabeling of the invasive cholangiocarcinomas showed retained expression in 16 cases (62%), and lost expression in 10 cases (38%). All 15 cases with concurrent COD lesions showed a matching pattern of SMAD4 expression.

Conclusions: Cancerization of ducts or ductules was identified in 31% of the hilar cholangiocarcinomas we studied. Among the cases with available immunolabeling, there was a high concordance in the immunolabeling pattern of invasive cholangiocarcinoma and COD for p53 (15/16 cases) and SMAD4 (15/15 cases), validating the prevalence of COD observed on H&E.

1734 Microsatellite instability and PD-L1 expression in pancreatic ductal adenocarcinoma

Li Zhang, Peking University Cancer Hospital, Beijing, China

Disclosures: Li Zhang: None

Background: Immunotherapy has become a new modality of cancer treatment, but has had a limited success in treating pancreatic ductal adenocarcinomas (PDACs). Microsatellite instability (MSI) is a genetic feature of sporadic and familial cancers of multiple sites and is related to defective mismatch repair (MMR) protein function. dMMR and MSI have been associated with responses of metastatic tumors to immune checkpoint inhibitor therapy. Programmed death ligand 1 (PD-L1) has shown potential as a therapeutic target in numerous solid tumors. Immunotherapy has shown promise against solid tumors. However, the clinical significance of PD-L1 in PDAC remains unclear. The present study aimed to explore PD-L1 expression in PDAC cases in a Chinese cohort to provide further insight into the potential value of programmed cell death protein 1 (PD-1) as a therapeutic target.

Design: Aims of the study were to determine the prevalence of MSI, PD-L1 expression and clinicopathological features in surgically resected pancreatic cancers in a retrospective study. We performed immunohistochemical analyses of a 120 PDAC paraffin specimens and matched adjacent tissue specimens, collected from consecutive patients at Peking University Cancer Hospital, to identify those with dMMR, based on loss of mismatch repair proteins MLH1, MSH2, MSH6, and PMS2.

Results: We detected dMMR in 12% of tumor samples. PD-L1 positivity were observed in 6% of cases. PD-L1 showed a predominantly membranous pattern in tumor cells. Increased PD-L1 expression was associated with inferior prognosis ($p = 0.040$). No statistically significant association was identified between PD-L1 status and MMR status or tumor infiltrating lymphocytes. PDAC patients with high expression levels of PD-L1 had significantly reduced OS. The PD-L1 positive rate was associated with PDAC T stages. The PD-L1 positive rate in the T3-4 group was higher than that in the T1-2 group ($P < 0.001$).

Conclusions: This data suggests that there is an inverse relationship between PD-L1 expression and disease specific survival times in resected PDAC. High PD-L1 expression levels predicted a poor prognosis in PDAC patients. Increased PD-L1 expression has an effect on tumor biology. PD-L1 status helps determine treatment in PDAC patients. MSI caused by mismatch repair deficiency (dMMR) is detected in a small proportion of PDAC. Studies are needed to determine whether these features of PDACs with dMMR or MSI might serve as prognostic factors.